# SCIENCE PLAN

# United Arab Emirates
# Unified Aerosol Experiment (UAE$^2$)

## Prepared for DWRS, NASA, NRL, and ONR

**Version 1.0 September 15th, 2004**

**Compiled & Edited by: Jeffrey S. Reid, Charles Gatebe, Brent N. Holben, Michael King, Stuart Piketh, and Douglas L. Westphal.**

**With Contributions from: Garret de Leeuw, Phillip Durkee, Christina Hsu, Becky Eager, Piotr Flatau, Tara Jensen, Ralph Kahn, Ming Liu, Steve Miller, Sethu Raman, Elizabeth Reid, Benjamin Ruston, Robin Schoemaker, Alexander Smirnov, Dominick Vincent, and Ellsworth Judd Welton**

# Executive Summary:

The United Arab Emirates Unified Aerosol Experiment ($UAE^2$) is an international science initiative designed to make a detailed characterization of atmospheric aerosols in the Gulf region while simultaneously characterizing the lower boundary condition with measurements over bright and dark surfaces, under cloud-free conditions, and coincident with satellite overpasses such as National Aeronautics and Space Administration (NASA) Terra and Aqua. The experiment, based from several sites in the UAE, will be carried out from 5 August–30 September 2004.

Recent reports and various satellite data show that the Arabian Gulf region hosts one of the largest confluences of aerosol types in the world. Emissions, smoke transported from the Indian subcontinent, and natural dust episodes result in a unique aerosol laboratory. To further complicate the intricate consortium of aerosols in this region, the Arabian Gulf also has an exceedingly complex meteorology that includes variable sea surface temperatures, enormous latent heat fluxes, strong land sea gradients, and strong mesoscale circulations. Remote sensing systems are hindered by the bright surfaces over the deserts, the Gulf's shallow waters and variable sediment loads. These factors combine to make the Arabian Gulf a significant challenge to climate and meteorology models, as well as satellite sensors that carry out environmental monitoring. A mission was required to characterize this demanding region, and develop and improve the next generation of remote sensing algorithms.

In the fall of 2003, the Unified Aerosol Experiment-United Arab Emirates ($UAE^2$) was initiated between the University of the Witwatersrand (South Africa), the Department of Water Resources, Office of the President (DWRS-United Arab Emirates), and NASA Goddard Space Flight Center (GSFC-United States). The $UAE^2$ mission was originally proposed to be an extension of a currently operating United Arab Emirates Dept of Water Resources, South African, and Nation Center for Atmospheric Research (NCAR) cloud seeding experiment. By leveraging with this ongoing research program, additional research would be cost effective. As the $UAE^2$ program developed, however, mission objectives and participants expanded greatly. This document outlines the current mission plan for the $UAE^2$ experiment.

In response to invitations by the ongoing UAE cloud seeding program, NASA, the Naval Research Laboratory (NRL), the UAE Department of Water Resources Studies, the University of the Witwatersrand, and 18 other US and foreign research laboratories have embarked on a measurement campaign, the $UAE^2$. Ultimately, scientists wish to gain insight on the properties and concentrations of aerosols in the gulf region, and understand how these aerosols might affect the atmosphere with respect to climate change and numerical weather prediction. To accomplish this task, 15 Aerosol Robotic Network Sun Photometers (AERONET), the NRL Mobile Atmospheric Aerosol And Radiation Characterization (MAARCO), and the NASA's Surface-sensing Measurements for Atmospheric Radiative Transfer (SMART) will be deployed and utilized in the gulf, coast, and desert region of the UAE, respectively. Numerous coordinated aircraft experiments involving in situ and remote sensing sensors such Cloud Absorption

Radiometer (CAR) will be conducted under a variety of conditions and during satellite overpasses to provide essential information to the remote sensing and meteorological modeling communities.

Currently, there are 4 overarching goals of UAE[2]. 1) Evaluate and improve the suite of satellite aerosol and ocean products commonly used by e scientific community in this optically complicated region of the world. 2) Determine the fundamental microphysical, optical and transport properties of aerosol particles in this mostly un-sampled region. 3) Understand how aerosol particles interact with the regional radiation budget in bright surfaced locations. 4) Model and explain the complicated flow patterns in the coastal regions of the Arabian Gulf and Gulf of Oman.

## 1.0 Introduction

In the past decade environmental monitoring technology has advanced at an almost exponential rate. Whereas in the middle 1990 most satellite observations techniques of aerosols and clouds were coming to their terminal fruition with the NOAA polar orbiters, new satellite senor systems such as those on Terra and Aqua give unprecedented data views of the earths land, ocean, and atmospheric environments. This highly advanced data has spurred new ideas and algorithms in aerosol, cloud, and ocean retrievals. Similarly, meteorology and aerosol modeling has advanced greatly in the last few years. Computational power is at a state where global and mesoscale aerosol models can be run in forecast mode. Between remote sensing and models in the past 4 years, our monitoring of the biosphere has been improved many fold.

With advances in sensor and model algorithm development, the required complexity of our understanding of the atmospheres and ocean's physical, chemical and optical properties that goes into algorithm's must also be advanced. Whereas in the past optical depth errors on the order of 30% were often considered acceptable, current demands place errors well under 10%. To meet such goals retrieval and modeling issues once ignored as "second order" must now be considered. Monitoring of regions once thought near impossible such as coastal zones or bright desert surfaces has not only become possible but is now considered absolutely necessary.

Further advances in algorithm and model development are often hindered in that atmosphere, ocean and land algorithms often feedback into one another. Ocean color retrievals must correct for aerosol particles in the atmosphere, and aerosol algorithms must correct for variable ocean reflectance and color. Quality assurance screening of dust interference in sea surface temperature (SST) retrievals in turn depends on aerosol and ocean color information. The SST retrieval is then assimilated in meteorology models that in turn drive the aerosol models. The aerosol models are sometimes used in the remote sensing algorithms for specifying particle properties, but at the same time aerosol models are now starting to assimilate optical depth retrievals.

With increasingly stringent requirements for environmental monitoring coupled with the interdisciplinary nature of such systems, it is essential that validation studies take

on numerous dimensions. Experiments and field trials need to be "unified", in that they must consider the many facets of environment being studied. Individual data sets must be constrained with respect to all other measurements in a study ensure that a "physical" picture is generated. However, the production of coupled datasets necessary for validating and optimizing interdisciplinary environmental monitoring systems is difficult. Not only must a wide array of highly calibrated instruments and sensors be used, but also they must be deployed in the proper conditions. Optimum locations include those areas with strong independent gradients in atmospheric, oceanographic, and land biosphere variables.

The Arabian Gulf region is arguably, based on satellite imagery especially in summer, one of the largest confluences of dust and anthropogenic emissions in the world. Emissions, smoke transported from the Indian subcontinent, and natural dust episodes result in a unique aerosol laboratory. In addition, the region has an exceedingly complex meteorology that includes variable sea surface temperatures, enormous latent heat fluxes, strong land sea gradients, and strong mesoscale circulation. These factors combined make the Arabian Gulf a challenge to our models and limit applications of satellite measurements.

In 2003, NASA GSFC initiated a surface-based radiation program to place advanced Sun photometers in the Arabian Gulf region. While there, they developed a strong cooperative relationship with the United Arab Emirates (UAE) government and with a UAE atmospheric research programs. As a result, a new NASA initiative was started to study the radiative properties of this region The Unified Aerosol Experiment-United Arab Emirates ($UAE^2$) was initiated to understand the complicated atmospheric environment of the southern Arabian Gulf region. $UAE^2$ was originally developed between the University of the Witwatersrand (South Africa), the Department of Water Resources, Office of the President (DWRS-United Arab Emirates), and NASA Goddard Space Flight Center (GSFC-United States) to be an extension of an ongoing cloud seeding experiment with the National Center for Atmospheric Research (NCAR). Expanding mission goals led to the involvement of the Naval Research Laboratory, and ten other government and university collaborators. At the writing of this plan, we anticipate a late summer 2004 utilization of the South African Aerocommander 690 A research aircraft, and the deployment of two radiation "super sites" (Mobile Atmospheric Aerosol and Radiation Characterization Observatory-MAARCO and GSFC Surface-sensing Measurements for Atmospheric Radiative Transfer-SMART) coupled with of fifteen AERONET Sun photometers. Combined, these instrument packages will form one of the densest mesonets of aerosol optical depth data ever deployed. These field assets will be utilized to provide critical information to the remote sensing and meteorological modeling communities to fulfill the mission goals as listed below.

## 2.0 Rationale for $UAE^2$

The latest generation of remote sensing algorithms has greatly expanded the utility of space-based sensors. Aerosol Optical Thickness (AOT), ocean color, and cloud can be retrieved at unprecedented accuracy. Recent studies have shown that using

passive microwave sensors can also now retrieve reasonable temperature profiles. Calibration/validation studies from missions such as the Southern African Regional Science Initiative (SAFARI 2000) and Chesapeake Lighthouse & Aircraft Measurements for Satellites Experiment (CLAMS), have shown that most satellite and ground based sensor algorithms are meeting their specified goals. However, other studies such as the Puerto Rico Dust Experiment (PRIDE) and the Aerosol Characterization Experiment – Asia (ACE-Asia) have shown that under some complicated aerosol mixtures and surfaces these retrievals can loose fidelity. If certain regions consistently have these types of artifacts, a consistent bias may develop in any long-term dataset. In addition to these quasi-operational products a new generation of remote sensing products need their first field trial. For example, the over desert dust detection method of *Miller* [2003] and the very recent over desert "Deep Blue" optical depth retrieval algorithm [*Hsu et al*., 2004] require additional primary validation.

Meteorology and aerosol models have similar issues as remote sensing systems, although the application differs significantly. Qualitatively these systems have repeatedly proven themselves. Mean flows are generally well represented in the models. However, there are issues in regions in sharp gradients of temperature and stability that in turn often covary with land use type. Aerosol source and sink functions must be specified, and various particle types must be validated.

The Arabian Gulf has one of the largest aerosol burdens in the world with frequent dust storms, smoke advection from the Indian subcontinent, and its own high emission rates of pollution from the petroleum industry. Particle size distributions and chemistries are highly variable. In addition, the Arabian Gulf exhibits extremely complicated meteorology, with variable sea surface temperatures, enormous latent heat fluxes, abrupt topography and strong mesoscale circulations. This combination of factors makes both modeling and remote sensing in the region extremely difficult. Consequently, this is one of the few regions of the world that can be used to fully stress aerosol algorithms and assumptions.

A preferable location for validating any visible/IR remote sensing product or model would be one that has strong independent gradients in the key variables required in the algorithm. For remote sensing systems these are typically surface brightness and color, particle scattering phase function (primarily through size and species), and particle absorption. It appears that the Arabian Gulf and the Gulf of Oman have these characteristics. First, surface albedos range from the dark open waters of the Gulf to the very bright surfaces of the inland deserts. Second, the limited data from the Gulf regions suggest that particle size distributions exhibit large dynamic range. Pollution from the region's petroleum industry can produce high concentrations of accumulation mode particles. Pollution from Pakistan may also reach the Gulf of Oman. Conversely, dust source regions in Saudi Arabia, Iraq, Iran and Afghanistan can inject optically thick layers of airborne dust. Lastly, there is absorption. Based on the high variability in both dust and pollution source regions feeding aerosol particles into the southern Gulf region, the absorption properties of particles also likely vary.

The Gulf regions also appear conducive to meteorology and aerosol modeling trials. The variability in fine and coarse mode aerosol species allows for the testing of aerosol source functions. The region also appears to be impacted by not only dust from Saudi Arabia, Iraq and Iran but long-term transport from Africa to Afghanistan have been reported (thus allowing for the validation of global models). On the micro and mesoscales, the relative high differences in surface temperatures over the ocean and the land can create complicated internal boundary layers during onshore/offshore flow. This will likely generate sea breezes and the formation of land plumes. Because the bulk of the UAE is near sea level, boundary layer effects can be studied without the complications of varying topography, land use, or roughness length. Conversely, mountain ranges on the eastern part of the UAE divide the airmasses between the Arabian Gulf and the Gulf of Oman allowing these regimes to be studied independently. Further, mountains on the UAE/Oman boarder may create atmospheric wave effects of interest to modelers.

In addition to the calibration and validation issues discussed above, there are fundamental scientific questions about the atmospheric environment of the Arabian Gulf of intense interest to the scientific community. Deployment to the UAE as part of this mission will greatly further our understanding of several aspects of the aerosol and radiation environment in the Arabian Gulf. First, because the ratio of small to large particles is highly variable, there exists a significant potential for artifacts and errors in remote sensing retrievals from Sun/sky inversions, satellite optical depth and lidar algorithms on which the research community depends. Can algorithms be developed to meet these challenges? Second, Aerosols in the region are almost completely un-sampled. What are the fundamental chemical and microphysical properties of aerosol particles in this region? Because there is a variable aerosol size, the formation of soluble secondary species on dust particles can also be studied under a range of aerosol conditions along with the impact of giant cloud condensation nuclei on cloud properties. It is likely that aerosol particles have a significant impact on cloud coverage and microphysics. Third, because cloudless skies are fairly common in the UAE and aerosol loadings are variable, the region is ideal for airborne and ground-based studies of direct radiative forcing. In addition, the variable partitioning of small/large aerosol particles makes infrared forcing studies feasible and will allow us, for the first time ever, to perform a complete accounting of the earth's radiative balance in this complicated environment.

Lastly, we must consider the recent prospects that have presented themselves. Thorough scientific studies on aerosol particles and their radiative effects have taken in most regions and aerosol regimes of the world. One notable exception is the Arabian Gulf, which is one of the last regional frontiers of aerosol research. There are virtually no in situ aerosol measurements available other than a few aircraft flights in the Kuwaiti oil fire smoke plumes of 1991. One study exists using Sun-sky inversion techniques in Bahrain [*Smirnov et al.,* 2000]. The opportunity the $UAE^2$ study is unprecedented in the region. While there were greater airborne assets in the Arabian Gulf for the 1991 Kuwait oil fires, never before has such a combination of ground and airborne, and space based sensors observed this region. The deployment of a research aircraft to the region of the caliber of the Aerocommander is indeed rare. This is coupled with the world-class

network of densely populated meteorology stations and environmental monitoring by the UAE DWRS. This is a cost effective opportunity that will not present itself again for some time.

All of the arguments suggest that the creation of an aerosol and meteorology experiment in the UAE would be highly beneficial to several disciplines in the atmospheric and ocean sciences. The combination of gradients in aerosol, meteorology, ocean, and land features coupled with available airborne and surface resources in the UAE will make allow the $UAE^2$ study to perform groundbreaking yet economical research.

## 3.0 Mission Objectives

The $UAE^2$ mission has a number of interrelated mission objectives in for fundamental areas of research: Satellite calibration/validation, radiative transfer, aerosol microphysics, and transport meteorology. Ultimately, these four areas will be unified for a regional evaluation. Goals are outlined below.

*3.1 Satellite Calibration/Validation*

3.1.1 Perform fundamental over water optical depth algorithm validation for MODIS, MISR, SeaWiFS, ATSR, & AVHRR under mixed (i.e., bi and tri-modal) aerosol conditions.
3.1.2 For over bright surface/desert areas evaluate Hsu et al., [2004] "Deep Blue" and Miller et al., [2003] significant dust product and new MISR aerosol algorithms.
3.1.3 Perform primary validation of high-resolution aerosol retrieval methods.
3.1.4 Evaluate MISR aerosol height algorithms.
3.1.5 Validate ocean leaving radiance and ocean color algorithms
3.1.6 Evaluate sea surface temperature algorithms and determine the relative bias dust particle induce in products.
3.1.7 Evaluate aerosol inversion algorithms.
3.1.8 Estimate land surface microwave emissivity.
3.1.9 Evaluate and improve passive microwave temperature and ground moisture inversions.
3.1.10 Over longer periods, evaluate GLAS systems.

*3.2 Radiation and Energetics*

3.2.1 Measure water leaving radiance, BRDF and desert/ocean albedo.
3.2.2 Measure, for the first time, UV through infrared sky radiance for retrievals of particle size distribution, single scattering albedo and complex index of refraction.
3.2.2 Generate 3-dimensional radiation fields using combined AERONET, CAR and flux radiometers.
3.3.3 Intercompare the CAR and AERONET aerosol retrievals.
3.3.4 Measure the shortwave forcing efficiency of aerosol particles in this region.
3.3.5 Model longwave forcing by aerosol particles.
3.3.6 Using lidar, AERONET, and satellite, develop algorithms that can determine the vertical distribution of extinction.
3.3.7 What is the atmospheric diabatic heating rate as a function of aerosol loading?

3.3.8 Do aerosol radiative effects make an appreciable difference to the Arabian Gulf's sensible and latent heat fluxes?
3.3.9 Combined analysis above to determine the energetics of the region.

*3.3 Aerosol Microphysics and Chemistry*

3.3.1 Determine the size-dependant vertical distribution of aerosol particles.
3.3.2 Understand how the microphysics and chemistry of the dust varies from the many sources that impact the Arabian Gulf region (e.g., Africa, Iraq, Afghanistan, etc...)?
3.3.3 Determine the basic chemical constituents of Arabian Gulf pollution.
3.3.4 Measure the spectral mass scattering and absorption efficiencies of the dust and pollution of the region (UV to IR).
3.3.5 Measure the spectral phase function of dust and haze.
3.3.6 Determine if the hygroscopic growth properties of aerosol particles in the region differ greatly from other 'anthropogenic" pollution owing to the presence of more organic species?

*3.4 Meteorology and Aerosol Transport*

3.4.1 Determine the temporal and spatial scales of aerosol and meteorological features in this region
3.4.2 Validate meteorology and aerosol transport model forecasts such as those from NOGAPS, NAAPS, COAMPS, and GOCART.
3.4.3 Understand the development of land and sea breeze circulations and the sensitivity of these phenomena to surface properties and processes. Evaluate forecasts of these features.
3.4.4 Explain the vertical distribution of aerosols relative to the PBL, MBL, and other meteorological features.
3.4.5 Evaluate the significance of local, fine-scale phenomena, such as the sharp inversion in the lowest 300 meters of the atmosphere. Can COAMPS even track small changes in inversion height?
3.4.6 Compare the aerosol direct heating and flux perturbations with the other diabatic heating and sensible and latent heat flux perturbations. Evaluate the importance of aerosol heating to accurate forecasts.
3.4.7 Estimate the impact of aerosols on the regional climate.

*3.5 Evaluation*

3.5.1 Build a realistic regional aerosol model/library for use in aerosol models and retrieval algorithms.
3.5.2 Develop a comprehensive receptor validation set suitable for any meteorology or aerosol transport models.
3.5.3 Perform the first ever-complete evaluation of aerosol and radiative properties for this region.
3.5.4 What are the relative contributions of local versus long-range sources to the region's dust, pollution and radiative properties?

## 4.0 The Arabian Gulf, Gulf of Oman, and Arabian Sea Environments

The Arabian Gulf, Gulf and Oman and Arabian Sea exhibit some of the most complicated environmental phenomenon in the world. An early understanding of the regional environment is required before a suitable scientific plan can be made. In this section, we discuss the geography, oceanography, meteorology, and aerosol characteristics of the region of the region.

### 4.1 Geology of the Region

Figure 1 presents topographical representations of the UAE and its surrounding regions. It is bordered by Saudi Arabia in the south and west, and Oman in the east. Its northern coast faces Iran across the Persian Gulf and the Strait of Hormuz, where the Persian Gulf narrows to roughly 40 km diameter. The mountain range in Oman and eastern UAE, coupled with the higher mountains across the Strait of Hormuz in Iran, functionally separate the airmasses and currents of the Persian Gulf and the Gulf of Oman/Arabian Sea.

Over eighty percent of the UAE is nearly flat desert plains of less than 200 meters of elevation, gently sloping toward the Arabian Gulf. The remaining twenty percent includes the northern edge of the Al Hajar al Gharam mountain range, which reaches 2,000 meters elevation and forms part of the eastern border of UAE with Oman. Across the Persian Gulf from UAE, the Zagros Mountains of Iran rise above 3000 meters, the result of folding along the edge of the Arabian Shield, underlying the Arabian Peninsula. Easterly tilting of the Arabian peninsula and downwarping associated with tectonic activities along the Iranian Zagros fold belt and the Oman Mountains, established the Persian Gulf, and the gently dipping central plains of UAE.

The coastal areas, and some drainage basins in the UAE, include sebkhahs: flat, barren plains having a shallow (salt) water table. Minerals such as gypsum, anhydrite, calcite, and dolomite precipitate at the surface, trapping and consolidating windblown sand and silt, while evaporites, including chloride (salts) and nitrate minerals form on the surface where they can also be eroded by wind and sand storms, or washed away by UAE's rare rainfall. The non-sebkhah plains consist of aeolian materials eroded from the continental and shallow-marine sediments of the Arabian Shield, including gravel, sand, silt, and clays. The plains merge with the gravel, sand and scrub-covered alluvial fans from the eastern mountain range, and with the rolling sand dunes of the Rub al Khali, the famous Empty Quarter of Saudi Arabia, to the south. Much of the central plains are a vast desert wasteland, punctuated by dry wadis (seasonal drainage channels) running down from the eastern mountains, and the sand dunes of the deep desert.

Sand storms and small vortices (dust devils) can rapidly entrain dust in the seabkhahs as well as the desert plains. However, more frequently, dust is transported into the UAE from sources to the northeast in Iraq and Saudi Arabia, from dry lakebeds and marshes in Iran and Afghanistan, or via long distance transport from Africa.

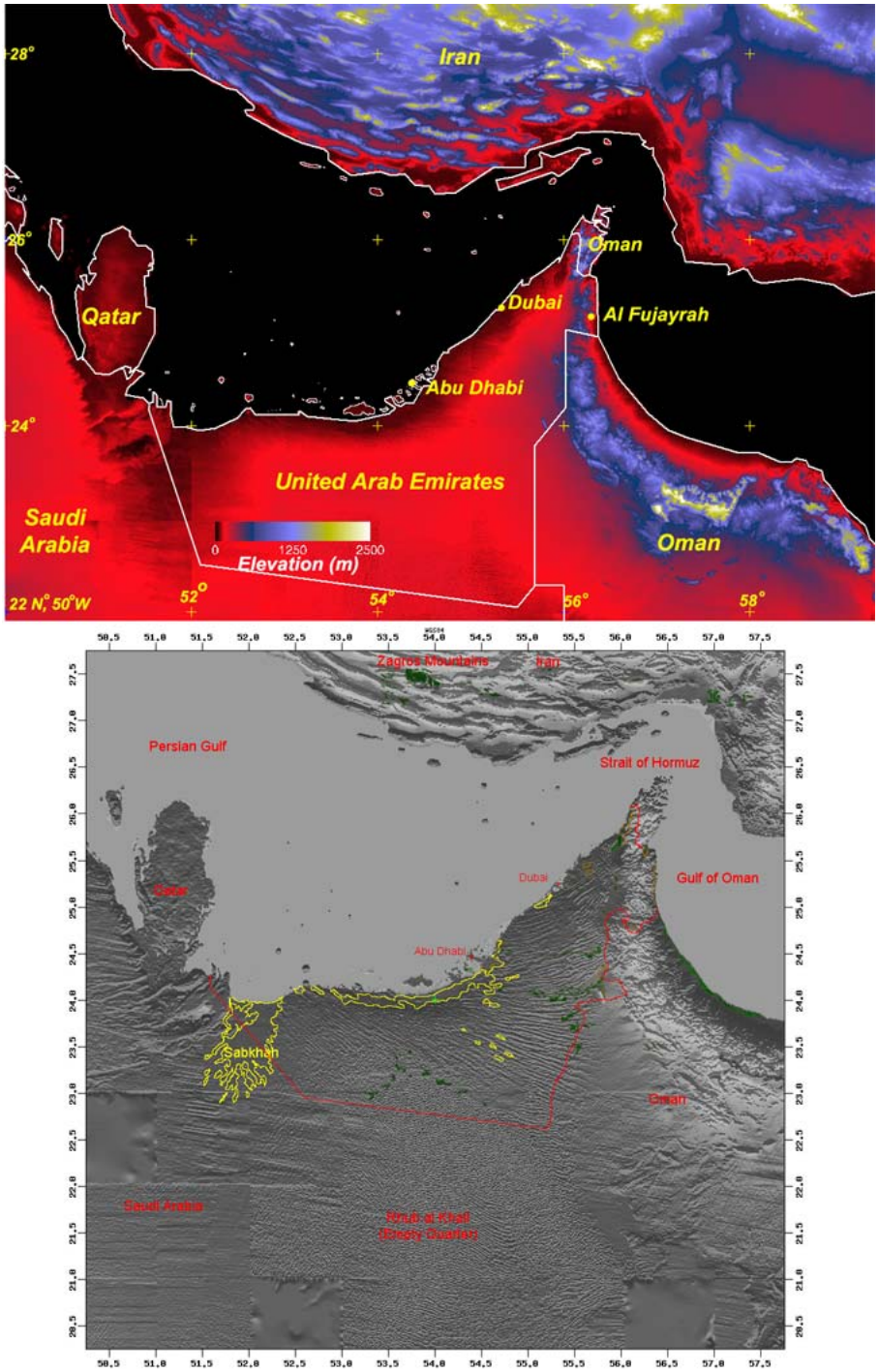


Figure 1. Regional elevation map of the United Arab Emirates and surrounding region

### 4.2 Oceanography Summary

The Arabian Gulf has shallow shelves with complex topography. There are numerous banks, shoals and small islands. It is not atypical to see bottom near the shore or around islands. The shallow waters coupled with limited fetch inhibit large swell production. Over the mission we should expect good conditions over the Arabian Gulf, and by implication less sun glint than most other coastal areas. Seas are typically calm with the National Climate Diagnostic Center (NCDC) reporting median significant wave heights less than 1 meter, although, wave heights as high as 4 meters have been reported in the August-September timeframe.

With the narrow 80 km Strait of Hormuz isolating the Arabian Gulf coupled with its shallow nature (20-70 m deep) and hot weather of the subtropical desert region, sea surface temperatures (SST) are of the highest in the world, particularly in the south. In winter months temperatures off the coast of UAE are at a low of ~23°C, but in summer months can reach over 35°C. Figure 2 presents average August 2003 SST retrievals for the Arabian Gulf/Gulf of Oman (AGGO) regions. Our field study should expect SSTs well over 30°C, with a dynamic range between the Arabian Gulf and Gulf of Oman of ~$3^{o}$ C. As the mission progresses through September, we expect only slight variations in any one location (<$1^{o}$ C).

The warm water of the Arabian Gulf is conducive to biological activity, despite being relatively nitrate-depleted [*Mantaoura et al.,* 1993]]. Positive dust fertilization effects in plankton populations have also been observed in the region [*Rao et al.,* 1999]. Chlorophyll retrievals have shown significant concentrations of microorganisms, particularly in the coastal waters. Like SST, we expect only minor changes in the chlorophyll concentrations during our period of study. However, unlike SST stronger gradients (more than a factor of three) however exist between the Arabian Gulf and the Gulf of Oman compared to SST.

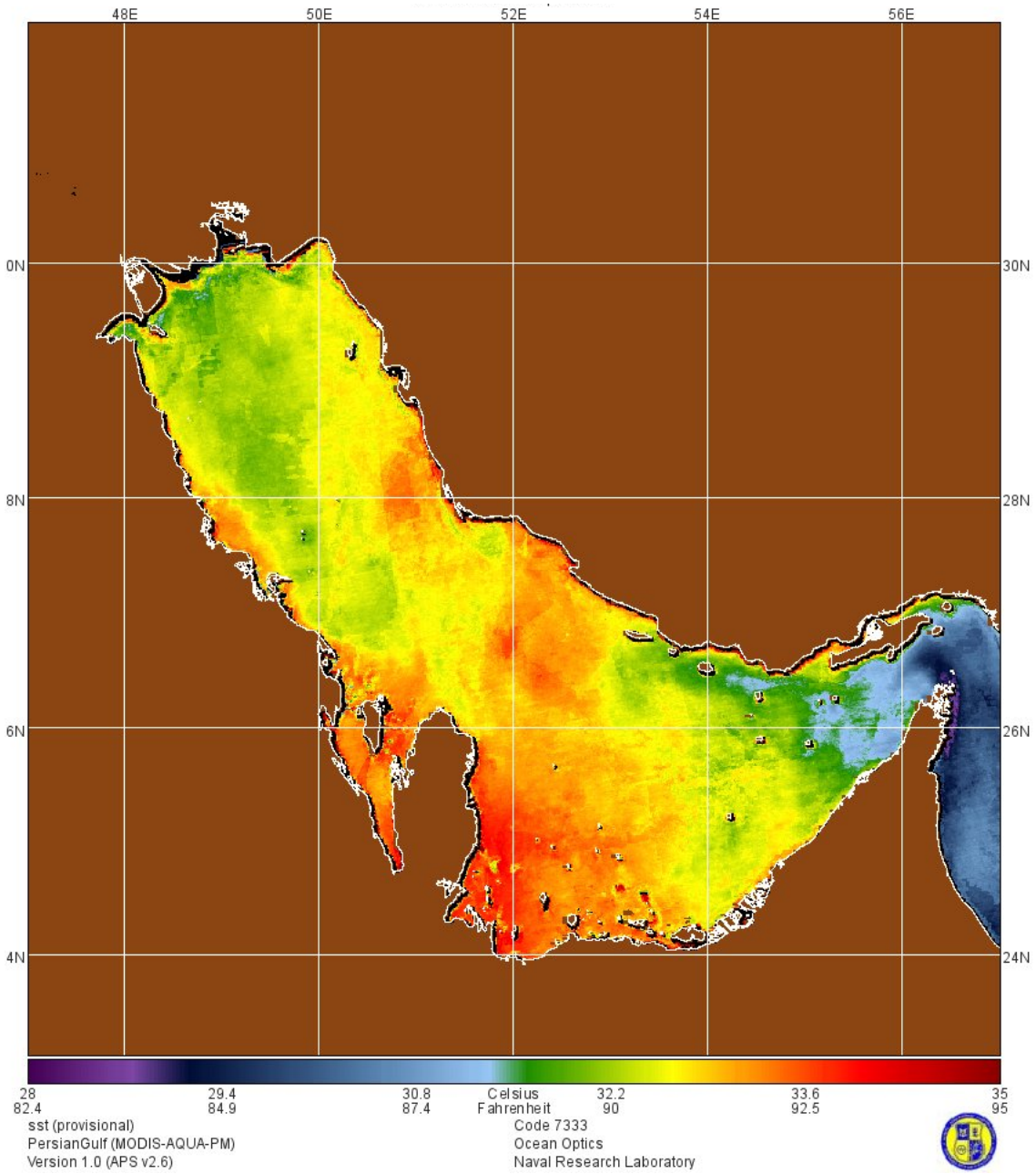


Figure 2. Average MODIS sea surface temperature retrievals for August 2003. Data courtesy of Naval Research Laboratory, Stennis code 7330

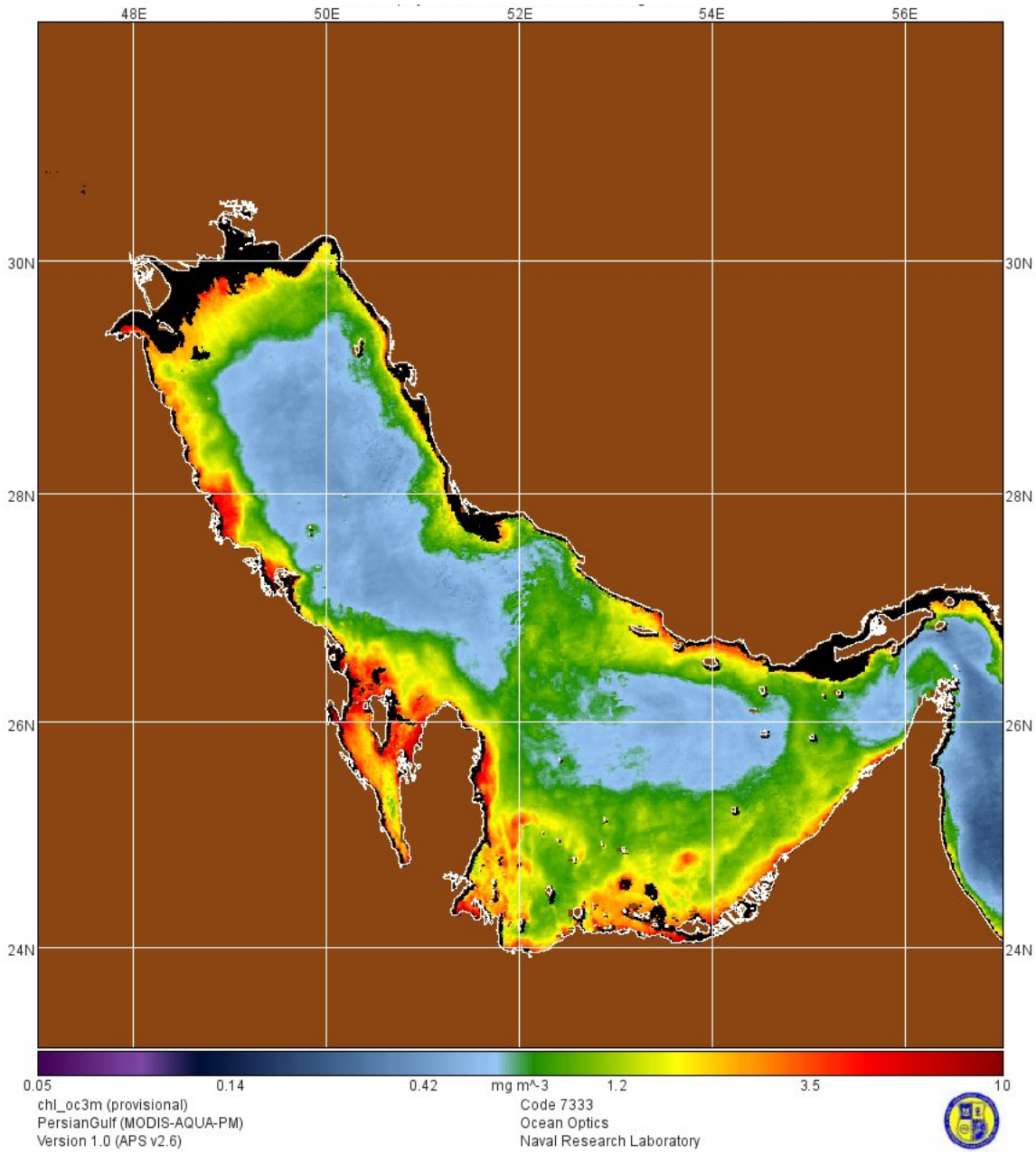


Figure 3. Average MODIS chlorophyll retrievals for August 2003. Data courtesy of Naval Research Laboratory, Stennis code 7330

## 4.3 Meteorological Characteristics

### *4.3.1 Seasonal Meteorology*

The meteorology of the Arabian Gulf follows a two-monsoon cycle: the wintertime Northeasterly monsoon and the summer Southwesterly "Shamals." These two monsoons are then coupled by two distinct intermediate periods. In this section we give an overview of the seasonal cycle. This analysis is mostly taken from the US Navy's Regional Weather Forecasters Handbook.

The onset of the winter monsoon is signaled by the development of wintertime cooling of the Indian plateau and the Middle East. Because SSTs remain relatively constant, a low-level pressure gradient forms between the land and ocean along the south coast of India. This results in northeasterly offshore winds off of the Indian sub-continent. However, mountain ranges such as the Himalayan Hindu-Kush prevent northerly cold air from ever reaching India. Consequently, the temperatures in India never drop too low and the land ocean gradient is not very strong, typically under 7 m $s^{-1}$. Differential heating between the Sahara and South Africa can extend this monsoon well into the southern hemisphere (Figure 4).

The wintertime monsoon period accounts for most of the precipitation in the lower elevations of the UAE. In winter months the westerly storm tracks dip far enough south. These are typically troughs and depressions, although occasionally a strong front can move through the region bringing precipitation across the UAE (Maybe once per year). Often such strong fronts will have imbedded convective cells. Topographic forcing enhances precipitation in the mountains. Annual rainfall amounts vary considerably in the UAE, and the last several years have been climatologically dry.

In April and May a spring transition period develops with a gradual reversal of the Northeasterly flow to a Southwesterly pattern. By June a strong and complex Southwest monsoon develops. This monsoon and its periodic intense wind storms (the Shamal) is a result of meteorological interactions across Africa to the Tibetan Plateau and is unrivaled in its size anywhere in the world. The intense spring summer solar insolation results in strong thermal low around the Arabian Sea. These eventually merge into a thermal trough from Somalia into Pakistan. Surface winds reverse becoming southwest while upper level flow are easterly to northeasterly. Just as the Himalayas prevent cooler air from descending into India and intensifying the winter monsoon, the Himalayas prevent the relatively cooler air from the north from flowing southward in the summer. Hence the intensity of the Somalian-Pakistani heat trough increases and intensifies the monsoon (Figure 4).

In the summer months (June-September) the UAE is very dry due to the combined effects of upper-level subsidence and limited sources of upper-level moisture. However, isolated convective cells can come through the region and produce precipitation over the mountains. This convective rainfall in the summer is widely known to local meteorologists but in the past has not been captured in any station data.

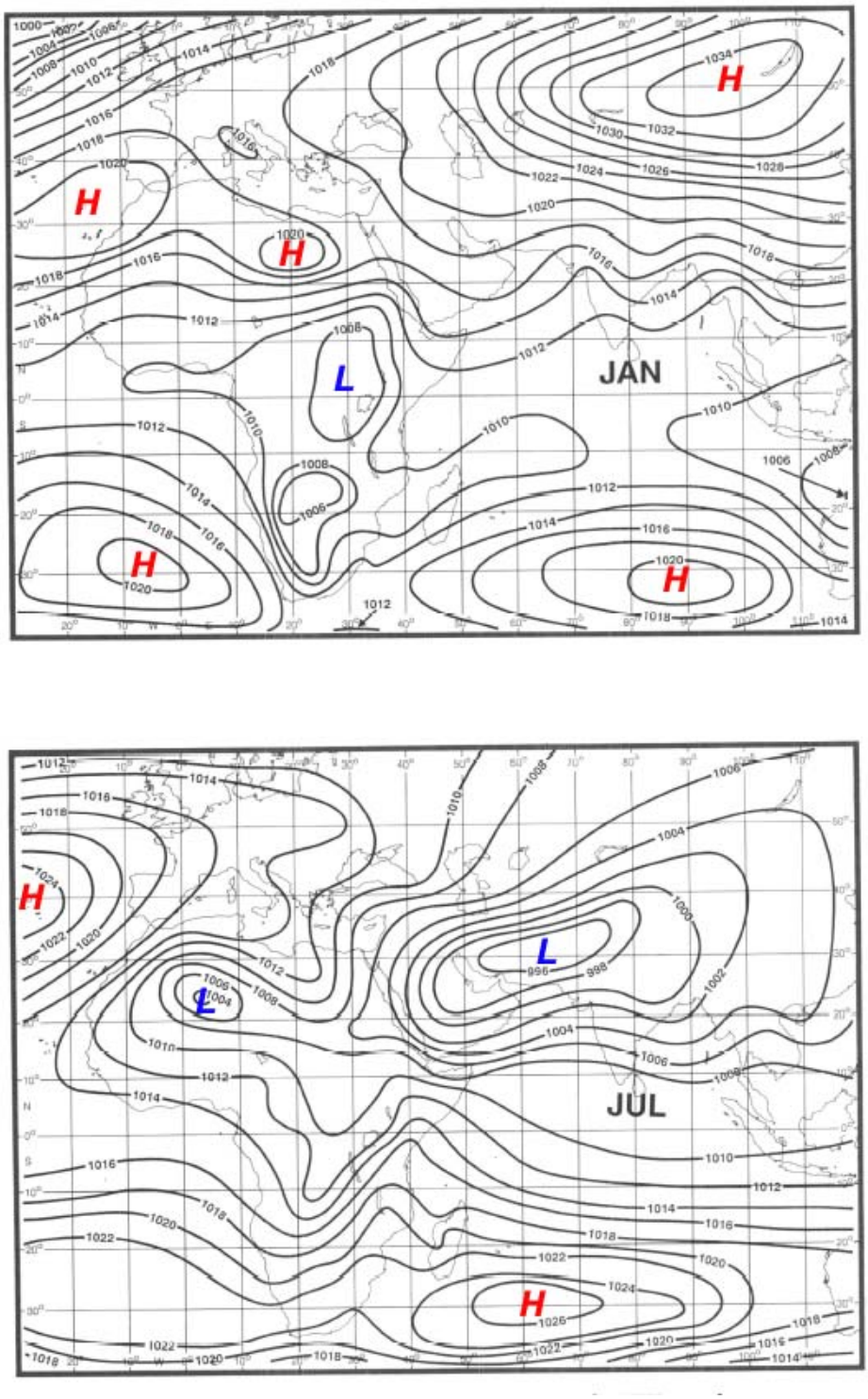


Figure 4. Climatological sea level pressure (in mb) showing the winter (January) and summer (July) monsoons. Figure is adapted from Naval Oceanography Command climatology [Brower et al., 1992].

In the fall transitional period (Oct-Nov) there is again a slow flow reversal from Northwest to Southeast flows. This typically occurs over a period of 30-45 days. The annual cycle then repeats itself.

*4.3.2 The Anticipated Meteorology of the Arabian Gulf During UAE*[2]

The UAE has a rich historical meteorological data set from which we have been able to develop a good understanding of the meteorological features we expect during the mission. Included in Appendix K are climatological summaries for the region as well as plots of station data for July-October, 2003. A summary of the regional meteorology during the mission is discussed here.

During the August and September timeframe of the mission, we will experience the end of the summer monsoon and the beginning of the fall transition period. High temperatures (>40°C), high humilities (>70%) and afternoon sea breezes (>6 m $s^{-1}$) will be typical along the coast for the study period. Arabian Gulf SSTs will reach their maximum of the year around the end of August. Consequently, September will likely be extremely humid and potentially we may see fog formation.

Winds will be most strongly influenced by the Northwesterly monsoon coupled with a strong sea breeze circulation. During the day, the monsoon and sea breeze reinforce one another bringing ~6 m $s^{-1}$ northwesterly onshore flow. Evenings can bring modest Southeasterly offshore flows on the order of 1-2 m $s^{-1}$. Despite the sea breeze circulation at the surface, winds aloft will be dominated by easterly trade winds south of UAE, and westerlies to the north. These flow reversal tend to occur at the 700 mb level.

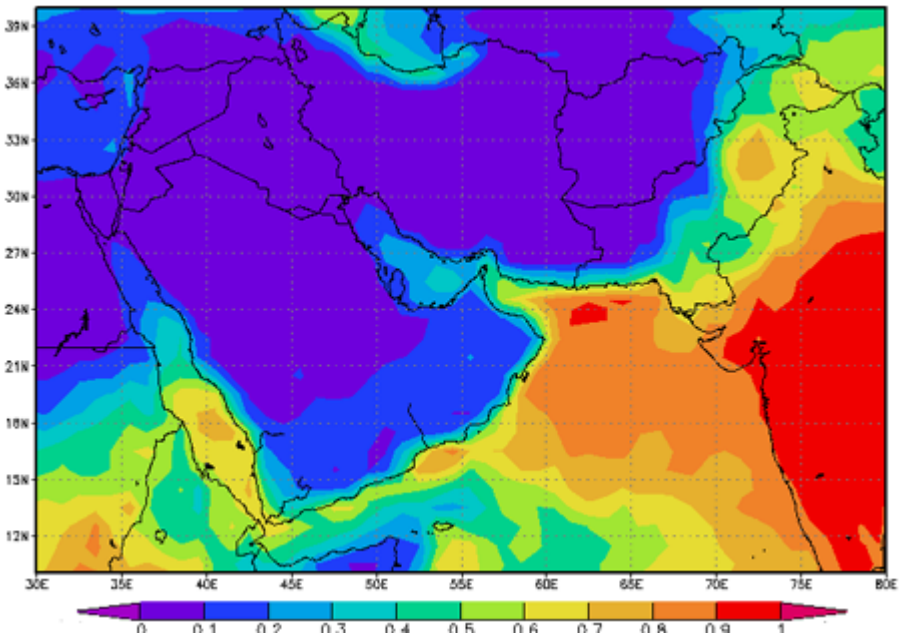


Figure 5. MODIS Level-3 mean daytime cloud fraction using the IR method. Image obtained from MODIS MOVAS website.
http://lake.nascom.nasa.gov/www/online_analysis/movas/monthly/index.shtml

coverage from cirrus. Average cloud top pressure is in the 800-850 mb range. Any flights over the Gulf of Oman will likely encounter low marine stratus.

There have been studies of the marine boundary layer (MBL) of the Arabian Gulf, notably the 1996 SHARAM experiment that utilized the UK met Office C-130 research Aircraft. *Brooks and Rogers* [2000] and *Atkinson et al.,* [2001] give the most extensive descriptions of this experiment and findings. These focused on the formation of the internal boundary layer (IBL) over the Arabian Gulf during the Northwesterly summer monsoon. Because of the enclosed nature of the Arabian Gulf, the boundary layer structure over land and over the ocean is heavily influenced by the formation of Thermal Internal Boundary Layers (TIBL). Typically, warm dry air from the land flows out over the cooler water resulting in the formation of a stable layer in the lowest 100-300 meters The warm water induces a positive latent heat flux while the warmer air results in a negative sensible heat flux. The relative humidity in this layer can be very high, reaching 90%.

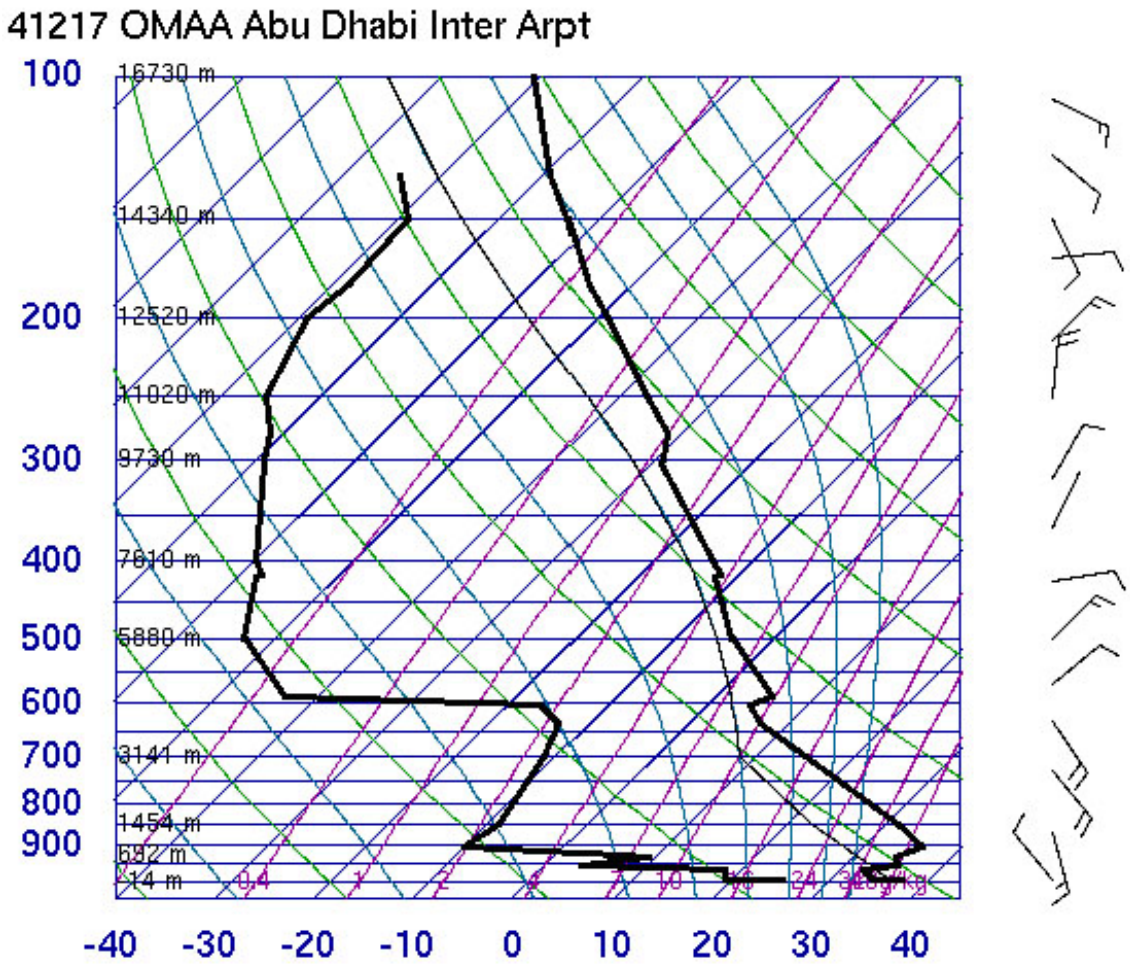


Figure 6. Abu Dhabi sounding valid 12 UTC (16 LST) 11 June 2004.

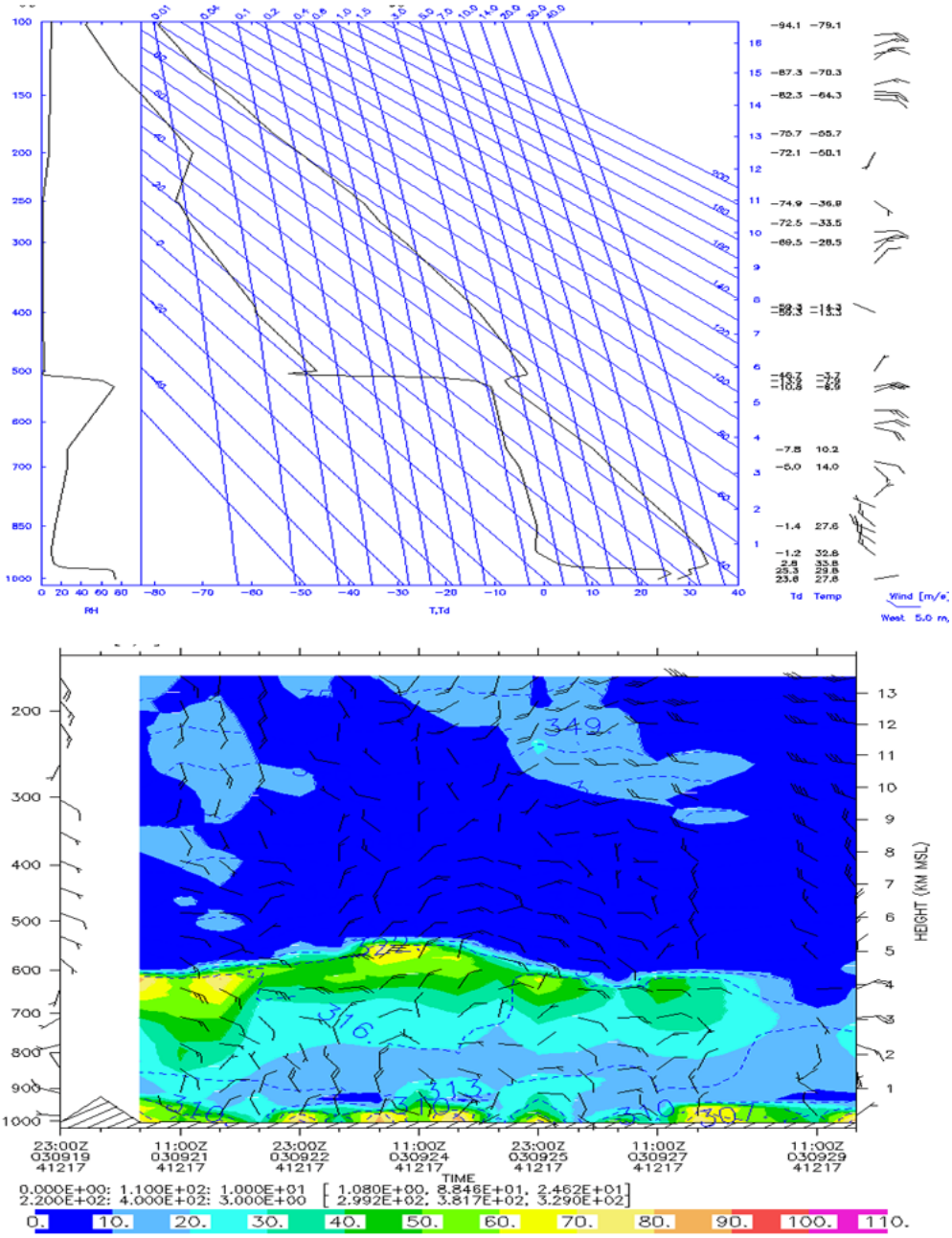


Figure 7. Example soundings from the Abu Dhabi Airport. Upper, sounding from Sept. 15, 2003 showing strong subsidence inversions and reversal of flow at 700 mb level. Lower, time-height cross-section showing potential temperature, (dotted line), humidity (color) and wind for the last week of September 2003.

The Abu Dhabi sounding at 11 UTC (16 LT) on 11 June 2004 is shown in Figure 6 for onshore flow. The sounding is representative of the conditions over the coastal ocean. There is a strong stably stratified layer near the surface to a height of 100 m. This is due to the advection of warmer air over relatively cooler ocean surface. A series of subsidence inversions will generally form above the IBL and MBL. Example soundings are presented in Figure 7. Here a "typical" sounding is presented along with a 1 week time-height cross section of potential temperature humidity and winds.

The soundings of Figure 7 also show the main upper level features we expect to experience during the mission. The upper level subsidence (or "trade") inversion is the most pronounced feature and dominates the sounding. Above this inversion is extremely dry free tropospheric air descending from the Hadley Cell. This inversion is typically several kilometers deep and moves between the 600 and 500 mb level. Near the surface is the shallow and moist IBL/MBL discussed above. In between these two inversions are intermediate well mixed layers. These are residual deep planetary and convective boundary layers from the surrounding deserts. Between these layers we often find a shift in the lower level Northwesterly summer monsoon Shamals and upper level trade winds, usually around the 700 mb level. This shift in wind direction is often accompanied by a slight shift in water vapor mixing ratio. Climatologically, the transition in upper level winds between the northern latitude westerlies and the southern easterly trades occurs in the vicinity of the UAE. Hence, by flying south was can experience Indian sub-continent air and by flying North we can experience layers from Africa. During the two-month study period we should expect the upper level flow to reverse several times. An example of such a reversal is presented in the lower box of Figure 7.

Critical to our mission is the understanding of the sea-breeze circulation that forms along the UAE coast. Weak synoptic forcing over the Arabian Gulf region allows for the formation of sea and land breeze circulations during the summer months on both the coasts of the Arabian Gulf. Hourly surface observations from stations on the coasts of the UAE and Iran have indicated the presence of the sea and land breeze circulations. Abu Dhabi (24° 28' 34'' N, 54° 19' 44'' E) is located on the southwest-northeast aligned coastline of the UAE. During the 27-30 July 1995 time period, both the sea breeze and the land breeze are evident in the wind direction, wind speed, temperature, and dew point temperature data. During the daytime hours, wind directions range between northwesterly and northeasterly, indicating onshore flow (Figure 8). During the night, winds range from east-southeast to southwest creating the offshore land breeze. The sea breeze reinforces the northwesterly flow over the region due to the monsoon circulation induced by the heat low, causing wind speeds of 10-18 mph or 4-8 m $s^{-1}$ (Figure 9). The land breeze opposes the prevailing flow and is much weaker with a magnitude of 2-8 mph or 1-4m $s^{-1}$. The sea breeze causes a decrease of about 15°F (8°C) in the air temperature shortly after it begins (not shown). In addition, it also causes an increase of about 10°F (5°C) in the dew point temperature due to the advection of moist air from the Gulf (not shown).

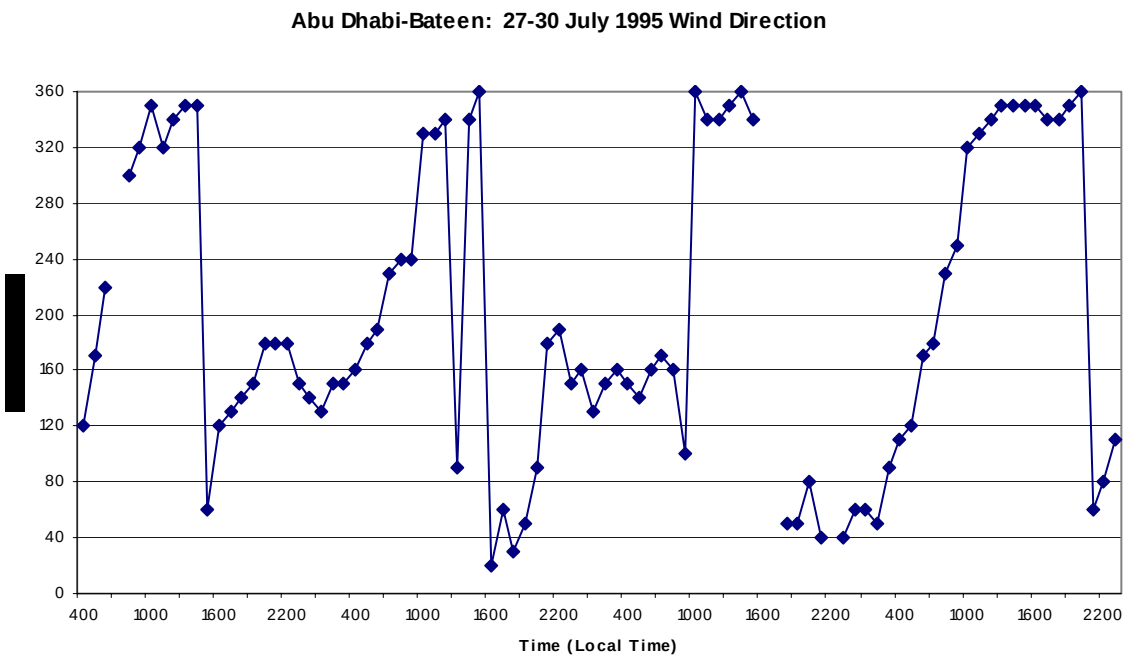


Figure 8. Wind directions at Abu Dhabi-Bateen for 27-30 July 1995. Daytime northerly flow indicates the sea breeze, while nighttime southerly flow indicates the land breeze.

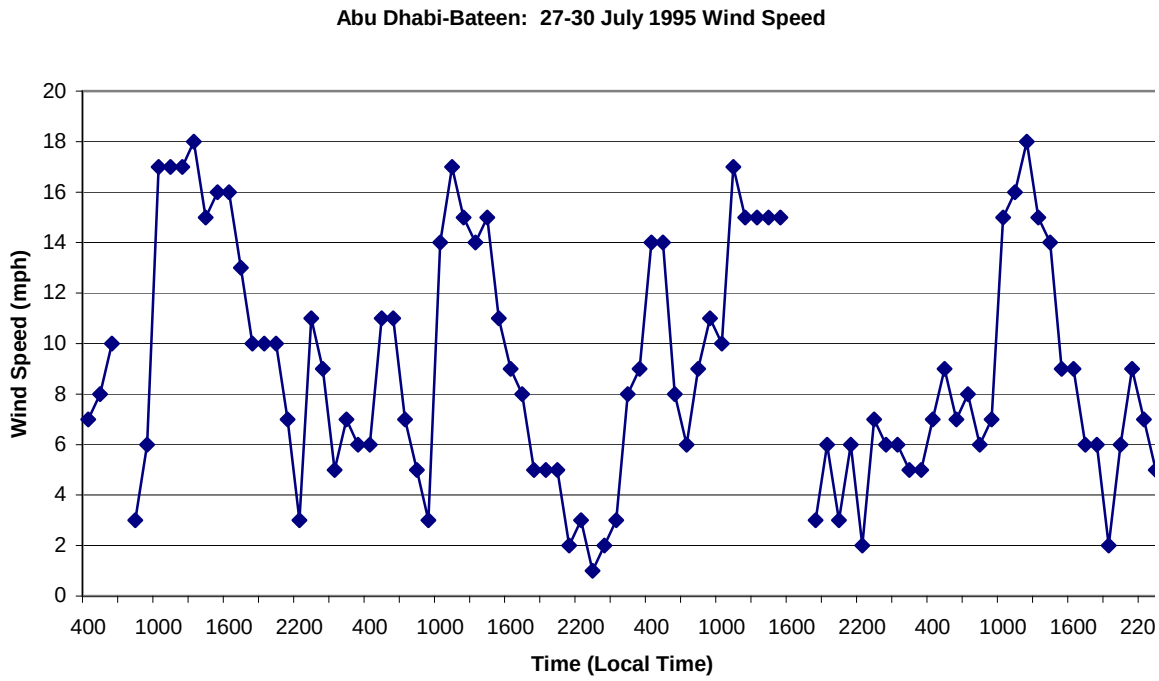


Figure 9. Wind speeds at Abu Dhabi-Bateen for 27-30 July 1995. Higher wind speeds occur during the sea breeze when the sea breeze and the prevailing winds are in the same direction.

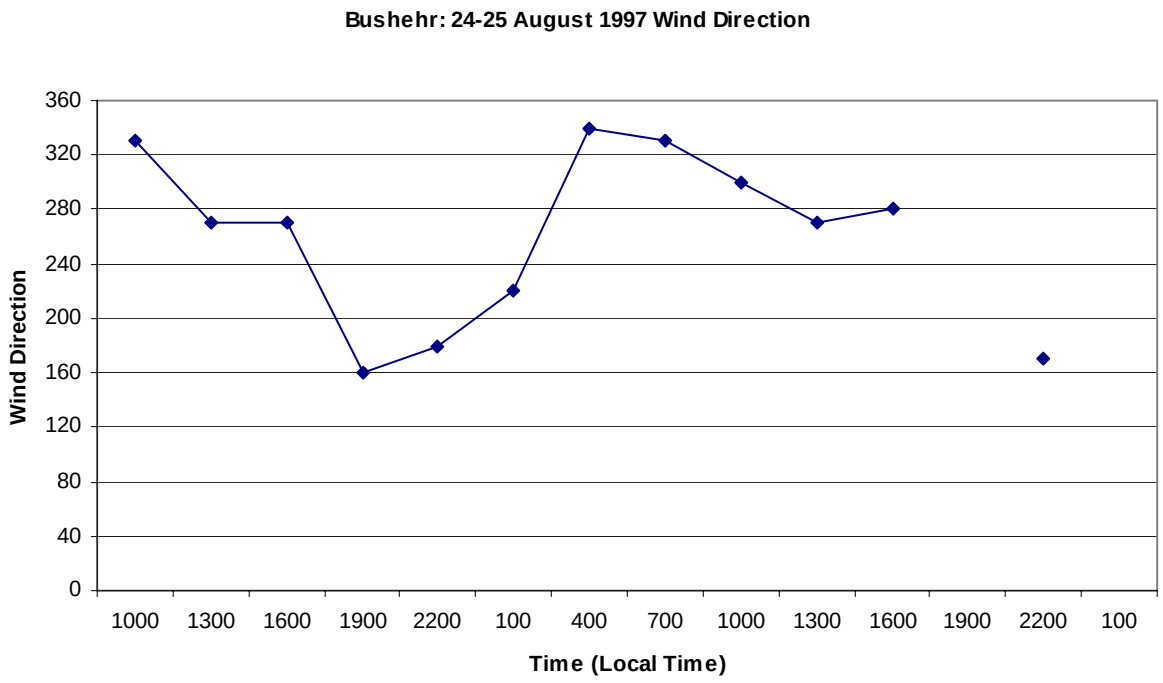


Figure 10. Wind direction variation at Bushehr, Iran for 24-25 August 1997. Southerly flow is indicative of the sea breeze, while northerly flow is indicative of the land breeze.

50° 50' 60'' E). The coastline at Bushehr is oriented northwest to southeast. During the daytime, wind directions are onshore and range from westerly to southerly (Figure 10). At night the winds exhibit a more north-northwesterly offshore flow. Temperatures decrease 4°F (2°C) after the onset of the sea breeze (not shown). Dew point temperatures increase by 8°F or 4°C (not shown). The orientation of the coastline causes the sea breeze and the land breeze to be at right angles to the prevailing northwesterly surface winds.

Due to the short distances across the Arabian Gulf in some locations, interactions between opposite the sea breezes at the opposite coasts is possible.
Interaction between land breezes will be less common because of their smaller horizontal extent except in regions where distance between the opposite coasts is small. In such cases, there could be strong convection because of the merger of two convergent flows.

The onshore winds cause a thermal internal boundary layer (TIBL) to form over the land. The TIBL will continue to grow until it reaches the return flow of the sea breeze, at which point it will mix to the height of the boundary layer over land. The return flow from the sea breeze will cause a stable layer over the Gulf. During nights, PBL over land will be stable with the cooling of the land surface. Horizontal gradient between the land and the ocean during nights causes land breezes to form. The thermal structure over the ocean will be convective due to cooler air flowing over relatively Warmer Ocean. When the synoptic flow is weak, land breezes occur on both sides of the

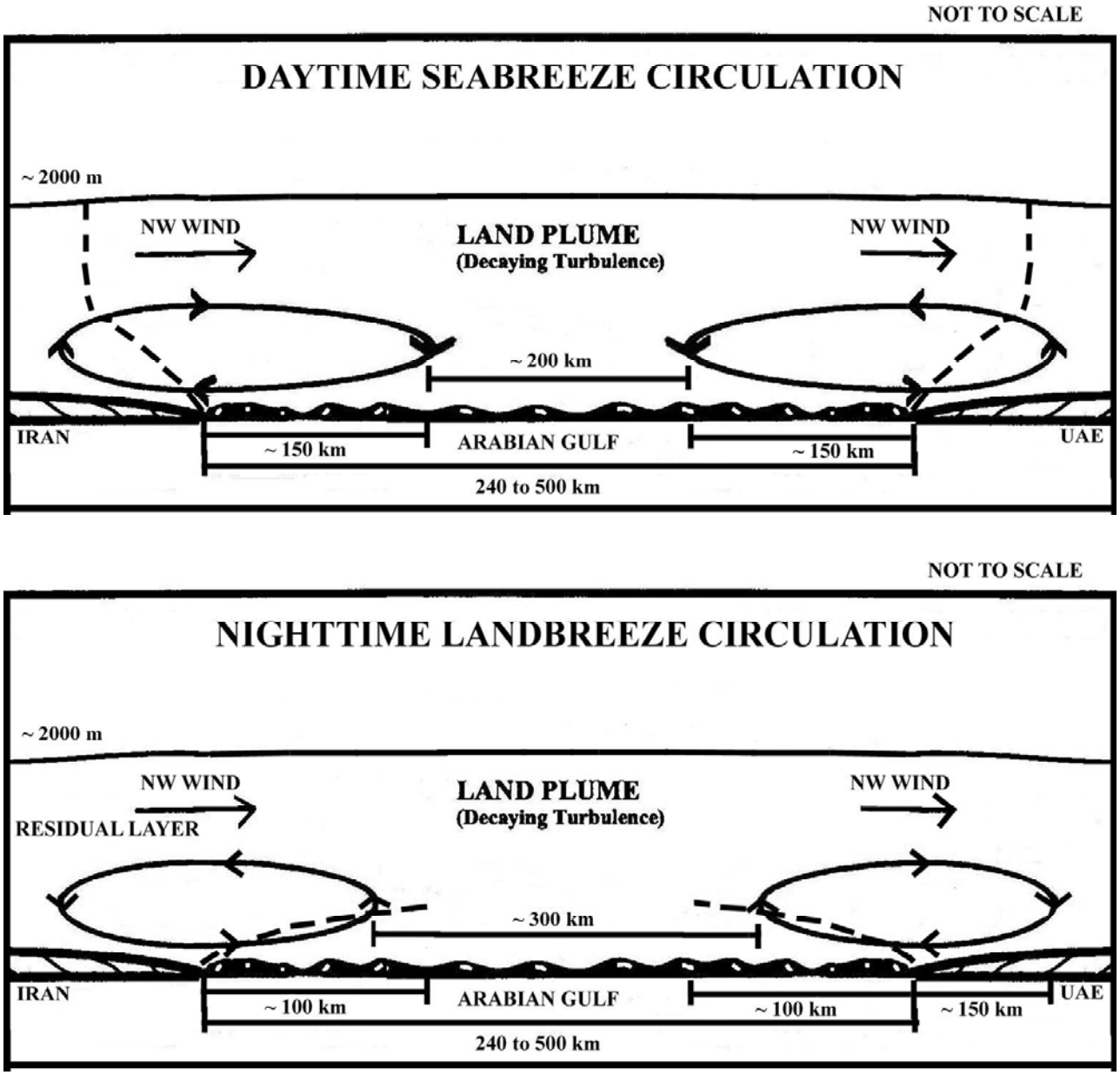


Figure 11. Schematic diagram of sea and land breeze circulations.

Similarly to that found over the Arabian Sea during INDOEX [*Raman et al.,* 2002, *Simpson and Raman*, 2004], we expect to find a land plume form over the Arabian Gulf off both the Kuwait/Iraq and UAE coasts due to the land and sea breezes. The land plume extended for hundreds of kilometers over the Arabian Sea in a well-mixed layer above the boundary layer (about 800 m) to a height of about 3 km. The land plume over the Arabian Gulf transports dust from Qatar, Kuwait, Iraq, or Iran, depending on the wind direction, to the UAE. An elevated jet has also been found within the land plume over the Arabian Sea at the top of the marine boundary layer. This should also be evident in the lower tropospheric northwesterly flow over the Arabian Gulf. The concentration of

dust in land plumes formed during the night is expected to be slightly less because the boundary layer over land becomes stable and the residual layer is cut off from the surface. A depiction showing this mechanism is shown in Figure 11.

### *4.4 Aerosol Characteristics*

Despite the large numbers of papers of aerosol properties in the Arabian Sea (most in relation to the INDOEX program), the properties of aerosol particles in the Arabian Gulf region were until very recently mostly unstudied. The one exception is the international field measurements surrounding the 1991 Gulf war/Kuwaiti oil fires incident. These circumstances are certainly an anomaly and are problematic to apply to more typical conditions. Climatological visibility data indicates high aerosol loadings in the region, especially in the summer months where visibility drops below 10 km more than 30% of the time. However, there are a few studies that can be used to understand some fundamental properties.

The first widely cited paper on Arabian Gulf aerosol properties was Ackerman and Cox [1982], who studied summertime dust properties and radiative effects during the Summer Monsoon Experiment (SMONEX). Aerosol size and vertical distribution were measured with a FSSP and compared to solar radiometers. Mean flow patters during offshore flow conditions were also measured. During the mission they found highly variable atmospheric dust loadings. Dust was frequently found to 6 km with a fairly consistent decrease in loading with altitude. They also detected the influence of the oceanic stable layer (in the lowest 500 meters) on aerosol concentration with dust concentrations over the ocean were an order of magnitude less than values over the desert. Radiative, they found that the dust did not appreciably perturb infrared forcing, although in the solar spectrum the atmospheric heating rate was doubled.

In the past several years there has been a substantial advances in the study of aerosol particles in the Arabian Gulf Region. Most significant is the paper by Smirnov et al., [2002] based on AERONET data in Bahrain. A synopsis of this manuscript is presented in Appendix H, but we will briefly summarize major points here. Based on the work of Smirnov and the available data from the Solar Village (Saudi Arabia), Al Dhafra and the new Abu Dhabi sites, we should expect relatively high aerosol loading in both the fine and coarse mode. The only AERONET site to capture an entire seasonal cycle in this region is Bahrain, operating from 1998 to early 2000.

In Figure 10 we plot daily average AOT and 440-870 nm Angstrom exponent for Bahrain. The seasonal cycle is quite clear. During the winter monsoon, the atmosphere is relatively clear and optical depth is dominated by fine mode particles (High angstrom exponent). Optical depths reach a minimum of 0.1 to 0.2 in December (the height of the winter monsoon). This is a result of the advection of relatively clean air from the southeast. Even so, an occasional dust event can move though region. During the transition period, wind intensity picks up and the region can experience large dust events from the North Westerly Shamals as well as dust from Afghanistan. Optical depths peak

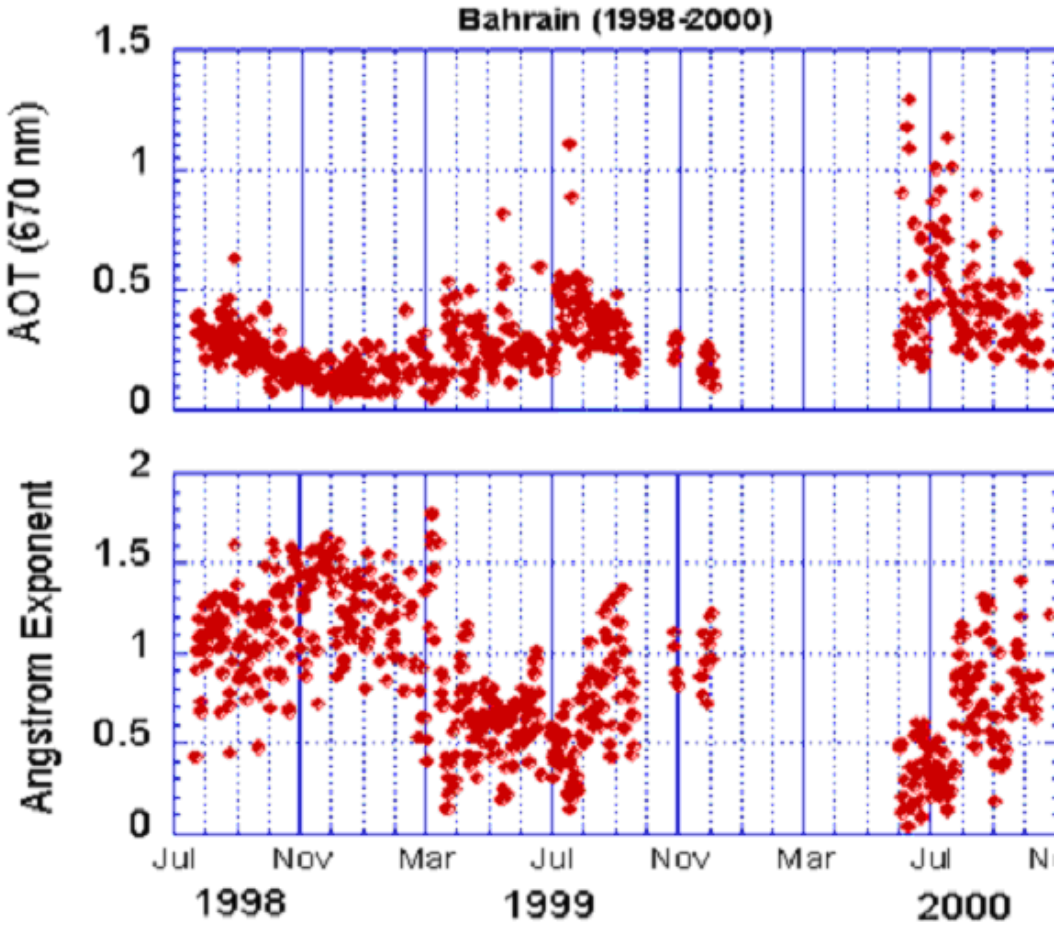


Figure 12. Daily average Aerosol Optical Thickness (AOT-Upper) and Angstrom Exponent (lower) for the Bahrain AERONET site.

in mid summer (July) with average values on the order of 0.4 and significant dust events reaching 1.5. While the bulk of this increase in AOT is due to dust, there is also a significant increase in fine mode particles as well.

MODIS data suggests that the aerosol properties should be relatively constant over the region. Figure 13 presents mean August and September optical depths for the Arabian Gulf/Arabian Sea region for the years 2001, 2002 and 2003. Mean optical depths are on the order of 0.3 and appear to be static over most of the Arabian Gulf region. This value is close to those from the Bahrain AERONET site. Along the southern Arabian Gulf coast optical depths appear to increase by 20%. This could be a result of ocean color artifact. However, it is also possible that this is due to the formation

of an offshore land plume. In appendix I are plots of diurnal visibility. It is clear that the high humidity of the morning hours results in an extremely strong haze formation. When transported out to sea in the land plume, these particles will remain hydrated and create a hazy coastal zone.

MODIS data also suggests that optical depths tend to be higher in the Gulf of Oman and Arabian Sea. This is likely due to a number of mechanisms. First, dust is frequently advected from Afghanistan into the Gulf of Oman. Due to the proximity to the source region these events can be quite intense with optical depths well over one. The Gulf of Oman is also a receptor for pollution advected off of the Indian subcontinent. Smoke from rice stubble combined with home bio-fuel produces a thick smog layer over Pakistan and northern India. The land plume that forms off of India regularly bring such particles into the region.

It is also noteworthy that Arabian Sea is often covered with stratocumulus clouds. Typically the cloud deck extends over the Oman coastline to Yemen. Seasonal cloud cover reached 80% in some areas. The presence of these clouds likely biases the MODIS data in Figure 13 although we still expect increased AOT over the region. The physics and chemistry of stratus cloud processes in this northern region of the Arabian Sea is almost unstudied. But we would expect modifications to particle size distributions as well as significant secondary particle production (sulfate and organic acids).

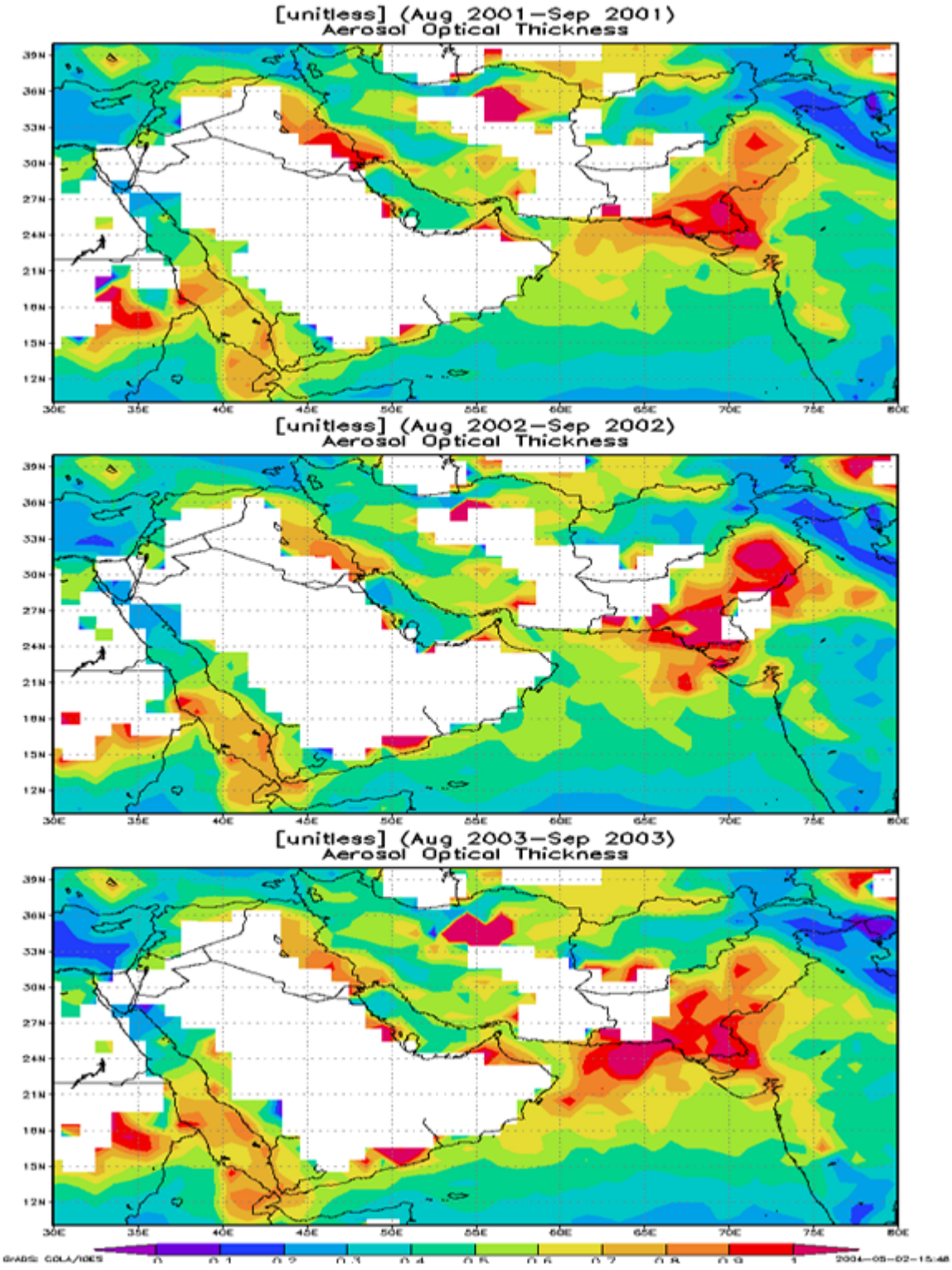


Figure 13. MODIS level 3 climatology for 2001, 2002, and 2003 for the Arabian Gulf region. Image obtained from MODIS MOVAS website. http://lake.nascom.nasa.gov/www/online_analysis/movas/monthly/index.shtml

During the UAE$^2$ mission, we expect all of the climatological aspects of the region described by the Bahrain Sun photometer and MODIS to hold for operations in the UAE. As a hypothesis test we can examine two short duration AERONET time series from sites just outside of Abu Dhabi, UAE. The first site, Al Dhafra, was deployed in 2001. The new Dhabi site was deployed in October 2003, less than 20 km from the Al Dhafra site.

Time series of AOT and Angstrom Exponent for these two sites is presented in Figure 14. Like Bahrain, AOT reached a maximum during the month of July. During the UAE$^2$ experiment, we should expect a slow decrease in total AOT for the region as the summer monsoon transitions into winter. Even so, daily variability in AOT can exceed 50%. We should also expect an increase in the fine/coarse partition, as dust production will be reduced and a pollution-based haze will settle into the region. At the end of the study, humidity may drop thus reversing her fine/coarse partition.

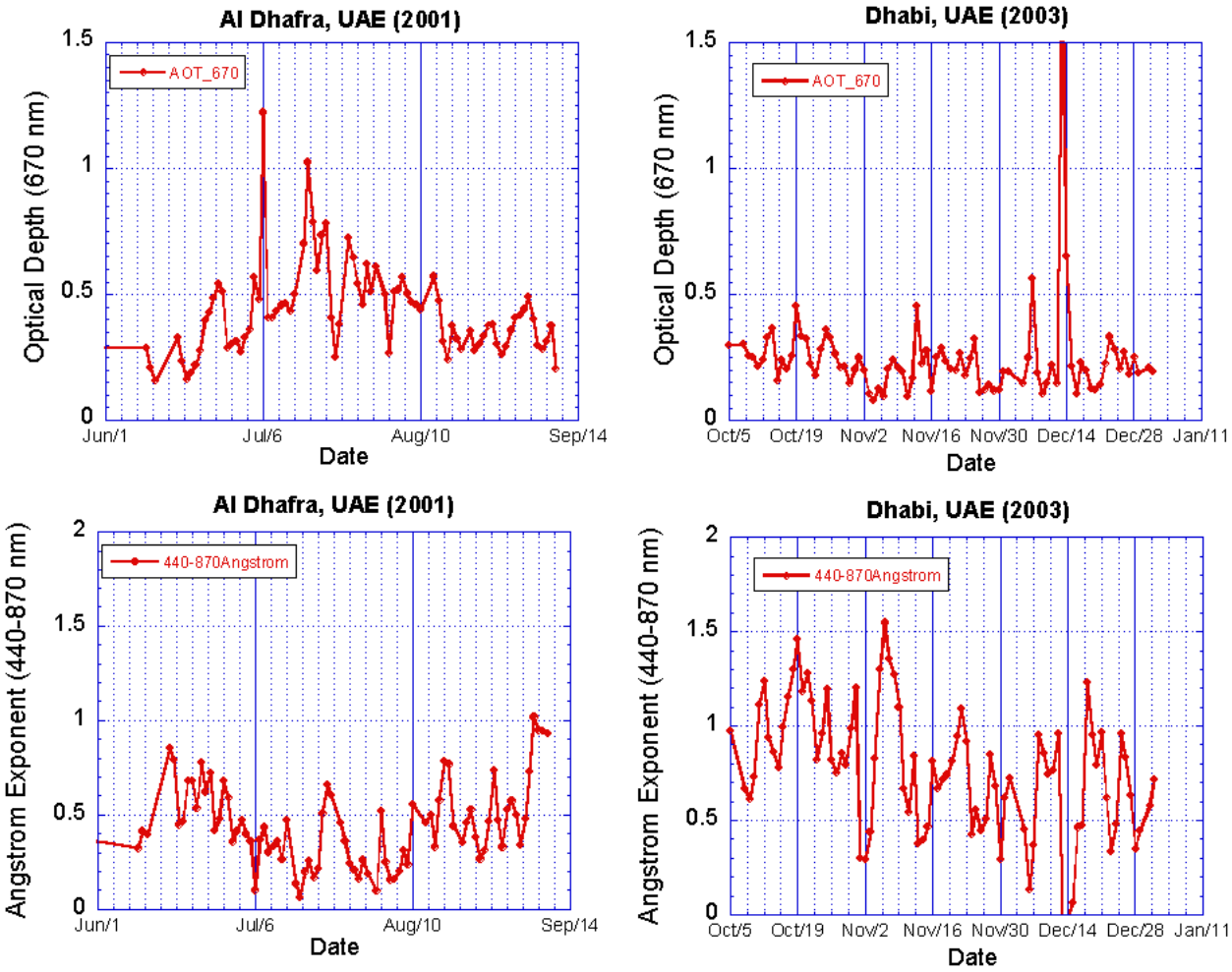


Figure 14. AERONET time series of Aerosol Optical Thickness and Angstrom Exponent for sites near Abu Dhabi

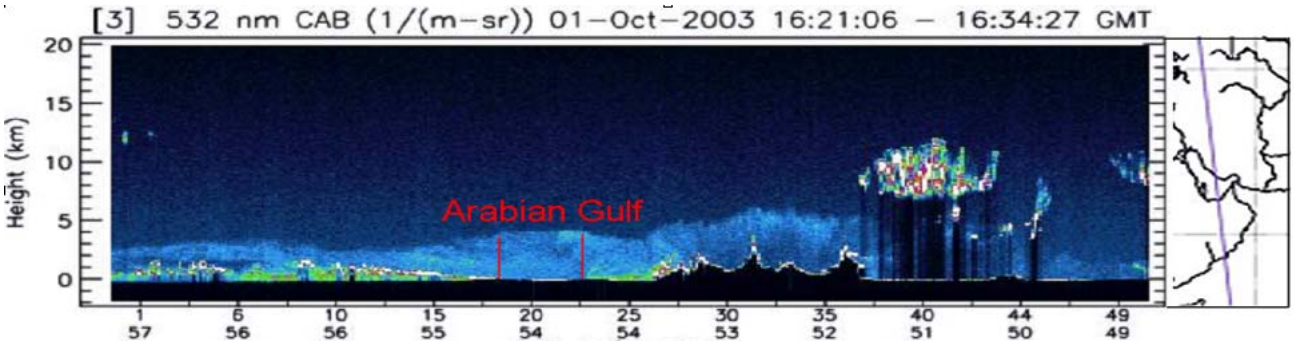


Figure 15. GLAS 532 nm overpass over the Arabian Gulf region for Oct 1 2003.

Particle vertical distributions should be fairly similar to the profiles listed in *Ackerman and Cox* [1982], although more layering should be present than in their averaged values. Figure 15 shows a recent overpass of the GLAS satellite. Dust and pollution is clearly observable to 5 km. Over the Arabian Gulf region, GLAS can also detect the evolution of the internal boundary layer.

## 5.0 Mission Assets and Measurements

Given the expected environmental conditions in the Arabian Gulf region UAE$^2$ mission objectives can only be achieved by a combined surface and airborne effort. In this section we summarize the UAE$^2$'s mission assets and their capability. In section 6 we will then relate these assets into a coherent plan.

### *5.1 AERONET Mesonet*

Paramount to UAE$^2$'s objectives is the calibration and validation of a number of satellite and aerosol model systems. Consequently, the cornerstone of the UAE$^2$ mission is a network of at least 12 Sun photometers. The AEROsol RObotic Network (AERONET) is an internationally collaborative network of sun and sky scanning spectral radiometers designed to retrieve aerosol optical properties from direct sun and diffuse sky radiance measurements. The program developed in 1993 from a need to remove atmospheric effects in RS satellite data but evolved to meet a need for satellite validation of aerosol extinction (aerosol optical depth) and more recently has developed into a globally distributed network for accurately characterizing basic properties of size (particle size distribution) and absorption, (single scattering albedo) for natural and anthropogenic marine, urban, biomass burning and desert aerosols. Since the inception of the program, the supported AERONET sites have grown from 3 to approximately 220 systems distributed on all continents. A standard AERONET system is an eight channel filtered radiometer that is pointed under robot control at the sun and scans the sky nominally at 15 minute intervals in predefined protocols. Within hours of collection, the data are transmitted via geostationary satellites to receive stations, FTP'd to the AERONET server, processed, analyzed, stored and posted to the AERONET website (http://aeronet.gsfc.nasa.gov) for use by the scientific community, policy makers, educators and the general public.

For the UAE$^2$ mission, 8 standard AERONET Sun photometers will be deployed in the Arabian Gulf region. The AERONET Sun photometers measured spectral aerosol optical thickness (AOT, $\tau_a$) at 6 wavelengths (340, 380, 440, 670, 840 and 1020 nm) plus column-integrated water vapor from the 960 nm channel. An additional 1.6 μm channel will be added on a limited number of other Sun photometers. Through the *Dubovik and King* [2000] algorithm to assess column integrated size distribution and index of refraction. From these algorithms other optical parameters such as single scattering albedo and asymmetry parameter are derived. The algorithm of *O'Neill et al.* [2001] will also be used to separate out fine versus coarse mode optical depth.

Figure 14 presents a plot of possible AERONET sites. Currently 1.6 μm Sun photometers are operating at Solar Village, Saudi Arabia and Abu Dhabi United Arab Emirates. At least 5 others will be deployed on the UAE mainland and 3 on island sites. Possible candidate countries outside of the include Bahrain and Qatar.

Figure 14. P AERONET Sun photometers during the UAE$^2$ field campaign. All sites are operational at the time of this report exepct for Abu Al Bukhoosh

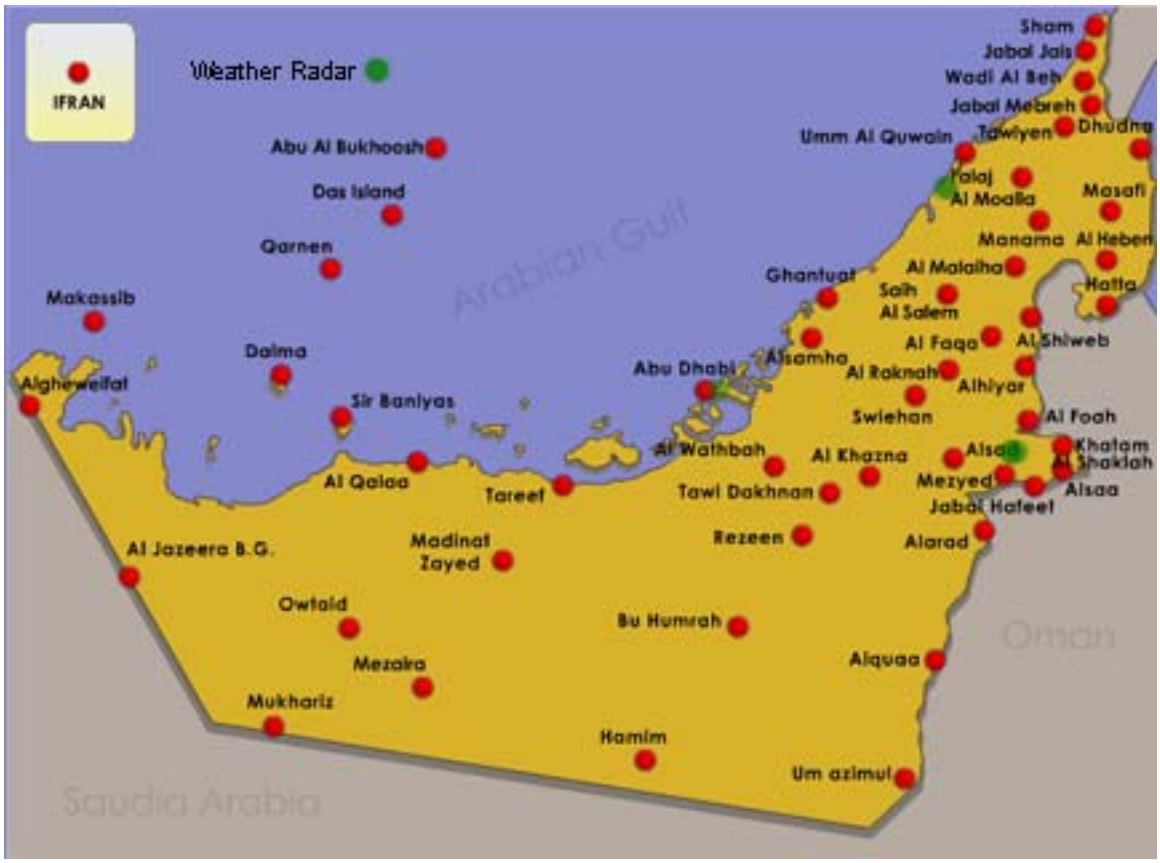


Figure 15. Map of DWRS surface meteorological stations. Map taken from DWRS website: http://www.almiyah.gov.ae/st/dwrs.asp

*5.2 Meteorology Mesonet*

While AERONET Sun photometers provide regional optical depths and aerosol properties, the regional mesonet of surface meteorological stations provide a very high-resolution data of the region's atmospheric patterns. The UAE Dept. of Water Resource Studies (DWRS) has deployed the densest network of surface stations in the Middle East region (Figure 15). Each of these almost 50 sites (including 6 island sites) is equipped with temperature, humidity, pressure and wind sensors. Eighty percent also have solar flux radiometers, soil temperature, and soil moisture at 10, 20, 30 and 50 cm depths. In addition, DWRS in association with NCAR has deployed five Doppler weather radars covering the entire UAE region.

Abu Dhabi airport (lat=24. 26 N; lon=054.39 E) is also a primary site for regular radiosonde releases every 12 hours. These are typically at 11:00 and 23:00 Z, or 14:00

and 2:00 LST. Vertical distributions of temperature, pressure, humidity and winds are provided. Other regional radiosonde sites include Bandar Abbas, Iran at the Strait of Hormuz (lat=27.13° N lon=56.22° E), Muscat in Oman (lat=23.35° N; lon=58.17° E), and King Fahd airport in Saudi Arabia (lat=26.27° N; lon=49.49° E).

5.3 Surface Super Stations

While the AERONET and meteorology mesonets provide information on a large regional picture of the atmospheric state, two aerosol super-stations will be deployed in the UAE to study the microphysical and radiative properties of aerosol particles in detail. Full descriptions of the super-sites are given in the appendices. However, a brief description is presented here. The primary aerosol super-site for UAE$^2$ is the NRL Mobile Atmospheric Aerosol and Radiation Characterization Observatory (MAARCO). MAARCO is a standard 20'x8' climate controlled CONEX shipping container that has been modified to function as an easily-shipped laboratory for sitting overseas, in remote areas, or on sea-going vessels. Its purpose it to perform basic research on atmospheric aerosols, gasses, and radiation (visible and IR light) in difficult to deploy regions. MAARCO will assist in validating aerosol and weather models as a ground station and is often used in conjunction with research aircraft. All MAARCO requires is input power (110, 220, or 240 3-phase), though it can utilize generators. MAARCO also has the capability to utilize telecommunications links for real time remote displays when available.

The MARCO container is 'mobile' in the sense that it can be easily moved it to new sites to perform research. One of the primary obstacles in performing research overseas is the difficulty in finding adequate facilities at good site locations. Most aerosol instruments prefer, if not require, climate controlled environments for stable, consistent operation. These conditions are not readily available in remote or foreign sites. Radiation instruments are for the most part less sensitive to changes in the environment, but are also much more valuable when run in conjunction with other instruments to fully characterize the local environment.

MAARCO is an integrated laboratory for atmospheric characterization. It has the capability to measure most atmospheric parameters at the surface (temperature, humidity, pressure, winds, precipitation, cloud base, cloud fraction through an all sky imager and fluxes through eddy correlation methods) as well as characterize the atmospheric profile through radiosonde system. Aerosol particle vertical distribution is measured through an eye-safe Micropulse Lidar system (MPL) connected to the NASA GSFC MPL net system as well as a high gain ceilometer. Optical depth is measured with an AERONET Sun photometer including a 1.6 μm channel. Aerosol particle mass, chemistry and particle size/shape is measured via filters for total suspended particulate matter (TSP) and behind a 2.5 μm cyclone. Continuous mass monitoring is also performed with a Tapered Element Oscillating Mass Balance (TEOM). Ozone and $SO_2$ are also measured. Particle size distribution can be measured with a PCASP and APS systems for fine and coarse mode particles, respectively as well as particle light scattering though a 3-λ nephelometer. For this mission MAARCO will have 2 nephelometers for measuring light scattering at ambient

and dried humidities. The radiative properties at the surface are measured with a suite of pyranometers, pyrgeometers, and pyrheliometers.

Also deployed for UAE$^2$ will be the NASA Goddard Space Flight Center (GSFC) Surface-sensing Measurements for Atmospheric Radiative Transfer (SMART) research container. SMART is similar to MAARCO in many respects, but focuses on atmospheric radiative balance. SMART includes an AERONET Sun photometer, MPL lidar, several sets of solar and infrared pyranometers, pyrgeometers, and pyrheliometers, and a microwave radiometer (to measure column integrated water vapor). SMART has been sent to six field campaigns on three continents.

For the UAE$^2$ mission several investigators have decided to deploy along side these two super-sites. Particle spectral absorption from the UV to near IR will be measured off of polycarbonate filters. IR sky radiance will be measured with the CLIMAT instrument will be deployed with SMART. There is also the possibility that a 7 wavelength Aethalometer will also be deployed with MAARCO.

*5.4 Aerocommander Research Aircraft*

Tying together field measurements during the UAE$^2$ mission is the South African 690A Aerocommander research aircraft. This aircraft is owned by the South African weather service and is under contract to the University of the Witwatersrand and the UAE DWRS to perform cloud seeding research in the southern Arabian Gulf region during the UAE$^2$ study period. For this mission the UAE$^2$ science team will have access to the aircraft on cloud free days. The UAE DWRS and NRL 6.1 platform support will provide 30 and 50 flight hours respectively for the mission. The aircraft has an endurance of 5.5 hours and can operate at a cruise speed ranging from 60 to 120 m $s^{-1}$.

The Aerocommander comes equipped with the ability to measure all atmospheric state parameters and navigational/attitude variables. These include temperature, pressure, humidity, dew point temperature, liquid water content, position, altitude, pitch, role and azimuth. From these variables winds can be derived. The Aerocommander can carry six PMS can probes, two on the nose and 4 on wing pylons. However, for this mission two PMS cans will be taken off periodically so as to not interfere with the car radiometer (see below). Typical PMS probes carried include a Forward Scattering Spectrometer Probe (FSSP 100), a Optical Array Probe (OAP2DP or OAP2D2P), a Two Dimensional Cloud Probe (2DC or 2D2C) probe and a Passive Cavity Aerosol Spectrometer Probe (PCASP 100X). For the mission an additional NRL PCASP and FSSP modified by DMT will be made available for selected flights.

For the UAE$^2$ mission, a number of additional instruments will be incorporated onto the Aerocommander. Key will be the NASA GSFC Cloud Absorption Radiometer (CAR), an airborne multi-wavelength scanning radiometer [King et al., 1986; see appendix C]. The CAR scan mirror rotates 360° in a plane perpendicular to the direction of flight and the data are collected through a 190° aperture that allows observations of the earth-atmosphere scene around the starboard horizon from local zenith to nadir.

The CAR instrument has the potential to play a strong role in UAE$^2$. The strength of the instrument is its unique ability to measure almost simultaneously, both downwelling and upwelling radiance at 14 narrow spectral bands located in the atmospheric window regions of the UV, Visible, and near-infrared. When combined with simultaneous airborne measurements of sun/sky radiance, CAR sky radiance measurements provide information on aerosol (size distribution, single scattering albedo, refractive index) both above and below the aircraft, and the surface bidirectional distribution function (BRDF) for any type of surface (Appendix C, Figure C2).

The second key instrument to be deployed on the Aerocommander is the 532 nm University of Hawaii lidar system. Unlike most other lidars, the University of Hawaii system can change its scan angle in flight (upwards, downwards and forward). This allows useful aerosol vertical profile data to be collected at all times during a flight.

To round out the Aerocommander instrumentation package, NRL will deploy a suite of aerosol instrumentation. For the mission, the University of Witwatersrand will install an aerosol inlet system. Onto this system we will plumb a 3-$\lambda$ nephelometer, an aerodynamic particle sizer (APS 3321), and a filter sample manifold. Filters for chemical analysis, organics, and spectral absorption will be collected. Also installed will be an infrared thermometer for measuring sea surface and land skin temperature.

*5.5 Remote Sensing Support*

The goals of UAE$^2$ will be achieved with the help of the comprehensive data sets from existing satellite sensors. Perhaps the most important of these is the Terra and Aqua platforms, which were launched by NASA in December 1999 and May 2002, respectively. Terra carries five environmental sensors, including the Moderate-Resolution Imaging Spectroradiometer (MODIS), Multiangle Imaging SpectroRadiometer (MISR), Clouds and the Earth's Radiant Energy System (CERES), Measurements of the Pollution in the Troposphere (MOPITT) and Advanced Spaceborne Thermal Emission and Reflection (ASTER). Aqua carries six state-of-the-art instruments in a near-polar low-Earth orbit. The six instruments are the Atmospheric Infrared Sounder (AIRS), the Advanced Microwave Sounding Unit (AMSU-A), the Humidity Sounder for Brazil (HSB), the Advanced Microwave Scanning Radiometer for EOS (AMSR-E), the MODIS, and CERES. Each has unique characteristics and capabilities, and all six serve together to form a powerful package for Earth observations. These satellites will be complemented by other highly successful sensors, including Landsat 7 Enhanced Thematic Mapper Plus (ETM+), National Oceanic and Atmospheric Administration's (NOAA's) Advanced Very High Resolution Radiometer (AVHRR), Sea-viewing Wide Field-of-view Sensor (SeaWiFS) and Tropospheric Ozone Mapping Spectrometer (TOMS) and several experimental NASA sensors, including the Vegetation Canopy LIDAR (VCL) and Earth Observing-1.

The European Organization for the exploration of Meteorological Satellites (METEOSAT), in geostationary orbit, can provide continuous images of the region at the highest temporal resolution. High spatial resolution sensors such as ASTER and ETM+ will detect fine scale land-cover change and use, and facilitate the scaling of point and short transect measurements over much larger areas. Likewise, coarser resolution sensors like MODIS, SeaWiFS, and AVHRR will be used for full regional views and retrospective analysis. Particularly encouraging is the anticipated ability of MODIS to more accurately detect thin cirrus clouds, fire temperature, areal extent and thermal

energy, and detect surface features through the occasionally pervasive smoke layers. The highly variable aerosol-forcing problem will largely be attacked with the accurate aerosol and 3-D cloud products expected from MISR. This sensor may also help resolve surface variability through its bidirectional sampling capabilities. Finally, MOPITT will help resolve large-scale source, sink and transport questions associated with carbon monoxide and methane emissions.

The use of satellite data and its comparison with field-measured data in $UAE^2$ will provide a critical regional-scale validation over bright and dark surfaces. This large range of measurements will combine to make this field experiment a large coordinated validation activity for NASA satellites such as Terra and Aqua.

### *5.6 Modeling Support*

The $UAE^2$ mission will relay heavily on two aerosol models for mission planning purposes as well for detailed analyses after the mission. One is global (the NRL Aerosol Analysis and Prediction System-NAAPS); the other is mesoscale (Coupled Ocean Atmosphere Prediction System-COAMPS™). The Naval Research Laboratory (NRL) in Monterey, CA, has developed these near-operational models for analyzing and forecasting the distribution of tropospheric aerosols.

#### 5.6.1 NAAPS

NAAPS will eventually comprise three components: data gathering and quality control, data assimilation, and transport modeling. Only the third component is available for use in $UAE^2$. The transport model is a multi-specie, three-dimensional, global transport model derived from the hemispheric SO2 and sulfate model of *Christensen* [1997]. Details of the model are given in that reference, and only an overview is presented here, with emphasis on modifications made to the original model.

The NRL version uses global meteorological fields from Navy's Operational Global Analysis and Prediction System [NOGAPS; *Hogan and Rosmond*, 1991*; Hogan and Brody* 1993] analyses and forecasts on a 1 X 1 degree grid, at 6-hour intervals and 18 vertical levels reaching 100 mb. (The original model used northern hemispheric, 12-hourly ECMWF fields on a 2.5 X 2.5 degree grid.) Forecasts are made daily out to 5 days and is posted at the NRL aerosol website (http://www.nrlmry.navy.mil/aerosol/.) The required NOGAPS fields are the topography, sea ice, surface stress, surface heat flux, surface moisture flux, surface temperature, surface wetness, snow cover, stratiform precipitation, convective precipitation, lifting condensation level, cumulus fractional coverage, cumulus cloud height, surface pressure, three components of the wind field, temperature field, and relative humidity. Transport is calculated using a 3-d semi-Lagrangian scheme [*Staniforth and Cote*, 1991] with departure points calculated using the method of *Ritchie* [1987]. Modifications have been made to the interpolation of wind and concentration fields across the poles and the interpolation method was changed from a 3rd order Lagrange to 5th order Lagrange. Horizontal and vertical diffusion are calculated with a finite element scheme. The diffusion coefficients are determined from the input NOGAPS data, based on Monin-Obukhov similarity theory. The horizontal diffusion coefficient is set to a constant. The moisture fields are used in an inverse

precipitation scheme to diagnose vertical profiles of cloud water and precipitation rate consistent with the input precipitation rates. These profiles are used to calculate the wet removal and reaction rates of the various species. The dry deposition velocity is based on the resistance method (*Voldner et al.,* 1986; *Walcek et al.,* 1986' and *Slinn and Slinn*, 1980), where the deposition velocity depends on the turbulence of surface layer and surface type (ocean, grassland, etc.).

NAAPS currently has three aerosol species: Sulfate, smoke and dust. Sulfur dioxide emissions are based on the GEIA inventory, version 1A, for the year 1985 with a seasonal variation and two-level vertical distribution [*Benkovitz,* 1996]. Natural emissions of DMS are immediately converted to 95% sulfur dioxide and 5% sulfate. The gas-phase chemistry is described by a set of reaction equations, which depends on the time of year and latitude.

Smoke emissions in NAAPS are based on geostationary satellite and MODIS fire products generated under the joint Navy, NASA, NOAA, and university Fire Locating and Modeling of Burning Emissions (FLAMBE) project [*Reid et al.,* 2004a,b]. To compute fluxes, half-hourly WF_ABBA and twice daily MODIS fire products are assigned smoke particle flux rates in 9 land cover sub-categories derived from the 1 km GLCC classification (e.g., tropical forest, woody savanna, etc.). These flux rates are a function of estimated fuel load, emission factors, and combustion fractions. For WF_ABBA, fire products are directly assimilated into the NAAPS source function algorithms. For MODIS products, a static diurnal cycle is imposed based on characterizations from North America WF_ABBA analyses. Specifics and references are listed on the FLAMBE web site listed above and in *Reid et al.,* 2004a, b].

NAAPS is most widely known for its dust component, which we expect to use heavily during the UAE$^2$ campaign. Dust emission occurs in the model whenever the friction velocity exceeds a threshold value, snow depth is less than a critical value, and the surface moisture is less than a critical value. The critical surface moisture is set to 0.3. The critical snow depth value is set to 0.4 cm. These choices are based on a qualitative analysis of these NOGAPS fields and synoptic dust observations. The forecasted friction velocities are used for the NAAPS dust forecasts.

The threshold friction velocity is set to infinity except in known dust-emission areas. These areas originally were defined as areas covered by eight of the 94 land-use types used in the USGS Land Cover Characteristics Database. In June 2000, we began using an analysis of TOMS AI data to further refine the source regions in the Sahara, Middle East, Arabia, and Australia. Our method bases the erodibility fraction on the frequency that high TOMS AI values are observed for a 1-degree grid box. Our source regions agree with those of Prospero, et al. who have conducted a thorough study of dust source regions using the TOMS data, terrain data, and other information.

When the threshold friction velocity is exceeded, the vertical dust flux Fa (in gm $cm^{-2}$ $s^{-1}$) is given by (Westphal et al., 1988) as Fa = Cf u*4 where Cf = 2.9 x 1014 and u* is the friction velocity in cm s-1. The flux is injected into the lowest two layers of the

model. As the immediate goal of this modeling effort is to develop a practical operational global aerosol forecast, the model microphysics are simplified in this early implementation and sophisticated flux parameterizations are not used. Furthermore, this model is best suited for long-range transport, because of the coarse resolution. Hence the model treats only those particles likely to be transported long distances. These are considered to be particles less than 5 μm in radius. To represent the mass flux of particles less than 5 μm, Equation 1 is scaled by the percentage of the total vertical mass flux with these sizes.

Based on observational evidence, we have made subjective modifications to the land use database when determining the dust source regions. (1) Low sparse grassland is a source region only in China and Mongolia. This excludes areas of the Steppes, Turkey, New Zealand, and N. America (2) Bare desert and Semi-desert shrubs north of 60N are excluded.

5.6.2 COAMPS

The US Navy's operational Coupled Ocean/Atmospheric Mesoscale Prediction System (COAMPS$^{TM}$) is a nonhydrostatic and compressible dynamics model. It predicts turbulent kinetic energy (TKE) for sub-grid-scale diffusion, uses a force-restore method in the surface energy budget, and contains explicit cloud microphysics [*Hodur* 1997]. Mesoscale data assimilation is performed at 6 to 12-hour incremental update cycles using the meteorological data from the world weather station network. The analyses and forecast fields of the Navy's operational global atmospheric prediction system (NOGAPS) [*Hogan and Rosmond* 1991] are used for updating the lateral boundary conditions every 6 hours during forecasts.

A dust microphysical aerosol model is fully embedded in COAMPS$^{TM}$, i.e. an on-line module of the prediction system, using the exact model's meteorological fields at each time step and at each grid point [Liu et al. 2003]. Therefore, the dust module has the same grid structure and feature as the dynamics model. It solves mass conservation equation in bins with source production, transport and sedimentation, wet and dry deposition. About 10 particle bins ranging from 0.05 to 35 μm in diameter is specified. The particle size increases in geometrical volume at a constant ratio following an algorithm described in *Toon et al.* [1988]. Dust is modeled as a generalized species with density of 2650 kg m$^{-3}$, and assuming an initial bimodal lognormal size distribution. The mass median radius and geometric standard deviation in the size distribution are predicted by the sandblasting model of *Alfraro et al*. [1997] at each time step, based on the particle's saltating kinetic energy in a dynamical environment using the wind speed and particle size.

The dust emission takes the formula of *Nickling and Gillies* [1993] that describes the vertical dust flux as proportional to friction velocity raised to the forth power (or the square of surface wind stress). Dust source areas are identified based on the 1-km-resolution land cover database produced by the U. S. Geological Survey (USGS) and a new 1-km dust dataset specifically developed for SW Asia by *Walker* [2003]. As a further refinement, the land survey by *Clements et al.* [1957] is used to estimate that an

average of 13% of each 1-km pixel in the USGS database is erodible. The threshold of friction velocity is chosen having a mean value of 0.65 m $s^{-1}$ based on previous modeling work [*Westphal et al.* 1987 and 1988] and field experiments [*Gillette and Passi* 1988]. Dust emission is further restricted to erodible areas where the soil is relatively dry when COAMPS predicted ground wetness is less than 0.3, a threshold derived from long-term dust modeling in the Asia dust source areas.

Dust advection in both horizontal and vertical directions uses a $5^{th}$-order accurate flux-form scheme developed by *Bott* [1989a and 1989b]. Sub-grid scale turbulent mixing is solved implicitly with the eddy diffusivities for scalar generated by TKE closure. Particle terminal velocity for sedimentation is calculated using Stokes Law with Cunningham correction. Dry deposition velocity is calculated based on surface wind stress and wind speed at 10-m height [*Stull* 1988]. Wet deposition by convective and stable precipitation is calculated at all vertical levels based on the scavenging rates of washout and rainout processes obtained from *Pruppacher and Klett* [1978]. COAMPS dust model has been used in SW Asia operational forecasting since March 2003.

## 6.0 Operations Plan

The base of operations for the $UAE^2$ mission is the Dept of Water Resource Studies facility in Abu Dhabi, UAE. Access is available 24 hrs per day, 7 days per week. As all DWRS staff are housed there, most meetings and planning will be conducted from the DWRS meeting room. Air operations for the Aerocommander are out of the Al Bateen military airfield in Abu Dhabi, UAE. Crews are allowed access to the Hanger from 4:30 to 19:00, 7 days a week. The hanger area is also the base of operations for the CAR radiometer and Porter lidar. In addition to these two main facilities, the MAARCO and SMART containers at Al Tawilah and Al Ain, respectively, will be staffed daily.

A daily operations meeting will be held at the DWRS every evening at 19:30 (8:30 AM PDT, 11:30 EDT) to review recent events and coordinate ground and air operations for the following day. Particular attention will be paid to the integration of the NCAR cloud seeding and $UAE^2$ flights. Other topics for discussion include:

- Report and critique of previous day's activities
- Report on current day's activities and environmental assessment
- $UAE^2$ forecast
    - General flow assessment
    - Strength of land/sea breeze
- Aerosol forecast:
    - Source activity
    - Arabian Gulf/Gulf of Oman
- Gulf of Oman/Arabian Stratus
- Regional cloud (cirrus/stratus/convective) forecast
- Precipitation and convection forecast
- Schedule/Plan Determination

In addition to the 19:30 meeting, there will be a 10:00 weather update to assess afternoon conditions

6.1 Surface Operations

AERONET stations will be serviced as necessary. The MAARCO and SMART containers will be visited each morning for maintenance and radiation instrument cleaning. Filter changes at MAARCO will be conducted at 9:00 AM. While the filters are being changed, additional aerosol measurements can be made including ramping the nephelometer heater and running the APS in correlated mode.

6.3 Aircraft Operations

Approximately 80 flight hours have been budgeted for the $UAE^2$ mission. Given that the average flight will be 4 hours in length and flight operations will begin no earlier than 21 August, we expect roughly a two-day-on /one-day-off schedule. $UAE^2$ flight operations will be closely coordinated with the NCAR cloud seeding program. As most convection is in the middle afternoon, and the principle $UAE^2$ platform of support is Terra, the two programs naturally separate between morning $UAE^2$ and afternoon NCAR flights.

*6.3.1 Fundamental Aircraft Maneuvers*

Radiation and aerosol chemistry flights tend to be fairly straightforward. Consistency in flight maneuvers is, however, imperative to ensure comparability between data from different flights. This consistency is not only in the flight components but extends to regional geography in which these flights take place. The Gulf region is vast and diverse. Consequently, in the short span of this mission we cannot hope to characterize the entire UAE in high detail. Instead, focus will be on the MAARCO and SMART super-sites as well key AERONET stations within easy reach of the aircraft such as the Sur Bu Nair Island and Hamim sites.

6.3.1.1 Typical Vertical Profile

Fundamental to the air campaign is the vertical profile over super-sites and AERONET Sun photometers. Vertical profiles will begin at the surface or the top of the haze layer (~5,000 to 6,000 m). To reduce the effect of response time bias on the profile, assent/descent measurements will be made at no faster than 350 ft/min (~2 m $s^{-1}$). Thus, to descend/climb 20,000 ft requires 1 hour. For circumstances when the aircraft must change altitude rapidly, 1,000 ft/min (5.4 m $s^{-1}$) ascent/decent is possible, although thermodynamic data can be collected qualitatively. Vertical profiles will be performed in an elongated race-track facing towards and away from the sun. Legs will be 8 km (2 minutes long). Approximately 4 straight and level legs of 2 minutes will also be included in the profile. During vertical profiles at least one integrated set of filters will be taken (Teflon, quartz, Millipore) plus electron microscopy grids as necessary. Typically, CAR radiometer scans will be performed at the top of the haze layer and surface (see next section).

6.3.1.2Measurements Plan for CAR BRDF

6.3.1.2 CAR circles

To measure the bidirectional reflectance distribution function (BRDF) of the surface-atmosphere system, the aircraft needs to fly at a roll angle of ~20° flying in a circle about 3 km in diameter above the surface, taking roughly 2–3 minutes to complete an orbit (Appendix C). Targets include AERONET sites in the desert and at sea. UAE[2] measurements will generally be obtained at an altitude of between 30 and 200 m above the targeted surface and under clear sky conditions. This implies that at a 1° IFOV the pixel resolution is about 0.5-4 m at nadir and about 17-116 m at an 80° viewing angle from the CAR. Multiple circular orbits (6 to 10) will need to be acquired over a selected surface so that small-scale surface and atmospheric inhomogeneities are averaged out. With this configuration, the CAR is expected to collect between 76 400 and 114 600 directional measurements of radiance per channel per complete orbit.

•

6.3.1.3 Porter Lidar

The University of Hawaii/Porter lidar system will be deployed on the starboard side of the aircraft and will have the capability to be pointed upwards, downwards and forwards. In most cases the lidar will be pointed downwards except in the lowest 3000 meters when it will be pointed upwards. During straight and level flight in the vertical profiles, the lidar will be pointed straightforward in front of the aircraft to test if aerosol extinction can be determined (see Porter proposal).

6.3.1.4 Marine Boundary Layer Curtain Walls

Because there are strong stable layers over the surface of the Arabian Gulf, it is critical that the lowest 1000 meters are characterized during the marine meteorology flights. During long over-water transects it is common to simply perform a saw tooth pattern along the flow. The aircraft travels 42 km for one up or down maneuver (or 85 km for one set). At such a rate the aircraft could only perform two profiles between MAARCO and Sur Bu Nair. However, in UAE waters it is likely that there will be significant variability in offshore conditions. Consequently, near-surface vertical profiles need to be performed orthogonal to the mean flow. During an outbound/inbound near-surface run the aircraft will porpoise between the 100- and 300-meter levels to characterize the stable boundary layer. Periodically the aircraft will turn normal to the mean flow and climb in a similar racetrack pattern as for the column vertical profile. However, the aircraft will only travel 1 minute per long leg. Intermittent 1-minute straight legs will be included to retrieve wind speed. These curtain walls will be performed in regions of suspected land plume convergence (from lidar, in situ measurements or model prediction)

*6.3.2 Flight Plans*

Flights typically have 70 m $s^{-1}$ sampling speed, ceiling of 20,000 ft (6,200 km), and 4-hour endurance. Free fuel can be acquired at Al Bateen, Al Ain and Al Fujarah if necessary.

Exact flight plans will be developed on a daily basis at the discretion of the science team. However, in order to meet our scientific objectives, we have identified 6 basic types of flight plans:

1. Basic Atmospheric Characterization: Vertical profile over MAARCO, SMART, Sir Bu Nuair, Bukhoosh, Dhadnah, Hamim at satellite overpass time
2. Land Breeze: Low level Al Khazhah-MAARCO-Sir Bu Nuair + AERONET Sir Bu Nair vertical profile at NOAA overpass.
3. Sea Breeze: North/South transects from coast to Mezaira/Hamim for profile (3:30 pm)
4. Afternoon Coastal Haze Front: Transects between MAARCO and SMART
5. Regional BRDF
6. Gulf of Oman/Arabian Sea Stratus: Characterization of stratus in the Gulf of Oman and further south.

Because of the distance between sites and the 4 hour endurance, flight plans need to be simple and straightforward. As an example, consider flight plan 1 for basic atmospheric characterization

| | Maneuver | Total |
|---|---|---|
| Takeoff: | 0.10 | 0:10 |
| Trans climb to Sir Bu Nair (lidar) | 0:30 | 0:40 |
| CAR Scan | 0:20 | 1:00 |
| Descending vertical profile w/5 lev. | 1:15 | 2:15 |
| Car scan | 0:20 | 2:35 |
| MAARCO return surface layer | 0:30 | 3:05 |
| w/3 curtain walls-3000 ft | 0:30 | 3:35 |
| Return home | 0:20 | 3:55 |
| Landing | 0:10 | 4:05 |

Many of these flight plans can serve multiple mission requirements. For example, aerosol microphysics work can be performed on all flight plans. Similarly, atmospheric radiation work fits well with satellite cal/val operations. Some orthogonality does exist between meteorology and radiation experiments, but even here common ground can be found. Even so, the aircraft is a limited resource and some conflicts may occur. Hence priorities must be established. Stakeholders with the most restrictive needs and limited opportunities for validation or science will be given higher priorities. The priorities and investigators are

1. ASTER/Quickbird (Durkee)
2. MISR (Kahn)
3. Land Breeze (Raman/Reid)
4. MODIS/SeaWiFS (Hsu)
5. Stratus (Bruintjes/Platnick)

6. Supplemental BRDF survey (Gatebe)
7. Sea Breeze (Raman/Reid)
8. Coastal Haze (Reid)

Targets for remote sensing and BRDF scans are also prioritized in order of utility. These are

Ocean:

1. South of Sir Bu Nair Island
2. Dalma – southwest of the island
3. Abu al Bu (Deep water case)
4. Al Qlaa (coastal waters)

Desert:

1. Mezaira/Hamim
2. Umm al Quwain
3. Saih Salam
4. Al Khaznah

Lastly, stratus work would be preferable in the Gulf of Oman over Muscat due to the availability of free fuel and the closer location

## 7.0 Current Timeline (as for Aug 16, 2004)

| | |
|---|---|
| **August 1st:** | **Deployment crew begins to arrive** |
| **August 4th:** | **MAARCO delivered to Al Tawilla site** |
| **August 5th:** | **SMART delivered to Al Ain site** |
| **August 10th:** | **Limited aerosol and radiation sampling at MAARCO begins** |
| **August 12th:** | **SMART in operation save lidar** |
| **August 20th:** | **MAARCO and SMART fully operational** |
| **August 21st:** | **First test flight** |
| **September 24th** | **SMART begins takedown** |
| **September 25th:** | **MAARCO begins move to Mussafa site.** |
| **September 28th:** | **Last flight** |
| **October 7th:** | **Last member of IOP crew departs** |

## References


Ackerman, S. A., and S. K. Cox, The Saudi Arabian heat low: Aerosol distribution and thermodynamic structure, *J. Geophys. Res.,* **87**, 8991-9002, 1982.

Alfaro, S. C., A. Gaudichet, L. Gomes, and M. Maille, Modeling the size distribution of a soil aerosol produced by sandblasting, *J. Geophys. Res*., **102**, 11239-11249.

Atkinson, B. W., J.-G. Li, and R. S. Plant, Numerical modeling of the propagation environment in the atmospheric boundary layer over the Persian Gulf, *J. Appl. Meteor.,* **40**, 586-602, 2001.

Benkovitz, C. M., T. Scholtz, L. Pacyna, L. Tarrson, J. Dignon, E. Voldner, P. A. Spiro, and T. E. Graedel, Global gridded inventories of anthropogenic emissions of sulphur and nitrogen. *J. Geophys. Res.,* **101**, 29239-29253, 1996.

Bott, A., A positive definite advection scheme obtained by nonlinear renormalization of the advective fluxes, *Mon. Weather Rev*., **117**, 1006-1015, 1989a.

Bott, A., Reply, *Mon. Weather Rev*.,**117**, 2633-2636, 1989b.

Brooks, I. M., and D. P. Rogers, Aircraft observations of the mean and turbulent structure of a shallow boundary layer over the Persian Gulf, *Bound. Layer Meteor.,* **95**, 189-210, 2000.

Brower, W. A., R. G. Baldwin, and P. L. Franks, *US Navy Regional Climatic Study of the Persian Gulf and the Northern Arabian Sea*, NAVAIR 50-1C-561, July 1992.

Christensen, J. H., The Danish eulerian hemispheric model - A three-dimensional air pollution model used for the Arctic. *Atm. Env*., **31**, 4169-4191, 1997.

Christopher, S. A. and J. Wang, (2004), Intercomparison between MISR and Sunphotometer AOT in Dust Source Regions over China: Implication for satellite retrievals and radiative forcing calculations, *Tellus B*, submitted.

Clements, T., T. H. Merriam, R. O. Stone, J. L. Eimann, and H. L. Reade, A study of desert surface conditions, Tech. Rep. EP-53, pp. 130, U.S. Army, Natick Lab., Natick, MA, 1957.

Dubovik, O., B. N. Holben, T. Lapyonok, A. Sinyuk, M. I. Mishchenko, P. Yang, and I. Slutsker, Non-spherical aerosol retrieval method employing light scattering by spheroids, *Geophys. Res. Lett.,* **29**, 10.1029/2001GL014506, 2002.

Dubovik, O., B. N. Holben, T. F. Eck, A. Smirnov, Y. J. Kaufman, M. D. King, D. Tanré, and I. Slutsker, Variability of absorption and optical properties of key aerosol types

observed in worldwide locations, *J. Atmos. Sci.*, **59**, 590-608, 2002.

Dubovik, O., and M. D. King, A flexible inversion algorithm for retrieval of aerosol optical properties from sun and sky radiance measurements, *J. Geophys. Res.*, **105**, 20,673-20,696, 2000.

Dubovik, O., A. Smirnov, B. N. Holben, M. D. King, Y. J. Kaufman, T. F. Eck, and I. Slutsker, 2000: Accuracy assessments of aerosol optical properties retrieved from AERONET sun and sky radiance measurements, *J. Geophys. Res.,* **105**, 9791-9806, 2000.

Eck, T. F., B. N. Holben, J. S. Reid, O. Dubovik, A. Smirnov, N. T. O'Neill, I. Slutsker and S. Kinne, Wavelength dependence of the optical depth of biomass burning, urban, and desert dust aerosol, *J. Geophys. Res.,* **104**, 31,333-31,350, 1999.

Gatebe, C. K., M. D. King, S. Platnick, G. T. Arnold, E. F. Vermote, and B. Schmid, 2003: Airborne spectral measurements of surface-atmosphere anisotropy for several surfaces and ecosystems over southern Africa. *J. Geophys. Res.*, **108**, 8489, doi:10.1029/2002JD002397, 2003.

Gatebe, C. K., M. D. King, A. Lyapustin, G. T. Arnold and J. Redemann, Airborne spectral measurements of ocean directional reflectance. *J. Atmos. Sci.* (in press), 2004

Gillette, D. A. and R. Passi, modeling dust emission caused by wind erosion, *J. Geophys, Res.*, **93**, 14233-14242, 1988.

Heishman, J., Commanding Officer, Forecaster's Handbook, US Navy Central Meteorological and Oceanographic Center, Bahrain, 1999.

Hodur, R. M., The Naval Research Laboratory's Coupled Ocean/Atmosphere Mesoscale Prediction System (COAMPS), *Mon. Weather Rev.*, **125**, 1414-1430, 1997.

Hogan, T. F., and T. E. Rosmond, The description of the Navy operational global atmospheric prediction system's spectral forecast model. *Mon. Wea. Rev.*, **119**, 1786-1815, 1991.

Hogan, T. F., and L. R. Brody, Sensitivity studies of the Navy's global forecast model parameterizations and evaluation of improvements to NOGAPS. *Mon. Wea. Rev.*, **121**, 2373-2395, 1993.

Holben, B.N., et al., An emerging ground based aerosol climatology: Aerosol optical depth from AERONET, *J. Geophys. Res.*, **106**, 12067-12097, 2001.

Holben, B.N., et al., AERONET - A federated instrument network and data archive for aerosol characterization, *Rem. Sens. Env.,* **66(1),** 1-16, 1998.

Hsu N. C., S. C. Tsay, M. D. King, J. R. Herman, Aerosol properties over bright-reflecting source regions, *IEEE Trans. on Geophys. and Remote Sens.,* **42**, 557-569, 2004.

Kahn, R., R. West, D. McDonald, B. Rheingans, and M. I. Mishchenko, (1997), Sensitivity of multi-angle remote sensing observations to aerosol sphericity, *J. Geophys. Res.* **102**, 16861-16870.

Kahn, R. A., B. J. Gaitley, J. V. Martonchik, D. J. Diner, K. A. Crean, and B. Holben, (2004a), MISR global aerosol optical depth validation based on two years of coincident AERONET observations, *J. Geophys. Res.,* submitted, 2004a.

Kahn, R., J. Anderson, T.L. Anderson, T. Bates, F. Brechtel, C. M. Carrico, A. Clarke, S. J. Doherty, E. Dutton, R. Flagan, R. Frouin, H. Fukushima, B. Holben, S. Howell, B. Huebert, A. Jefferson, H. Jonsson, O. Kalashnikova, J. Kim, S-W. Kim, P. Kus, W-H. Li, J.M. Livingston, C. McNaughton, J. Merrill, S. Mukai, T. Murayama, T. Nakajima, P. Kalashnikova, O. V., R. Kahn, I. N. Sokolik, and W-H. Li, The ability of multi-angle remote sensing observations to identify and distinguish mineral dust types: Part 1. Optical models and retrievals of optically thick plumes, *J. Geophys. Res*., submitted, 2004.

King, M. D., Directional and spectral reflectance of the Kuwait oil-fire smoke. *J. Geophys. Res*., **97**, 14545-14549, 1992.

King, M. D., M. Strange, P. Leone, and L. R. Vlaine, Multi-wavelength scanning radiometer for airborne measurements of scattered radiation within clouds, *J. Atmos. Oceanic Tech.,* **3**, 513- 522, 1986.

Lienert, B, J.N. Porter, N. Ahlquist, D. Harris, S. Sharma, A 50 MHz Logarithmic Amplifier for use in Lidar Measurements, *J. of Atmos. and Oceanic Tech.,* **19**, 654-657, 2002.

Lienert, B. R., J. N. Porter and S. K. Sharma, Aerosol Size Distributions from Genetic Inversion of Polar Nephelometer Data*, J. Atmos. and Oceanic Tech*., **20**, 1403-1410, 2003.

Liu, M. D. Westphal, S. Wang, A. Shimizu, N. Sugimoto, J. Zhou, and Y. Chen, 2003: A high-resolution numerical study of Asia dust storms of April 2001. *J. Geophys. Res*., **108,** (D23) 8653, doi:10.1029/2002JD003178.

Liu, M., D. L. Westphal, and T. R. Holt, Numerical study of a low-level jet over complex terrain in southern Iran, *Mon. Wea. Rev.,* **128**, 1309-1327, 2000.

Mantaoura, R. F. C., C. S. Law, N. J. P. Owens, P. H. Burkill, E. M. S. Woodwar, R. J. M. Howland, and C. A., Lewellyn, Nitrogen Biogeochemical Cycling in the

Northwestern Indian Ocean, Deep See res. Part II- Tropical Studies in Oceanography, **40** (3), 651-671, 1993.

Martonchik, J.V., D.J. Diner, R. Kahn, B. Gaitley, and B. Holben, Comparison of MISR and AERONET aerosol optical depths over desert sites, *Geophys. Res. Lett*., submitted, 2004.

Miller, S. D., A consolidated technique for enhancing desert dust storms with MODIS, *Geo. Res. Lett*., **30**(20), Art. No. 2071 Oct 30 2003.

Nickling, W. G. and J. A. Gillies, Dust emission and transport in Mali, West Africa, *Sedimentology,* **40**, 859-868, 1993.

O'Neill, N. T., T. F. Eck, A. Smirnov, B. N. Holben, and S. Thulasiraman, Spectral discrimination of coarse and fine mode optical depth, *J. Geophys. Res.*, **108**(D17), 4559, doi:10.1029/2002JD002975, 2003.

O'Neill, N. T., O. Dubovik, and T. F. Eck, A modified Angstrom coefficient for the characterization of sub-micron aerosols, *Appl. Opt.,* **40**(14), 2368-2375, 2001b.

O'Neill, N. T., T. F. Eck, B. N. Holben, A. Smirnov, O. Dubovik, and A. Royer, Bimodal size distribution influences on the variation of Angstrom derivatives in spectral and optical depth space, *J. Geophys. Res.,* **106**, 9787-9806, 2001a.

Porter, J. N., T. F. Cooney, C. Motell, Coastal Aerosol Phase Function Measurements With A Custom Polar Nephelometer, Ocean Optics XIV Conference, Kona, Hawaii, pp. 5, 1998.

Porter, J. N., Lienert, B., S. K. Sharma, Using the Horizontal and Slant Lidar Calibration Methods To Obtain Aerosol Scattering Coefficients From A Coastal Lidar In Hawaii, *J. of Atmos. and Oceanic Tech.*, **17**, 1445-1454, 2000.

Porter, J. N., B. Lienert, S. K. Sharma, and H. W. Hubble, A Small Portable Mie-Rayleigh Lidar System to Measure Aerosol Optical and Spatial Properties, *J. of Atmos. and Oceanic Tech.*, **19**, 11, 1873-1877, 2002a.

Porter, J. N., K. Horton, P. Mouginis-Mark, B. Lienert, E. Lau, S.K. Sharma, J. Sutton, T. Elias, and C. Oppenheimer, Lidar and Sun Photometer Measurements of The Hawaii Pu'u O'o Volcano Plume: Estimates of $SO_2$ and Aerosol Flux Rates and $SO_2$ Lifetimes, *Geo. Res. Lett*., **29**, 2002GL014744, 2002b.

Pruppacher, H. R. and J. D. Klett, Microphysics of Clouds and Precipitation, D. Reidel Publishers, pp. 389, 1978.

Quinn, J. Redemann, M. Rood, P. Russell, I. Sano, B. Schmid, J. Seinfeld, N. Sugimoto, J. Wang, E.J. Welton, J-G. Won, S-C. Yoon, Environmental Snapshots From ACE-Asia, *J. Geophys. Res*., submitted, 2004b.

Raman, S., D. S. Niyogi, M. Simpson and J. Pelon (2002): Dynamics of the elevated land plume over the Arabian Sea and the northern Indian Ocean during northeasterly monsoon (INDOEX), *Geo. Res. Lett.*, **29**, 641- 644.

Rao D. V. S., F. Al-Yamani F, and C. V. N. Rao, Eolian dust affects phytoplankton in the waters off Kuwait, the Arabian Gulf, *NATURWISSENSCHAFTEN* **86** (11): 525-529,1999.

Reid, J. S., E. M. Prins, D. L. Westphal, C. C. Schmidt, K. A. Richardson, S. A. Christopher, T. F. Eck, E. A. Reid, C. A. Curtis, and J. P. Hoffman, Real-time monitoring of South American smoke particle emissions and transport using a coupled remote sensing/box-model approach. *Geo. Res. Lett.*, **31**, L06107, doi:10.1029/2003GL018845, 2004.

Ritchie, H., Semi-Lagrangian Advection on a Gaussian Grid, *Mon. Wea. Rev.*, **115**, 608-619, 1987.

Simpson, M., and S. Raman (2004): Role of the land plume in the transport of ozone over the ocean during INDOEX (1999), *Bound. Layer Meteor.*, **111**, 133-152.

Slinn, A. A., and W. G. N. Slinn, Predictions for particle deposition on natural waters. *Atm. Env.*, **14**, 1013-1016, 1980.

Smirnov, A., B. N. Holben, O. Dubovik, N. T. O'Neill, T. F. Eck, D. L. Westphal, A. K. Goroch, C. Pietras, and I. Slutsker, Atmospheric aerosol optical properties in the Persian Gulf region, *J. Atm. Sci.,* **59**, 620-634, 2002.

Smirnov, A., B. N. Holben, T. F. Eck, O. Dubovik, and I. Slutsker, Cloud screening and quality control algorithms for the AERONET data base, *Rem. Sens. Env.,* **73***(3)***,** 337-349, 2000.

Staniforth, A. and J. Cote, Semi-Lagrangian Integration Schemes for atmospheric models - A Review, *Monthly Weather Review*, **119**, 2206-2223, 1991.

Stull, R. B., An Introduction to Boundary Layer meteorology, pp. 251-289, Kluwer Academic, Norwell, Mass., 1988.

Stunder, M. and S. Raman (1985): A comparative evaluation of the coastal internal boundary-layer height equations, *Bound. Layer Meteor.*, **32**, 177-204.

Toon, O. B., R. P. Turco, D. L. Westphal, R. Malone and M. S. Liu, A multidimensional model for aerosols: description of computational analogs. *J. Atmos. Sci.*, **45**, 2123-2143, 1988.

Voldner, E. C., L. A. Barrie and A. Sirois, A literature review of dry deposition of oxides of sulphur and nitrogen with emphasis on long-range transport modeling in North America. *Atm. Env.*, **20**, 2102-2113, 1986.

Walcek, C. J., R. A. Brost, J. S. Chang and M. L. Wesely, SO2, Sulfate and HNO3 deposition velocities computed using regional landuse and meteorological data. *Atm. Env.,* **20**, 949-964, 1986.

Westphal, D. L., O. B. Toon and T. N. Carlson, A two-dimensional investigation of the dynamics and microphysics of Saharan dust storms, *J. Geophys. Res*., **92**, 3027-3049, 1987.

Westphal, D. L., O. B. Toon and T. N. Carlson, A case study of mobilization and transport of Saharan dust. *J. Atmos. Sci*., **45**, 2145-2175, 1988.

Walker, A., S. Miller, K. Richardson, and D. Westphal, 2003: Revised Land Use Characteristic Dataset For Asia and Southeast Asia for NAAPS and COAMPS Dust. *Battlespace Atmospheric and Cloud Impacts on Military Operations Conference*. Sep 9-11, Monterey, CA.

# Appendix A. Science Teams

**Steering Committee:**
Roelof Bruintjes (NCAR): Cloud research mission scientist
Piotr Flatau (Scripps): Radiation sciences leader
Charles Gatebe (GEST/GSFC) US mission deputy, remote sensing team co-leader
Brent Holben, (NASA GSFC): Ground team leader
Ralph Kahn, (Jet Propulsion Laboratory): Remote sensing co-leader
Michael King, (NASA GSFC): Radiation sciences
Hal Maring (NASA HQ): Lead program manager
Abdulla Al Mandoos, (DWRS): UAE mission scientist
Stuart Piketh (Univ. of Witts): South Africa mission scientist, cloud physics
Jeffrey Reid (NRL): US mission scientist, microphysics & chemistry
Douglas Westphal (NRL): Meteorology team leader, Aerosol transport

**Funding Agencies:**
Dept. of Water Resources, Office of the President, United Arab Emirates (Mangoosh)
NASA HQ, Washington DC (Maring)
Naval Research Laboratory Base Funding, 6.1 Platform Support (Hartwig)
Office of Naval Research Code 32 (Ferek)
Office of Naval Research Code 35/NAVSEA PMS 405 (Graf/Nolting)

**Participating Institutions**
Dept. of Water Resources, Office of the President, United Arab Emirates
Droplet Measurement Technologies, Inc.
Jet Propulsion Laboratory, Pasadena, CA.
National Center for Atmospheric Research, Boulder CO.
NASA Goddard Space Flight Center, Greenbelt MD.
Naval Research Laboratory, Monterey, CA
Naval Research Laboratory, Stennis, MS
North Carolina State University, Raleigh, NC
Orsmond Aviation, South Africa.
Scripps Institution of Oceanography
South African weather Agency
TNO Physics and Electronics Laboratory, The Hague, Netherlands
Universite de Sherbrooke, Sherbrooke, Quebec, Canada
University of Alabama, Huntsville, AL
University of California, Davis, CA
University Corporation for Atmospheric Research
University of Hawaii, Honolulu HI
University of Maryland, Baltimore County, Baltimore MD
University of Maryland, Collage Park, MD
University of Witwatersrand, South Africa
Warsaw University, Warsaw, Poland

**Airborne Deployment Team (Piketh and Reid)**
Anthony Bucholtz (NRL Monterey): Radiometry
Dan Breed (NCAR): Cloud microphysics
Roelof Burger (SAWS/U. Witwatersrand): Cloud microphysics
Piotr Flatau (Scripps/UCSD): Airborne radiometers.
Charles Gatebe (GEST)/GSFC: CAR radiometer
Michael King (GSFC): CAR radiometer
Vanderlei Martins (GEST/GSFC): Aerosol particle absorption
Tara Jensen (NCAR): Cloud microphysics
Stuart Piketh (U. Witwatersrand): Cloud microphysics.
John Porter (University of Hawaii): Airborne lidar
Jeffrey Reid (NRL Monterey): Aerosol microphysics, land-sea meteorology
Kristy Ross (U. Witwatersrand): Aerosol chemistry

**Ground Deployment Team (Holben)**
Steve Cliff (UC Davis): DRUM impactor
Arie de Jong (TNO): IR differential radiance spectroscopy, transmissometry
Garrit de Leeuw (TNO): Transmissometry
Thomas Eck (GEST/GSFC): AERONET retrievals
Piotr Flatau (Scripps/UCSD): Surface radiative properties
Brent Holben (GSFC): AERONET Sun photometer
Jack Ji (GEST/GSFC): SMART/COMMIT
Krzysztof Markowicz (U of Warsaw): Aerosol radiative forcing
Vanderlei Martins (GEST/GSFC): Aerosol particle absorption
Norm O'Neill (Univ. of Sherbrooke): Aerosol optical properties.
Antonio Queface, (U Witwatersrand): Radiation
Elizabeth Reid (NRL Monterey): Single particle analysis, MPL lidar
Jeffrey Reid (NRL Monterey): Aerosol Chemistry & microphysics.
Joanna Remiszewska (Univ. of Warsaw): Aerosol forcing, data assimilation
Joel Schafer (GEST/GSFC): AERONET retrievals
Alexander Smirnov (GEST/GSFC): AERONET retrievals
Si-Chee Tsay (GSFC): SMART, surface radiation.
Ellsworth Judd Welton (GSFC): Micropulse lidar
Nicola Walton (U. Witwatersrand): Atmospheric chemistry
Marcin Witek (U of Warsaw): Radiative forcing

**Remote Sensing Team (Gatebe)**
Robert Arnone (NRL Stennis): SeaWiFS & MODIS ocean products
Sundar Christopher (Univ. of Alabama): CERES & MODIS integration
Phil Durkee (NPS): High-resolution AOT retrievals
Charles Gatebe (GEST/GSFC): Surface almucantar/CAR Fusion, BRDF
Hashem Al Hashemi (DWRS): Regional remote sensing/GIS
Christina Hsu (GEST/GSFC): AOT retrievals over bright surfaces
Ralph Kahn (JPL): MISR aerosol retrievals
Olga Kalashnikova (JPL): MISR aerosol retrievals
Jolanta T. Kusmierczyk (TNO): ATSR dust retrievals

Steve Miller (NRL Monterey): Dust products
Ben Ruston (NRL Monterey): Microwave radiance temperature inversions
Nazmi Saleous (GEST/GSFC): MODIS aerosol retrievals
Robin Schoemaker (TNO): ATSR aerosol retrievals
Adnan Sharaf (DWRS): Regional remote sensing/GIS
Dominick Vincent (NPS) High-resolution AOT retrievals

**Meteorology Team (Westphal)**
Hamid Brashdi (Dir. Gen. of Civil Aviation and Meteor., Oman): Regional meteorology
Steven Burk (NRL Monterey): near surface temperature/humidity profiles
Mian Chin (GSFC): GOCART aerosol modeling
Rebecca Eager (NC State): COAMPS, land-sea flow processes
Suffian Farrah (DWRS): Regional forecasting
Ahmed Ibrahim (DWRS): Regional forecasting
Ming Liu (NRL Monterey): COAMPS dust forecasting
Sethu Raman (NC State): COAMPS, land-sea flow processes
Annette Walker (NRL Monterey): Dust forecasting and source functions
Douglas Westphal (NRL Monterey): NAAPS dust forecasting

**South African Aerocommander Crew (Piketh)**
Steve Broccardo (Orsmond Aviation): South African project manager
Steve Edwards (Orsmond Aviation): Electrical engineer
Hans Kruger (Orsmond Aviation): Cloud seeding pilot
Steve Mandel (Orsmond Aviation): Aerocommander cloud seeding chief pilot
Harry McGarry (Orsmond Aviation): Chief mechanic
Gary Willis (Orsmond Aviation): Aerocommander $UAE^2$ chief pilot

## Appendix B. Airborne Platform Summary: South African Weather Service Research Aircraft – Aerocommander 690 A

**Stuart Piketh, University of the Witwatersrand**

The South African Weather Services are the sole owners of two research aircraft, namely Aerocommander 690 A's with registrations ZS-JRA and ZS-JRB. These aircraft have been utilized over the past fifteen years exclusively for atmospheric research. The aircraft are twin turbo prop aircraft with Garret turbine engines. The aircraft are pressurized and are able to operate between sea level and approximately 28 000ft. Over the past year one of the aircraft, ZS-JRB, has been utilized in the United Arab Emirates for both atmospheric chemistry and weather modification experiments. A picture of the aircraft is provided in Figure 1. The aircraft is operated in the United Arab Emirates under the lease to Orsmond Aerial Spray (PTY) Ltd. Orsmond Aerial Spray (Pty) Ltd ensures that the aircraft is fully maintained in the UAE, and is responsible for obtaining appropriate liability coverage for operating the aircraft for scientific purposes in the Middle East.

The airplane operates with standard aircraft avionic equipment. It is equipped with a GARMIN GNS430 Global Positioning System. The Aircraft has several atmospheric measurement capabilities that have been added over the past five years. The aircraft measures all atmospheric state parameters. These include temperature, pressure, humidity, dew point temperature and liquid water content (summary in Table 1).

| Parameter | Sensor and source |
|---|---|
| Position | GARMIN GNS 430 |
| Dynamic pressure | Rosemount / SAWS |
| Static pressure | Rosemount / SAWS |
| Temperature | Rosemount / SAWS |
| Relative humidity | Viasala Humicap / SAWS |
| Liquid water content | King |

In addition, the airplane is equipped to carry six PMS aerosol and water droplet probes. Two probes are mounted on the front nose of the aircraft and two probes are hung under each wing. Several PMS probes are available for use on the aircraft. These include a Forward Scattering Spectrometer Probe (FSSP 100), a Optical Array Probe (OAP2DP or OAP2D2P), a Two Dimensional Cloud Probe (2DC or 2D2C) and a Passive Cavity Aerosol Spectrometer Probe (PCASP 100x).

A series of other equipment can be mounted in the interior of the airplane. In general the equipment is housed in 19 " rack mounts. All data collected on the aircraft can be logged on a dedicated Airborne Data Acquisition System (ADAS). The ADAS is capable of storing data at 10 Hz on a flash card. The data is converted into NetCDF and ASCII format during post-processing. Depending on the configuration of the equipment

mounted in the aircraft, it is possible for two scientists in addition to the pilot to fly on board the aircraft during a research flight.

Modifications to the aircraft are possible as long as details of the equipment are provided in good time. All modifications are approved by the Civil Aviation Authority in South Africa.

Figure 1. Aerocommander 690A ZS-JRB. Identical aircraft to ZS-JRA.

The project operational manager for the United Arab Emirates is Dr Stuart Piketh. Contact details are as follows:

Dr Stuart Piketh
Climatology Research Group
University of the Witwatersrand
Johannesburg
Tel: +2711 717 6532
Fax: +2711 717 6535
E-mail: stuart@crg.bpb.wits.ac.za

# Appendix C. Cloud Absorption Radiometer (CAR)

**Michael King and Charles Gatebe, NASA GSFC**

## 1) Bidirectional Reflectance Properties of Surfaces

The Cloud Absorption Radiometer (King et al. 1986) has been used in the past to acquire BRDF measurements of the ocean, sea ice, snow, tundra, savanna (cerrado, mopane, miombo), smoke, vegetation, desert (Saudi Arabia, salt pans in Botswana and Namibia), and clouds between 0.5 and 2.3 μm. These measurements involved flights onboard the University of Washington C-131A or CV-580, and date from observations over the Kuwait oil fire smoke and nearby Saudi Arabian Desert and Persian Gulf in 1991 (King 1992), and extend to the more recent CLAMS experiment over ocean surfaces with sunglint (Gatebe et al. 2004).

Figure C.1 shows a typical flight pattern whereby the aircraft, with the CAR in the nosecone, flies a clockwise circular pattern above the surface or cloud repeatedly, drifting with the wind, and scans the underlying surface and much of the transmitted solar radiation from above, and makes radiometric observations about every 1° in azimuth and better than 1° in zenith angle with an instantaneous field-of-view of 1°. Often, multiple circular orbits are averaged together to smooth out the reflected solar radiation signal.

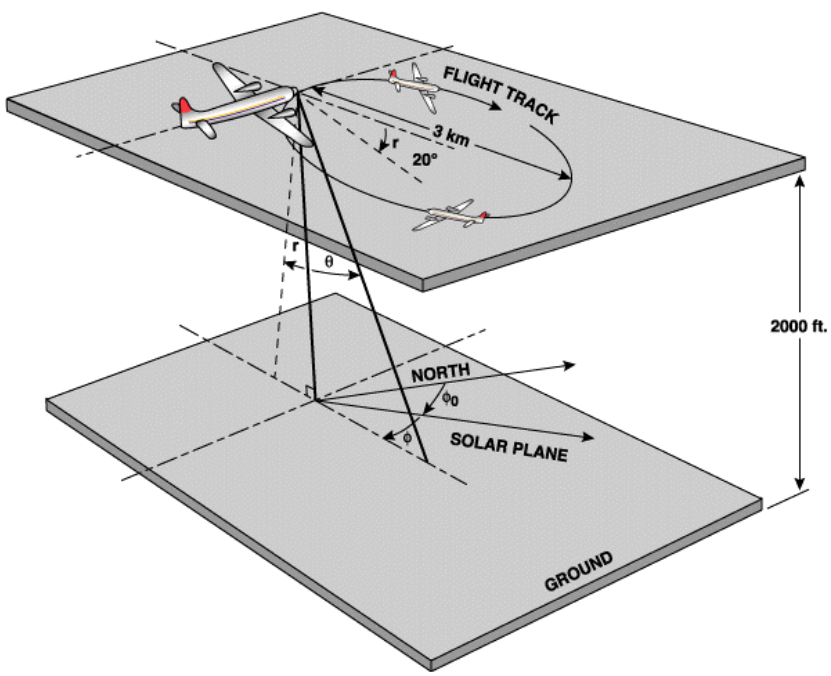


Figure C.1. Schematic illustration of a clockwise circular flight track for measuring surface bidirectional reflectance from nadir to the horizon as we as much of the transmittance pattern from near zenith to the horizon (adapted from King 1992).

Figure C.2 shows selected examples of the bidirectional reflectance observed over selected terrestrial surfaces, including Namibian stratus with a rainbow and glory, the Etosha Pan, Namibia, and savanna vegetation at Skukuza, South Africa (Gatebe et al. 2003), and ocean reflectance with sunglint off the Virginia coast in the western Atlantic (Gatebe et al. 2004).

**2) Measurements Objectives for UAE[2]**

Onboard the South African Weather Service Aerocommander 690A aircraft, the CAR will be used to acquire multiangular and multispectral observations suitable for satellite validation strategies. These observations will include:

- Measurements of the bidirectional reflectance pattern of desert and ocean at multiple wavelengths in the visible and near-infrared
- Measurements of the bidirectional reflectance pattern of desert and ocean at several vertical heights for characterization of aerosol radiative properties in the vertical
- Intercomparison of CAR/AERONET retrievals of aerosol properties to simultaneous retrievals of in situ microphysics measurements of aerosols
- Validation and comparison:
    - Lidar (vertical distribution of aerosol)
    - SeaPRISM (water leaving radiance)
    - MODIS/TOMS/SeaWiFS

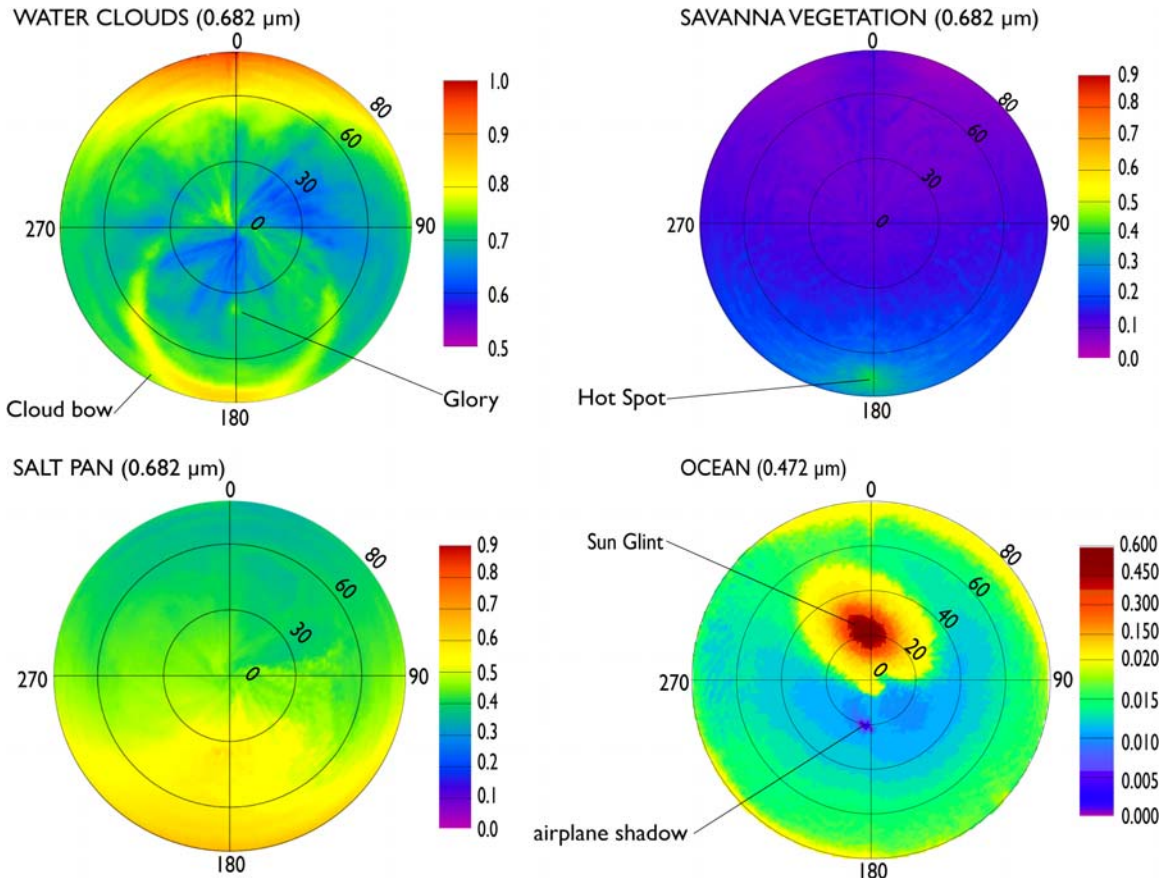


Figure C.2. Bidirectional reflectance of various natural surfaces observed by the CAR mounted on the University of Washington CV-580 research aircraft. These observations have all been atmospherically corrected, and include Namibian stratus clouds and the Etosha salt pans of Africa, savanna vegetation in South Africa, and ocean reflectance with sunglint over the western Atlantic Ocean off Virginia, US.

# Appendix D. Lidar and Polar Nephelometer Measurements During The UAE$^2$ Experiment (2004)

**John Porter, University of Hawaii**

## Aircraft Lidar Measurements

As part of the UAE$^2$ experiment, we will carry out aircraft lidar measurements with our small custom lidar system (Porter et al., 2002a). The lidar will be mounted in the side of the aircraft fuselage with a design, which allows it to be pointed either upward, or downward depending on the aircraft altitude. Using assumed aerosol and lidar optical properties, aerosol extinction values will be plotted in real time from the lidar measurements (Porter et al., 2000; Porter et al., 2002b) allowing informed decisions in flight planning. On select occasions, when the plane is flying level in an aerosol layer, the lidar will be pointed forward. These forward-looking lidar measurements will allow us to test a new lidar approach to derive quantitative aerosol extinction values. In order to make the system eye safe (at greater than 200 range) we will use a diverging laser beam combined with a non-imaging optics approach to collect the light (Porter et al., 2002a).

Specifications:

| | |
|---|---|
| Electrical Power | ~300 watts, 120V, 60 Hz, |
| Total Weight | ~ 100 pounds |
| Light power | ~ 15 mJ/pulse at 532 nm (20 Hz) |
| Lidar range | ~ 60 to 5000 m (larger range pos. if near field is extended) |
| Sampling resolution | ~ 10 m |
| Products | distribution of aerosol extinction values |
| Custom Electronics | LogAmp (Lienert et al., 2002) and TVG |

## Polar Nephelometer Measurements

Polar nephelometer will be carried out during the UAE 2004 experiment with our custom polar nephelometer. Aerosol scattering measurements are made externally so that no aerosol inlet losses occur (Porter et al., 1998). Angular scatter measurements will be made at 1064 and 532 nm wavelength. In collaboration with other investigators (aerosol size distributions, compositions, shape information) our angular scatter measurements will be used to test both forward and inverse calculations using spherical and non-spherical assumptions. In the past we have used Genetic Inversion approaches (with Mie theory) to invert aerosol size distributions from polar nephelometer data from sea salt aerosols (Lienert et al., 2003).

## Appendix E. AERONET UAE$^2$ Mission Plan

AERONET is an internationally collaborative network of sun and sky scanning spectral radiometers designed to retrieve aerosol optical properties from direct sun and diffuse sky radiance measurements. The program developed in 1993 from a need to remove atmospheric effects in RS satellite data but evolved to meet a need for satellite validation of aerosol extinction (aerosol optical depth) and more recently has developed into a globally distributed network for accurately characterizing basic properties of size (particle size distribution) and absorption, (single scattering albedo) for naturally and anthropogenically occurring marine, urban, biomass burning and desert aerosols. Since the inception of the program, the supported AERONET sites has grown from 3 to approximately 220 systems distributed on all continents (Fig. E.1). A standard AERONET system is an eight channel filtered radiometer that is pointed under robot control at the sun and scans the sky nominally at 15 minute intervals in predefined protocols. Within hours of collection, the data are transmitted via geostationary satellites to receive stations, FTP'd to the AERONET server, processed, analyzed, stored and posted to the AERONET website (http://aeronet.gsfc.nasa.gov) for use by the scientific community, policy makers, educators and the general public. The result is a systematically collected data set that allows analysis for short-term aerosol variations and long-term aerosol characterizations with an accuracy of 0.01 to 0.02 in optical depth and 0.03 in single scattering albedo.

**AERONET UAE^2 project goals:**

- Characterize aerosol optical and microphysical properties of the Gulf Region using the resources of the AERONET program
- Measure accurately and continuously the column integrated aerosol optical properties at a mesoscale to facilitate airborne and satellite validation efforts
- Measure, for the first time, UV through Infrared sky radiance for retrievals of particle size distribution, single scattering albedo and complex index of refraction
- Measure for the first time ocean leaving radiance for dust aerosol with the SeaPRISM.
- Intercompare CAR/AERONET/airborne lidar retrievals of aerosol properties to simultaneous retrievals of in situ microphysics measurements from MAARCO and Aerocommander platforms
- Study the dynamics of the single scattering albedo and establish regional variability for comparison to Saharan single scattering albedo observations
- Compare profile retrievals available from CAR to the column integrated AERONET retrievals
- Provide a comprehensive data set to validate ocean leaving radiances from the surface to

**Measurement Plan:**

AERONET will deploy a diverse suite of sun and sky scanning radiometers that will take the usual AERONET observations and additional protocols to measure ocean leaving radiances, and several test instruments for multispectral polarization of sky radiances, UV sky radiances and with a new filter configuration total column $CO_2$. The

sites anticipated will be distributed approximately according to Figure E.1 that includes small islands and oil platforms for ocean color, coastal sites, urban and desert landscapes. The sites themselves will likely be co-located with the site in of the extensive network of DWRS meteorological stations Figure E.2. We anticipate up to 15 AERONET sites distributed across the country with the bulk in the interior at sites uniform within a 10 by 10 km box. It is anticipated that data collected at most sites will be up-linked to Meteosat as is usual for most AERONET sites for near real time processing. Several higher volume sites will have direct Internet links where possible and some may have to rely on PC downloads with infrequent dumps to the AERONET server for processing. Table 1 shows the instrumentation to be included in the measurement program. Most equipment is expected to be deployed around June 20, 2004.

Table E.1 showing anticipated ground based equipment to be deployed during UAE^2

| Type of instrument | Number anticipated | Measurement characteristic* | Location | PI |
|---|---|---|---|---|
| Standard† | 10 | Sun & Sky | Interior | Holben |
| Extended λ | 5 | Sun & Sky +1.6μm | Interior | Holben |
| Polar Standard | 3 | Polar @870 nm | 1 Is & 2 interior | Goloub & Piketh |
| UV extended | 2 | Sun & Sky +UV Sky | 1 Urban & 1 Interior | Holben |
| Polar Multispectral | 1 | Sky Polarization all channels | Perhaps a rover but primarily urban | Holben/Goloub |
| SeaPRISM# | 2 | Sun and sky + ocean leaving radiances | Oil platforms in Gulf | Zibordi & Hooker |
| $CO_2$ | 1 | Sun & Sky +CO2 at 2.06 μm | Urban & interior | Holben |
| UV Shadowband | 1 | UV AOT, Direct and diffuse radiances | At DWRS site | Jim Slusser |

*All AERONET type instruments will make AOD measurements and almucantars @ 440, 675, 870 and 1020 nm, water vapor measurements at 940 nm
†includes AOD at 340 and 380 nm
#Ocean radiance @412 and 520 nm

Figure E. 1, Proposed AERONET site distribution for UAE^2

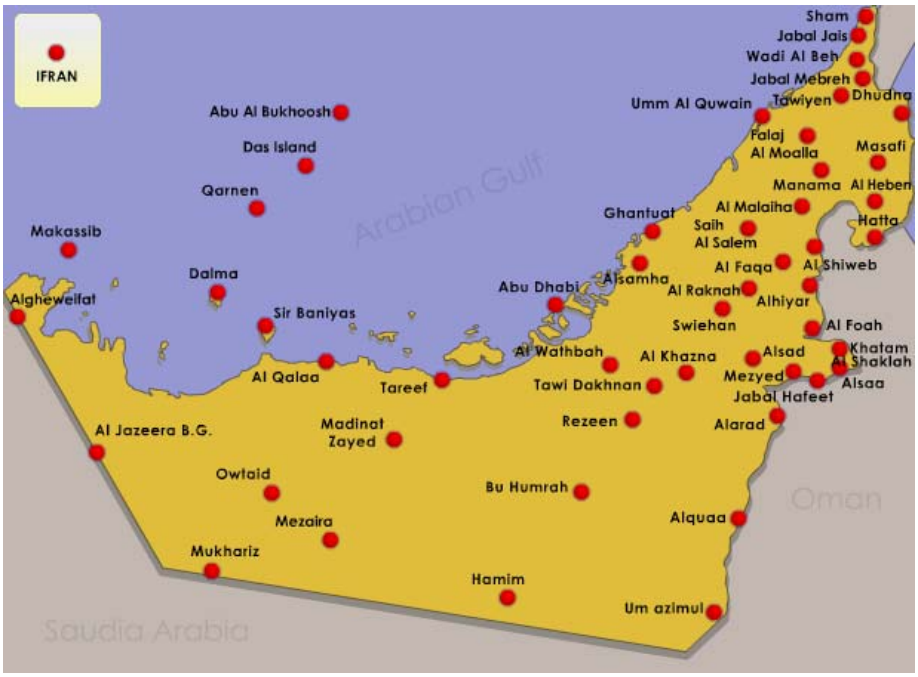


Figure E.2, DWRS meteorological site distribution and potential co-location sites w/ AERONET.

**AERONET Collaborator Requirements:**

Frequent profiles over AERONET sites with the Aerocommander emphasizing iso-altitude spirals with the CAR, lidar and onboard in situ measurements.

Technical Assistance: DWRS technician available to Set up equipment in June and be on call to maintain instruments as needed through September.

Management Issues: DWRS to clear customs and organize deployment transportation for all in-country equipment.

## Appendix F. MAARCO Instrumentation:

### NRL Monterey

The Mobile Atmospheric Aerosol and Radiation Characterization Observatory (MAARCO) is a standard 20'x8' climate controlled CONEX shipping container that has been modified to function as an easily-shipped laboratory for deployment overseas, in remote areas, or on sea-going vessels. Its purpose it to perform basic research on atmospheric aerosols, gasses, and radiation (visible and IR light) in difficult to deploy regions. MAARCO will assist in validating aerosol and weather models as a ground station and often be used in conjunction with research aircraft. All MAARCO requires is input power (110, 220, or 240 3-phase), though it can utilize generators. MAARCO also has the capability to utilize telecommunications links and the Internet for real time remote displays when available.

The MAARCO container is 'mobile' in the sense that it can be easily moved it to new sites to perform research. One of the primary obstacles in performing research overseas is the difficulty in finding adequate facilities at good site locations. Most aerosol instruments prefer, if not require, climate controlled environments for stable, consistent operation. These conditions are not readily available in remote or foreign sites. Radiation instruments are for the most part less sensitive to changes in the environment, but are also much more valuable when run in conjunction with other instruments to fully characterize the local environment.

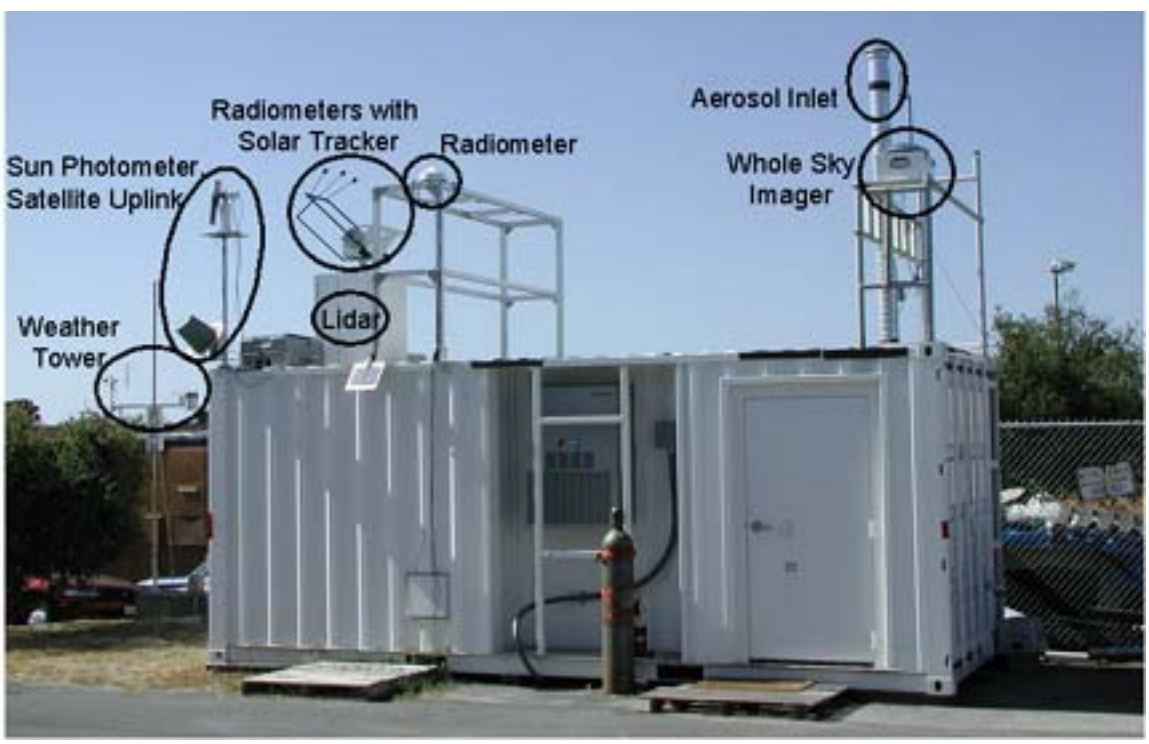


Figure F.1. Overview of MAARCO container with outboard radiation and meteorology equipment.

Table F.1 Listing of MAARCO available equipment.

| | Instrument | Power Usage | Net Power | Shipping Weight | Weight of Instrument | Net weight |
|---|---|---|---|---|---|---|
| 1 | Aeronet Sun Photometer: | solar | 0 | 30 kg | 26 kg | 30 kg |
| 2 | Pyranometers, 2 | solar | 0 | 1 kg | 930 g | 2 kg |
| 3 | Pyrgeometers, 2 | solar | 0 | 1.2 kg | 1050 g | 2.4 kg |
| 4 | Pyrheliometer | solar | 0 | 1 kg | 700 g | 1 kg |
| | CV2 ventilation unit – 4 total | 12 V DC, 1.25 A<br>5 W continuous, 10 W heating | 40 W | 1 kg | 1 kg | 4 Kg |
| | Solar tracker | 115 VAC<br>150 VA power | 150 VA | 45 kg | 30 kg | 45 kg |
| 5 | Total Sky Imager | 115 VAC<br>50-600 W depending on whether heater is on | 600 W | 30 kg | 20 kg | 30 kg |
| 6 | Nephelometer | 24 +/- 4 VDC at 5A, 175 W maximum | 175 W | 30 kg | 23 kg | 30 kg |
| 7 | Aerodynamic Particle Size | 85 to 264 VAC, 100 W | 100 W | 27 kg | 17 kg | 27 kg |
| 8 | TSP filter Pump | 115 V, 60 Hz, 15 Amp | 1725 W | 25 kg | 22 kg | 25 kg |
| 9 | Tapered Element Oscillating Mass Balance | 115 V, 60 Hz, 1 Amp | 115 W | 90 kg | 75 kg | 90 kg |
| | TEOM Pump | 115 V, 60 Hz, 5.3 Amp | 1000 W | 16 kg | 15 kg | 16 kg |
| 11 | Optical Particle Counters | 115 V, 60 Hz, 5.3 Amp | 400 W | 100 kg | 90 kg | 100 kg |
| 12 | SO2 Monitor | 105-125 VAC, 60 Hz, 10( Watts | 100 W | 24 kg | 20 kg | 24 kg |
| 13 | Ozone monitor | 90-110VAC, 60Hz, 150 Watts | 150 W | 20 kg | 16 kg | 20 kg |
| 14 | MOUDI sampler | 115 VAC, 60 Hz, 0.3 A | 35 W | 15 kg | 13 Kg | 15 kg |
| 15 | MPL LIDAR | 115 VAC, 60 Hz, ~ 5A | 575 W | 120 kg | 40 kg | 120 kg |
| 16 | Weather Station | solar | | 60 kg | 50 kg | 100 kg |
| 15 | Mini-Rawinsonde System (MRS) AN/UMQ-12 | | 100 W | 50 kg | 45 kg | 50 kg |
| | Radiosondes, 50 | battery | | 0.75kg ea | | 38 kg |
| 17 | Laptop computers, 5 | 5@ 80 W | 400 W | 3 kg ea | 2.5 kg ea | 15 kg |
| | Rack computers, 2 | 2@ 200 W | 400 W | 10kg ea | 9kg ea | 20 kg |
| | Racks, 3 | | | 30 kg | 30 kg | 90 kg |
| 18 | Scaffolding | | | 50 kg | 50 kg | 50 kg |
| | Ladders, 2 | | | 15 kg | 15 kg | 15 kg |
| | Batteries/UPS, 5 | | | 20 kg ea | 18 kg ea | 100 kg |
| | NET Equipment | | 7 kW | | | 1060 kg |
| | MAARCO container | 220V 3-phase, or 110 V, 60 Hz. Up to 200 Amps | AC/heater and light only:<br>4 kW | | 2040 kg | 2040 kg |
| | NET TOTAL | | 10 kW normal operation. | | | 3100 kg |

**1. The AERONET** (AErosol RObotic NETwork) Sun photometer. The AERONET program is an inclusive global federation of ground-based remote sensing aerosol networks. The goal is to assess aerosol optical properties and validate satellite retrievals of aerosol optical properties. Data from this collaboration provides globally distributed observations of spectral aerosol optical depths, inversion products, and precipitable water in geographically diverse aerosol regimes. Direct sun measurements are made in eight spectral bands to derive aerosol optical thickness (AOT). In addition, this instrument measures the sky radiance in four spectral bands to acquire aureole and sky radiances observations through a large range of scattering angles from the sun to retrieve size distribution, phase function and aerosol optical thickness.

**2. MPL LIDAR**: The MPL LIght Detection And Ranging is a single channel (523nm), autonomous, eye-safe system used to determine the vertical structure of clouds and aerosols. The MPL data is analyzed to produce optical properties such as extinction and optical depth profiles of the clouds and aerosols. It is valuable also for locating atmospheric layers of interest for aircraft sampling, and to assist in interpreting the sun photometer, pyrgeometers, pyranometers, and pyrheliometer radiation (visible and IR light) instrument data. The primary goal of MPLNET is to provide long-term data sets of cloud and aerosol vertical distributions at key sites around the world. The long-term data sets will be used to validate and help improve global and regional climate models, and also serve as ground-truth sites for NASA/EOS satellite programs.

**3. Pyranometers**. Kipp & Zonen CM 21 Pyranometers measure incoming global solar radiation (0.3 to 2.8 µm spectral range). We use two pyranometers on MAARCO: one in direct sunlight to give total solar irradiance, and one on the solar tracker shaded by tracker balls (that block the sun and shade the pyranometers) to measure diffuse sky irradiance.

**4. Pyrgeometers:** Kipp & Zonen CG 4 Pyrgeometers provide high accuracy infrared radiation (IR) measurements, from 4.5 to 42 µm. We use two pyrgeometers on MAARCO: one in direct sunlight to give total IR irradiance, and one on the solar tracker shaded by tracker balls (that block the sun and shade the pyranometers) to measure diffuse sky IR irradiance.

**5. Pyrheliometer:** Our Kipp & Zonen pyrheliometer is mounted on our solar tracker – allowing it to constantly point at the sun during daylight hours. It is designed for unattended normal incident direct solar radiation measurements, from 0.2 to 4.0 µm.

**6. Total Sky Imager:** Our total sky imager is an automatic camera system that collects real-time images of the entire visible sky at set intervals (up to 1 per minute), processes the data to determine percentage cloud cover, and saves the images for later reference. These data and images are valuable for determining the relative impact of clouds on the measurements taken by other instruments in the MAARCO observatory.

**6. Nephelometer:** MAARCO is equipped with a TSI three wavelength nephelometer with backscatter shutter. The nephelometer measures aerosol light scattering properties of the air pulled into the nephelometer chamber by subtracting light scattered by atmospheric gasses, the walls of the instrument and the background noise in the detector from the light scattering measurement. Besides characterizing the light scattering properties of particles in the air, it provides data on aerosol particle sizes and concentrations in the sampled air.

**7. Aerodynamic Particle Sizer.** We use an APS 3321 to determine aerodynamic diameter and light-scattering intensity. The APS provides high-resolution, real-time aerodynamic measurements in the range from 0.5 to 20 micrometers. It also measures light-scattering intensity in the equivalent optical size range of 0.37 to 20 micrometers.

Because it provides paired data (aerodynamic diameter and light-scattering intensity) for each particle, the APS provides clues to the makeup of the aerosol particles.

**8**. **Optical particle counters:** These are probes typically mounted on aircraft but have been modified for ground operation.

**9. TSP filter**: Total suspended particulates are collected in our air filter system for later mass, elemental composition, and particle morphology analysis.

**10. Tapered Element Oscillating Mass Balance:** TEOM is an extremely sensitive aerosol mass instrument; it continuously (real-time) measures the mass or 'weight' of the particles that are collected from air as it passes through a filter. This real-time mass measurement is valuable for correlation with the other particle and gas measuring instruments, and to understand current atmospheric conditions, allowing users to identify episodes and determine trends in real time.. Also, the filter can be later analyzed for elemental composition and particle morphology.

**11. $SO_2$ Monitor:** The SO2 monitor provides a continuous, and a time averaged measurement of sulfur dioxide in the atmosphere. As SO2 is a reactive compound that can modify aerosol particles, and is correlated to visibility degradation and industrial processes, we measure this compound for chemistry, and to gain clues to the origin of the air mass we are sampling.

**12. Ozone monitor:** The ozone monitor provides a continuous, and a time averaged measurement of ozone in the atmosphere. Ozone is also a reactive compound that can modify aerosol particles, and is correlated with industrial processes and smog. We track ozone to understand the changing atmospheric chemistry, and to get clues to the origin of the air mass.

**13. MOUDI sampler**: The MICRO-ORIFICE, UNIFORM-DEPOSIT IMPACTOR atmospheric aerosol particle sampler is a precision cascade impactor for collecting size-fractionated aerosol particle samples for gravimetric (mass or 'weight') and chemical analysis. It size-fractionates the sampled aerosol particles into ten size bins, over wide size range, 0.056 – 18 μm.

**14. Weather Station:** The weather station provides local weather conditions including wind speed, direction, humidity, temperature, and solar radiation.

**15. Radiosonde system**: The radiosonde system utilizes balloons to lift instrument packages though the troposphere to continuously measuring wind speed, direction, elevation, and humidity as the balloons ascend. This provides data to correlate with the vertical structure of clouds and aerosols observed by the MPL Lidar system, and to understand the local weather conditions.

## Appendix G. The SMART COMMIT System

**Si-Chee Tsay and Jack Ji , NASA GSFC**

The NASA/GSFC SMART (Surface-sensing Measurements for Atmospheric Radiative Transfer) and COMMIT (Chemical, Optical & Microphysical Measurements of In-situ Troposphere) is a mobile measurement facility. The SMART ground-based instrument suite (*cf.* Fig. G.1 and Table G.1) was integrated into a weather-sealed trailer with thermostatic temperature control, which facilitated good data quality in hot/cold and humid environments. It consists of many commercially available radiometers (pyranometer, pyrheliometer, pyrgeometer, etc.), a spectrometer, an interferometer, and many in-house developed remote-sensing instruments (e.g., micro-pulse lidar, scanning microwave radiometer, and sun-sky-surface photometer). During field deployments, SMART collocates with satellite nadir overpass for intercomparisons and for initializing model simulations. Many researchers (both experimentalists and theoreticians), as well as graduate students, have taken part in hands-on operation of the SMART instrumentation. The participation of graduate students has an educational/outreach component because the students have an unusual opportunity to expose themselves to the procedure of data acquisition by the state-of-the-art ground-based radiation instruments.

In complementing the capabilities of SMART, we have developed COMMIT to recognize the importance of measuring the in-situ properties of atmospheric constituents and particulates at (or near) the source/sink region and during transport. Remote sensing and retrievals of atmospheric constituents and aerosols from satellite measurements often lack sensitivity and accuracy in the planetary boundary layer. Improvement of our understanding of processes involving chemically and radiatively important aerosols and carbonaceous trace gases requires better monitoring of the characteristics of the boundary layer. The COMMIT facility contains in-situ instruments to measure trace gas (CO, $SO_2$, $NO_x$, and $O_3$) concentrations, fine-to-coarse particle size, concentration and chemical composition, and aerosol light extinction at one (green) and three (blue, green, and red) wavelengths with respective to the ambient and modulated relative humidity.

As part of $UAE^2$, SMART will be deployed in full to a remote desert site. Aerosol instrumentation form COMMITT will be deployed with the MAARCO container to a coastal site. This instrumentation includes an Aerodynamic particle sizer (APS), Scanning Mobility particle Sizer (SMPS), and TSI three-wavelength nephelometer.

Figure G. 1. The latest version of the SMART system shown in center panel: ($a_1$) an array of broadband-total radiometers in ultraviolet, shortwave and longwave regions, ($a_2$) broadband-direct radiometers, ($a_3$) broadband-diffuse radiometers, (b) shadow-band radiometer, ($c_{1\text{-}2}$) sun photometers, (d) meteorological probes for atmospheric pressure, temperature, humidity, wind speed/direction, (e) interferometer, (f) solar spectrometer, (g) whole-sky imager, (h) scanning microwave radiometer, (k) soil moisture probes, ($m_1$) physical rain gauge, ($m_2$) optical rain gauge, and (n) micro-pulse lidar.

Table G.1. NASA/GSFC Surface-sensing Measurements for Atmospheric Radiative Transfer (SMART) instrument and measurement parameter list.

| Instrument | Measurement Parameter |
|---|---|
| Broadband Radiometers | Solar Irradiance at 0.3~3, 0.4~3, 0.7~3 µm (Global, Diffuse & Direct on Solar Tracker); Global Irradiance at 302, 308, 315, 336, 377, 400~700 nm; Sky Irradiance at 4~50 µm |
| Sun Photometer | Solar Radiance at 8 or 14 Wavelengths |
| Shadow-band Radiometer | Solar Irradiance at 414, 498, 614, 672, 866, 939, and 300~1000 nm (Global, Diffuse, and Direct) |
| Micro-pulse Lidar | Aerosol profile in Normalized Relative Backscatter Intensity |
| Sky Imager | Hemispherical Sky Image |
| Spectroradiometer | Solar Spectral Irradiance 0.4~2.5 µm |
| Interferometer | Downwelling Spectral Radiance 500~3000 $cm^{-1}$ |
| Microwave Radiometer | Sky Radiance at 23, 23.8, and 36 GHz |
| Meteorological Sensors | Air Temperature, Relative Humidity, Pressure, Wind Speed/Direction |
| Optical/Physical Rain Gauge | Rain Rate |
| Garmin GPS | Geographical Location |
| Laboratory Container, 8’ x 8’ x 20’ | Air-conditioned Facility to Hold all Instruments |

# Appendix H. Other field deployments

## H.1 TNO Seven Wavelength Transmissometer

Transmission measurements using the 7 wavelength bands with the recently developed transmissometer will be made in UAE[2]. With these wavelengths, varying from the UV to the NIR, a good assessment can be made on the working of the aerosol models. Transmission is measured in the following seven wavelength bands: 0.40-0.49 µm, 0.57-0.65 µm, 0.78-1.04 µm, 1.39-1.67 µm, 2.12-2.52 µm, 3.55-4.15 µm, and 7.8-13.7 µm. The set-up consists of a double-source (optical and IR part). The modulation frequency is 1160 Hz and a reference signal is transmitted through a radio link. The bundle divergence is approx. 5 mrad and the alignment is performed using a target finder. The receiver is a 7-channel radiometer with linked-up lock-in amplifiers. The integration time is set for 1.1 seconds. Data are written to a data acquisition system that allows for continuous registration. The 4 µm and 10 µm detectors are cooled with liquid nitrogen. The radiometers have a FOV of approx. 1.5º, which is directed by the target finder. The sensitivity of the system is such that for all channels and in case of a "clean" range of 8 km, a S/N ratio of at least 100 is achieved. If the windows are regularly checked for and if calibration is conducted before and after the experiments, only then is an absolute accuracy of 10% achieved. The sensitivity makes it possible to determine the extinction coefficients in each of the channels. It also makes it possible from the mutual ratios, to seek the correlation with the size distributions as obtained from other equipment.

# Appendix I. Investigator Summaries and Plans for Remote-Sensing Research

## I.1 MISR Goals and Contributions

**Ralph Kahn, John Martonchik, Olga Kalashnikova, David Diner, and Barbara Gaitley.**

**Jet Propulsion Laboratory**

Among the strengths of the Multi-angle Imaging SpectroRadiometer (MISR) instrument, flying aboard the NASA Earth Observing System's Terra satellite, are its sensitivity to the shape of airborne particles [Kahn et al., 1997]. This means that the MISR data contain some information about mineral dust microphysical properties that we hope to extract in the aerosol retrieval process. The MISR aerosol retrieval algorithms have demonstrated success at retrieving mineral dust mid-visible optical thickness (AOT) over both land and water, and uniquely over bright surfaces, with a sensitivity of about ±0.07 [Martonchik et al., 2004; Kahn et al., 2004; Christopher and Wang, 2004]. We have also developed detailed models of mineral dust microphysical properties incorporating the most recent field campaign results, with the aim of further refining the algorithm [Kalashnikova et al., 2004].

The biggest challenge to achieving this goal is obtaining adequate ground truth. All published studies to date rely upon sun photometer data for validation, which has enormous strengths in terms of coverage and accuracy. But the sun photometer's column-averaged spectral AOT alone, and even the sky-scan size distributions, are not sufficient to constrain differences between medium and coarse mode SSA, particle shape, and vertical distribution. Currently, the only comprehensive field data coincident with MISR overpasses that contain dust are from ACE-Asia [Kahn et al., 2004b], which are mixtures that include considerable pollution and background maritime aerosols as well, and from PRIDE, which turned out to be significantly cloud-contaminated.

The upcoming campaign is our next opportunity to collect critical field data to refine and test our algorithm. We would aim for situations where as much as possible of the aerosol vertical structure, height-resolved aerosol micro-physical properties, aerosol optical properties, and surface BRDF were observed over a few-tens-of-km region, coincident with MISR overpasses. Over 40 MISR overflights are predicted between late June and early October, 2004, encompassing the intensive field operations period (Table 1, attached). The combination of surface-based sun photometer and lidar data, airborne sampling, optical, and physical particle characterization, and airborne remote sensing instruments promised for this campaign should provide most or all the key information needed to take the next step with our algorithm.

We are also ready to contribute MISR regional aerosol retrieval results both prior to and during the campaign. As an initial contribution, attached are time-series of MISR and AERONET data over the Solar Village AERONET site, for 2001 and 2002. The purple are the AERONET measurements, connected by straight-line segments for clarity. The dark green circles are MISR retrieval AOT results for the 17.6 km region that includes the AERONET site. The light green circles are the average of up to eight MISR retrieval AOT results for the 17.6 km regions surrounding the one that includes the AERONET site. The "surroundings" retrievals are plotted only if there is no successful central region retrieval. The four plots in each figure report AOT in each of the MISR spectral bands (centered at 446, 558, 672, and 866 nm). Note that the MISR AOTs for some dusty retrievals are high relative to AERONET. This is traced to old dust models in the MISR algorithm, having too much absorption [Kahn et al., 2004a]. New dust optical models that address this problem have been developed [Kalashnikova et al., 2004], and are being added to the MISR algorithm in the next few months. Further refinements of the MISR dust component retrieval await results of the forthcoming campaign.

## I.2 NRL Monterey Satellite Research: Proposed Science Plan

**Steven D. Miller, Arunas Kuciauskas, and Cristian Mitrescu**
**Naval Research laboratory, Monterey CA.**

For the past several years leading up to and including the conflicts in Afghanistan and Iraq, the Satellite Meteorological Applications Section (Code 7541; hereafter NRL-SatMet) at NRL Monterey has been involved in extensive satellite product demonstrations over the Southwest Asia domain. Included in this value added product suite are items of particular relevance to aerosol properties and derived parameters of particular tactical relevance to the Navy (e.g., laser attenuation and slant range visibility). Leveraging a cadre of near real-time satellite telemetries (including passive optical and microwave sensors aboard eight polar orbiting and one geostationary platform) and Linux-based cluster post-processing system, NRL-SatMet parlayed this “accelerated research/development/application transitional environment” into a pseudo-operational support mechanism during Operations Enduring and Iraqi Freedom, via the “Satellite Focus” webpage interface. We believe this near real-time framework is well posed for participation in any intensive observation periods (IOPs) emerging from the current United Arab Emirates campaign.

In particular, significant dust enhancements over land and ocean, based on Moderate Resolution Imaging Spectroradiometer (MODIS; aboard the National Aeronautics and Space Administration’s (NASA) Earth Observing System (EOS) Terra and Aqua satellites), Sea-viewing Wide Field-of-view Sensor (SeaWiFS; aboard OrbImage’s SeaStar satellite), and Meteosat-5 Visible/Infrared Spin-Scan Radiometer (VISSR) data, combined with model wind overlays matched to the data from the Navy’s Coupled Ocean/Atmosphere Mesoscale Prediction System (COAMPS™), would facilitate both the detection and tracking of dust regions advecting into the UAE

observing domain. Aerosol optical depths (AOD) retrieved from MODIS and the Advanced Very High Resolution Radiometers (AVHRR, aboard the National Oceanic and Atmospheric Administration's (NOAA) Polar Orbiting Environmental Satellites (POES), using the AOD retrieval technique developed at the Naval Postgraduate School (NPS), provides quantitative information speaking to the key operational metrics mentioned above. Various cloud detection and cloud property products may also play a role in IOP planning and execution.

We regard the UAE campaign as an opportunity for symbiosis in the areas pertaining to a) providing near real-time satellite information over the area of interest that potentially is of use in the definition/coordination of field campaign data collection strategies, b) obtaining in situ information (e.g., from the Aerosol Robotic Network (AERONET), Mobile Atmospheric Aerosol and Radiation Characterization Laboratory (MAARCO), Cloud Physics Lidar (CPL), and Cloud Absorption Radiometer (CAR)) useful in the quantification and/or validation of various NRL-SatMet products, and c) exploring potential multisensor applications. Specifically, these activities would potentially include:

1) Process a dedicated sector over the UAE domain upon the NRL-SatMet Satellite Focus Webpage, to include the full complement of cloud (convective cloud heights, nocturnal low cloud detection, multi-layered cloud product, cirrus detection product, and MODIS-L2 cloud optical properties), aerosol (the aforementioned dust enhancement and retrieval products), surface characterization products (e.g., fire/hot-spot, and normalized-difference vegetation index), satellite-derived precipitation (rainrate and accumulation), and general imagery products (visible, infrared, vapor, and 250m true color) with COAMPS™ model field overlays for meteorological characterization. The logistics of making these data available via a DoD-exclusive interface to members of the community involved in the current campaign would need to be explored.

2) Leveraging AERONET observations for the purpose of both validating the NPS-AOD algorithm and quantifying the significant dust enhancement. The NPS-AOD and NRL significant dust enhancement to date have had few opportunities for validation. If the NPS-AOD algorithm is found to be robust, the quantification of the significant dust enhancement can then be extended beyond the UAE domain.

3) Combining CPL cross-sections with NPS-AOD retrievals to approximate extinction profiles, derive slant-range visibility, and compare to surface observations and those derived from AERONET. Explore to what extent the assumption of horizontal homogeneity applies, potentially applying the significant dust enhancement and/or the Navy Aerosol Analysis and Prediction System (NAAPS) fields in this regard.

In anticipation of multisensor applications as described in (3), we have begun exploring the Geoscience Laser Altimeter System (GLAS) attenuated lidar backscatter and level-2

aerosol layer data from the Ice, Cloud, and land Elevation Satellite (IceSat), made available over limited segments by the National Snow and Ice Data Center (NSIDC). The hope is to match IceSat to greatest extent possible spatially and temporally with MODIS Terra/Aqua over southwest Asia during the time period of March 2003, when several notable dust events occurred. Provided sufficient data exists, this exercise will help develop the techniques applied with CPL data during the UAE experiment. Provided the continued availability sufficient resources and minimal conflicts with existing FY04 obligations, this work will be conducted under the auspices of the Office of Naval Research, under program element PE-0602435N, supporting the 6.2 "Key Parameters" NRL-SatMet work unit. Key performers are to include Dr. Steven Miller (Satellite Focus product suit and general POC), Mr. Arunas Kuciauskas (activities associated with NPS-AOD product), and Dr. Cristian Mitrescu (CPL and multi-sensor applications toward slant range visibility estimation.

## I.3 Aerosol Retrievals Over Deserts from SeaWiFS and MODIS

**N. Christina Hsu**
**University of Maryland Baltimore County/ NASA Goddard**

*Mission Objectives*
In this project, we will use the aircraft- and ground-based remote sensing and in situ measurements to help improve our satellite aerosol retrieval algorithm. Specifically, our mission objectives are to:

(1) Study the microphysical and optical properties of mineral dust, anthropogenic air pollutants and marine aerosols in the region of interest to build a more realistic aerosol library for use in the retrieval algorithm;
(2) Validate the SeaWiFS and MODIS aerosol products over bright surfaces produced from our algorithm not only with an airmass that is dominated by one single aerosol type and but also under mixed aerosol-type conditions; and
(3) Evaluate the effect of surface BRDF over deserts on the satellite retrieval of the SeaWiFS and MODIS aerosol products over bright surfaces through aircraft and ground based bi-directional surface reflectance measurements.

*Mission Plan*
In support of the UAE field campaign, we will use satellite measurements to provide a "big-picture" look at the aerosol loading distribution over the region. In particular, we will:

(1) Provide near-real time SeaWiFS aerosol products of aerosol optical thickness and Angstrom exponent over the region of interest during August and September 2004 to support flight planning;
(2) Provide post-mission MODIS aerosol products of aerosol optical thickness and Angstrom exponent over desert and semi-desert regions;

(3) Characterize the temporal and spatial variability of aerosol loading over the entire region of interest, including over desert and semi-desert areas for the duration of the intensive observation period;
(4) Identify the sources of wind-blown dust to help improve the ability to forecast dust storms in the region of interest; and
(5) Characterize the physical and optical properties of dust from different sources.

Our goal is to take advantage of the golden opportunity provided by the UAE field campaign to gain a detailed and comprehensive understanding of the mineral dust and air pollution aerosol properties. The use of aircraft and ground information will help us better interpret our studies that use satellite observations to determine aerosol effects on the radiation budget in the entire atmospheric column. Our participation in this campaign will also help us to learn the strengths and weaknesses of our algorithm, using SeaWiFS and MODIS data, in retrieving aerosol properties over bright surfaces.

## I.4 AATSR Dust Optical Depth Retrievals

**Robin Schoemaker and Gerrit de Leeuw**
**TNO Physics and Electronics Laboratory, The Hague, Netherlands.**

The Advanced ATSR (AATSR) instrument onboard the European ENVISAT satellite is a radiometer with seven wavelength bands of which four are in the visible and NIR (0.555, 0.659, 0.865, and 1.6 µm) and three are in TIR (3.7, 11, and 12 µm). The AATSR instrument is functionally the same as the ATSR-2 onboard ERS-2, but the mechanics and some components have been re-worked to match the environment of the ENVISAT platform. AATSR is a dual view imaging spectrometer with a conical scanning mechanism for forward view at a 55º incident angle to the surface and a nadir view at approx. 0º angle to the surface. The resolution of this instrument is 1 x 1 $km^2$ at nadir view and the swath width is 512 km, which provides in a global coverage every three days. While the four VIS/NIR channels are particularly useful for aerosol retrieval, the key problem in retrieval over land is to distinguish between atmospheric scattering contributions and the surface reflectance contributions to the TOA reflectance, contrary to retrieval over sea where surface reflection is negligible *a priori* and retrieval is less complex. To solve for the retrieval over land, the dual view technique is used which makes use of the along track scanning mechanism that enables sensing of the same point on the Earth's surface along the orbit through two different columns of atmosphere separated by a time interval of approx. 2.5 minutes. A so-called dual-view algorithm uses both the directional and the spectral information in the instrument data to separate between atmospheric and surface contributions for cloud-free scenes in the retrieval procedure. This procedure on its turn makes use of reflectance and AOD values of pre-modeled aerosol types that are to be compared to the TOA reflectance and aerosol extinction for the appropriate wavelengths. The quasi-operational algorithm requires as input the gridded brightness temperature/reflectance data product. Corrections, a fully automated cloud screening, and retrieval computations consequently yield the various

aerosol properties like AOD and Ångström parameter in the output. AOD is computed for a pixel size of 10 x 10 $km^2$ for a regional scale (e.g. Europe) and other statistical composites like standard deviation are likewise obtained. The retrieval of aerosol optical depth over land currently delivers an accuracy of 0.06, while over sea an accuracy of 0.04 is achieved – both based on comparisons with sun photometers.

The AATSR measurements aim for retrieval of dust optical depth maps for the given region, which are to be compared with sun photometer measurements and other space based measurements using MODIS and MISR data. The intention is to investigate whether the retrieval of dust optical depth using AATSR gives reliable results above the high reflecting desert surface. Implementation of the TIR bands of AATSR in the retrieval algorithm is part of the analysis.

## I.5 Satellite Retrievals of Land Surface Temperature and Microwave Emissivity over the Arabian Peninsula

**Benjamin Ruston**
**Naval Research Laboratory, Monterey, CA**

The atmosphere at most microwave frequencies is semi-transparent. Consequently, a radiance measurement from a microwave radiometer contains information from clouds, the atmosphere, and the underlying surface. Over land surfaces, particularly when in clear-sky or non-precipitating cloud regimes, the microwave satellite measurement is dominated by the contribution from the land surface itself. The emissivity of a surface is defined as its emission efficiency. If the microwave surface emissivity is well known, an atmospheric retrieval can then extract the greatest amount of information from the satellite radiance measurement. The accuracy of a microwave emissivity estimate relies on the precision to which the land surface temperature is known. The $UAE^2$ field campaign will provide the researcher with in-situ ground and aircraft based measurements to minimize the error in the retrieved land surface temperature, and subsequently reduce the error in the microwave emissivity. In addition, the United Arab Emirates Department of Water Resources Study stations are adequately equipped to provide soil moisture information required for a forward microwave emissivity model, which can be validated against the satellite-based retrievals.

# Appendix J: Summary of AERONET research in Southwest Asia, Alexander Smirnov (GEST/GSFC)

AERONET is a federated international network of sun/sky radiometers. AERONET has been operational for more than 10 years (since 1993) and maintains more than 150 automatic instruments (sun/sky radiometers) worldwide [*Holben et al*. 1998; *Holben et al*. 2001]. It deploys standardized instrumentation (automatic Sun and sky scanning radiometers CIMEL), measurement protocol, data processing, cloud-screening algorithm, and inversion techniques to retrieve information on columnar aerosol characteristics [*Holben et al.* 1998; 2001; *Eck et al*. 1999; *Smirnov et al*. 2000; *Dubovik and King* 2000; *Dubovik et al*. 2000]. Data are publicly available online in near real-time mode (http://aeronet.gsfc.nasa.gov). All of the measurements reported here were made with the automatic Sun and sky scanning radiometers CIMEL. The CIMEL Sun and sky radiometer measures direct sun flux in the eight spectral channels between 340 and 1020 nm (340, 380, 440, 500, 670, 870, 940 and 1020 nm). The 940 nm data is used for the columnar water vapor content estimations. Diffuse sky fluxes in the solar almucantar are acquired at 440, 670, 870 and 1020 nm wavelengths. Typical total uncertainty in $\tau_a(\lambda)$ for a field instrument is ±0.01-0.02 and is spectrally dependent with the higher errors (±0.02) in the UV spectral range [*Eck et al*. 1999].

Table J.1. Deployment history in the Persian Gulf region

| Site | Time period | CIMEL | Data Quality | N days/ N months |
|---|---|---|---|---|
| Bahrain | 07/23/1998-10/25/2000 | Standard | Level 2 | 517/24 |
| Solar Village, Saudi Arabia | 01/22/1999-present | Standard | Level 2 | 1240/49 |
| Al Dhafra, UAE | 01/11/2001-09/09/2001 | Standard | Level 2 | 119/6 |
| Dhabi, UAE | 10/05/2003-present | Standard | Level 1.5 | 158/6 |

AERONET has accumulated a significant amount of data at operational sites in the Persian Gulf region (Bahrain; Solar Village, Saudi Arabia; Al Dhafra and more recently at Dhabi, United Arab Emirates). Initial effort in Bahrain (July 1998) lasted for two years and then the site was abandoned because of the organizational difficulties. The site in Saudi Arabia, not far from the capital Riyadh (Solar Village) is currently operational and has been operational since June 1999. Detailed information on the seasonal, inter- and intra-annual variability of aerosol optical properties for Bahrain and

Solar Village sites can be found in the studies by *Holben et al*. [2001], *Dubovik et al*. [2002], and *Smirnov et al*. [2002]. The Table 1 presents the deployment history.

According to the Forecaster's Handbook [*Heishman*, 1999] the area's long-term climatology has enabled the following seasonal divisions to be established for the Persian Gulf: southwest monsoon (June-September), fall transition (October-November), northeast monsoon (December-March), and spring transition (April-May). During the southwest monsoon a northwesterly flow occurs at all levels over the Arabian Peninsula bringing extremely dry air and dust from the Iraqi deserts. During the fall transition season, winds remain northwesterly but speeds decrease, the frequency of occurrences of dust storms decreases significantly, and air temperatures drop. The northeast monsoon is characterized by a very complex airflow pattern, which can be a combination of land-sea breezes, outflow from the Persian Gulf and northeasterly flow off the Iranian coast. Dust usually is advected from Saudi Arabia, Iraq or southern Iran [*Liu et al.,* 2000]. In the April-May period winds are predominantly from the North or North-northwest, and the frequency of dust storms increases.

Figure J.1 illustrates the monthly averaged aerosol optical depth at 500 nm for the available record (see Table 1). Aerosol optical depth peaks in July and August, although for Solar Village it is a secondary maximum. It is noteworthy that monthly averages for Solar Village are not very high (less 0.40 as a 5 year average). Aerosol loading is higher for Bahrain and Al Dhafra although it might be a result of less robust statistics (much shorter record). For Solar Village, Bahrain and Al Dhafra the monthly average of the least turbid month is smaller than the maximal monthly $\tau_a$ (500 nm) by a factor of 3. Monthly averages of the Angstrom parameter $\alpha$ (derived from a multi-spectral log linear fit to the classical equation $\tau_a \sim \lambda^{-\alpha}$ and based on four wavelengths in the range 440-870 nm) for the whole period of observations are shown in Figure J.2. The notable decrease of the Angstrom parameter during April-September period is associated with the presence of dust in the aerosol loading. Specific pattern for individual sites may be slightly different, for example in Solar Village dust blowing starts in March and $\alpha$ reaches minimum in May when aerosol loading is the heaviest (see also Figure J.1).

Mean monthly values of the columnar water vapor content are presented on Figure J.1. Solar Village is situated in the middle of the Arabian Peninsula and consequently precipitable water monthly averages are lower than in Bahrain or UAE. Nevertheless, intra-annual trend shows a maximum in July-September for all the sites. Optical inversions of sky radiance and optical depth data indicate that the variations in aerosol volume size distributions were largely due to changes in the concentration of the coarse aerosol fraction. Using the alternative technique developed by *O'Neill et al*. [2003] we estimated the input of the coarse aerosol fraction in the total optical depth (Figure B.2.a). The separation of the fine and coarse mode optical depths from the spectral shape of the $\tau_a(\lambda$is purely optical technique and avoids intermediate computations of the particle size distribution [*O'Neill et al*., 2001a, 2001b, 2003]. Figure 4 shows the statistics of the sites in the Persian Gulf region. Frequency of occurrences (based on the daily averages) shows that variations in the aerosol optical depths were

mainly due to coarse aerosol fraction in $\tau_a(\lambda)$. Pollution aerosol affected statistics in Bahrain and the histogram is wider than for other sites considered.

Particle non-sphericity should be taken into account while modeling dust aerosol optical properties. A retrieval method based on the model of a shape mixture of randomly oriented polydisperse spheroids has been developed and applied to the AERONET measurements [*Dubovik et al*. 2002]. Application of this method to the data acquired in Solar Village during the dusty season (from March through September) is shown in Figure J.2 9b). The number of individual retrievals and number of the averaged days is also presented. Figure J.2 (b) illustrates that the spheroid model significantly reduces non-spherical artifacts, i.e. the amplitude of the fine aerosol fraction is smaller and mode radius is not shifted towards smaller radii.

Figure J.2 (c) shows columnar volume size distributions for heavy aerosol loading. The number of averaged retrievals for a particular site and optical depth grouping is also presented. The spheroid retrieval algorithm has been utilized with the residual error threshold less than 10% and the number of scattering angles in the measured sky radiance distributions not less than 21. Solar zenith angle was larger than 45 degrees. The peak in the coarse mode volume radius lays at 2.9 μm, although lognormal fit gives smaller value owing to asymmetry of the size distribution.

Single scattering albedos (SSA) are shown in Figure J.2 (d). When large particles dominate SSA either increases with wavelength or stays neutral (Solar Village). When dust is not a major contributor to the atmospheric optical state, the SSA has a selective spectral dependence (SSA decreases with Y). Also when aerosol mixture has an anthropogenic component the SSA values are lower because anthropogenically influenced aerosol absorbs more than dust. Figure J.2 (d) illustrates that in Bahrain SSA is lower and decreases with wavelength. Single scattering albedos from Cape Verde and Dakar (West coast of Africa) are shown for comparison. Spectral dependencies are similar to Solar Village, and SSA values are slightly lower.

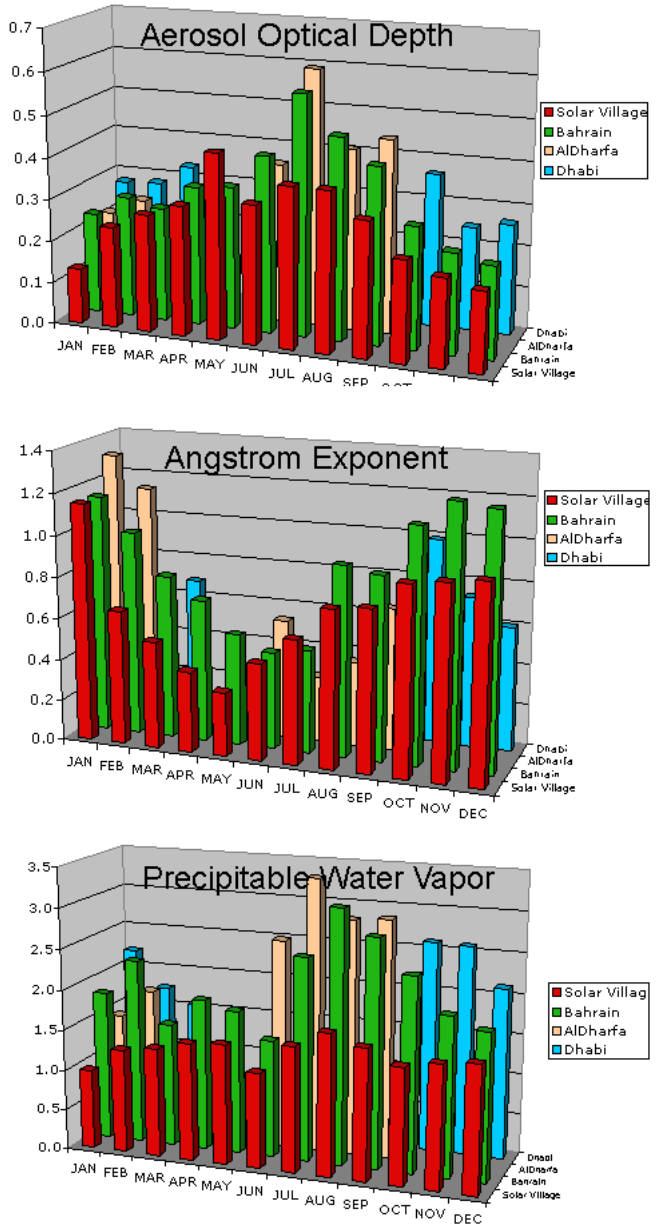


Figure J.1 AERONET optical depth (upper), Angstrom exponent (middle), and precipitable water vapor (lower) monthly averages for Middle-east sites.

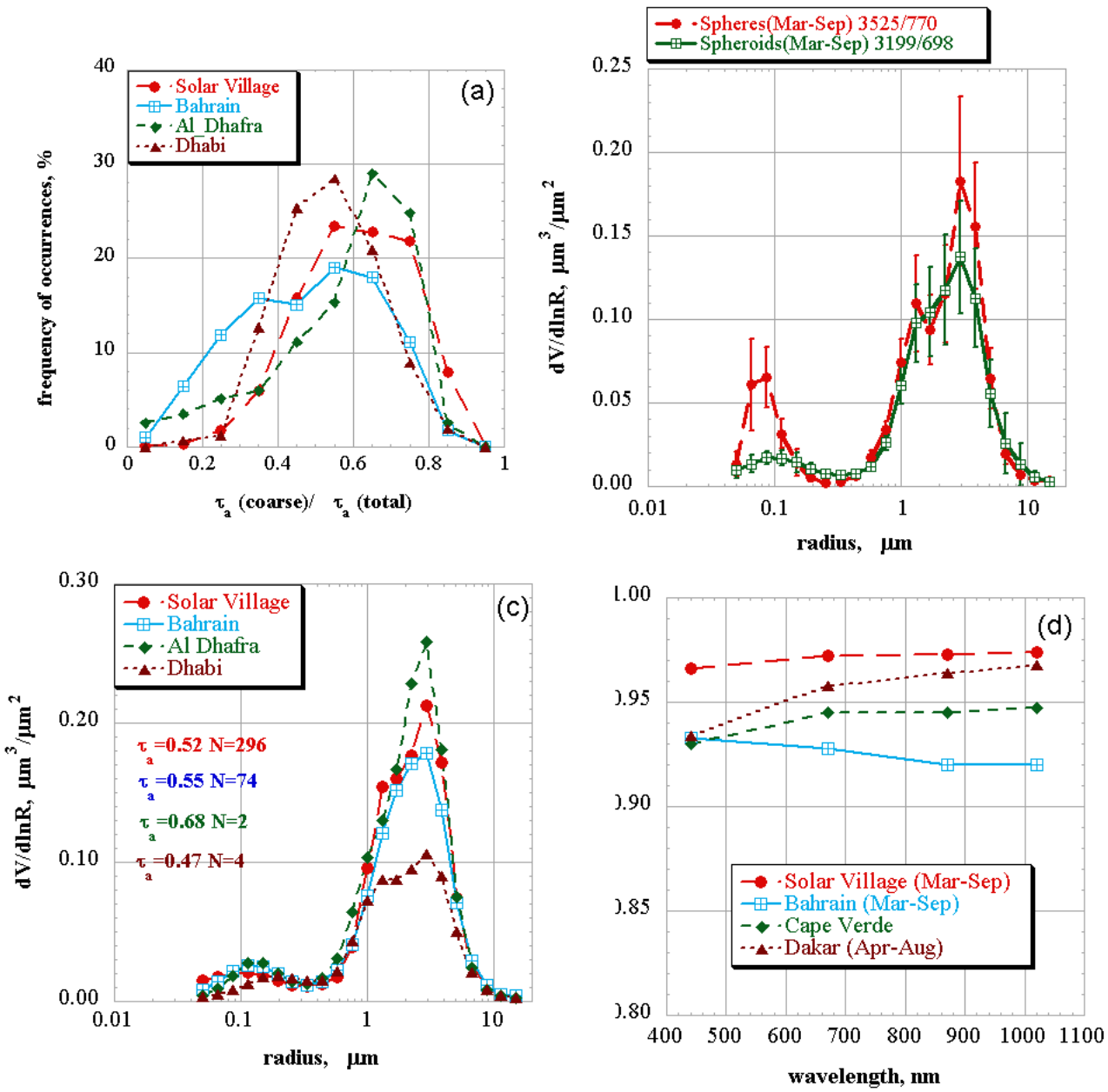


Figure J.2 Aerosol properties inverted from AERONET data. 9a), % frequency of coarse mode fraction. (b) Average volume distribution when using spherical and non-spherical inversions, (c) Average size distribution, (d) Average single-scattering albedo

## Appendix K. Additional Climatological Data for the Southern Arabian Gulf Complied from Fleet Numerical METOC Detachment, Ashville. http://navy.ncdc.noaa.gov/

**Table K.1 Climatological Properties of Abu Dhabi Airport**

| Parameter | August | September |
|---|---|---|
| State Variables | | |
| Abs. Max. Temp. | 115 F | 112 F |
| Avg. Max Temp. | 105 F | 103 F |
| Avg. Temp | 95 F | 91 F |
| Avg. Min | 85 F | 80 F |
| Abs. Min. Temp | 75 F | 66 F |
| Avg. AM Humid. | 71% | 75% |
| Avg. PM Humid. | 44% | 40% |
| Winds | | |
| Prevailing Wind | N @ 10 kts | E@ 5 kts |
| Avg. Onshore Flow | NW @ 13.1 kts 16:00 LST | NW @ 12.1 kts 16:00 LST |
| Avg. Offshore Flow | NE @ 5 kts 7:00 LST | NW @ 5 kts 7:00 LST |
| Visibility | | |
| % <5 mi Min. | 15% at 13:00 LST | 5% at 13:00 LST |
| % <5 mi Max. | 40% at 7:00 LST | 40% at 7:00 LST |
| % days with | | |
| Restricted Vis. | 75% | 67% |
| Smoke/Haze | 39% | 45% |
| Fog | 10% | 22% |

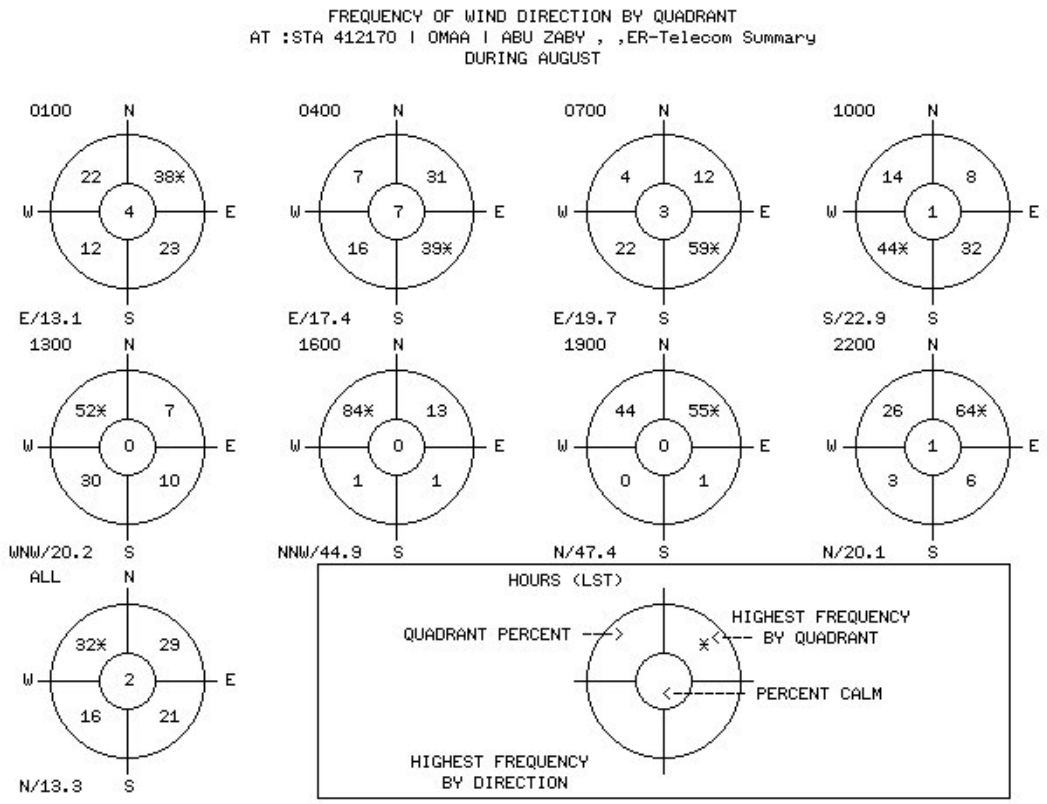


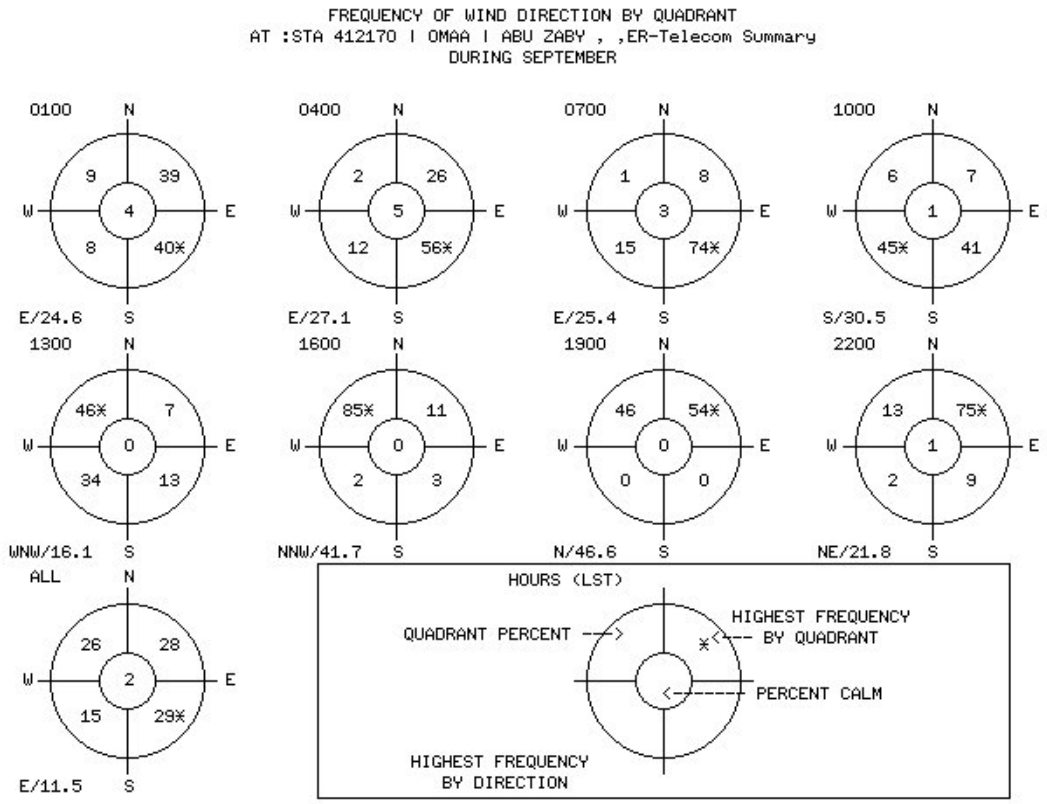


Figure K.1 August and September diurnal wind **directions for Abu Dhabi Airport.**

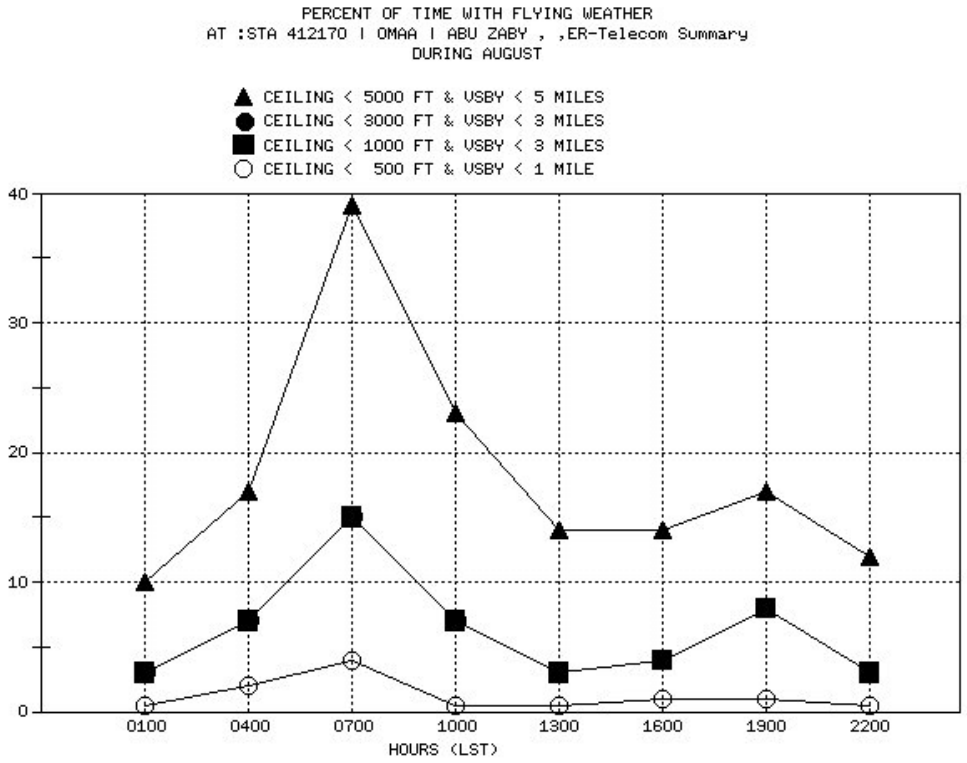


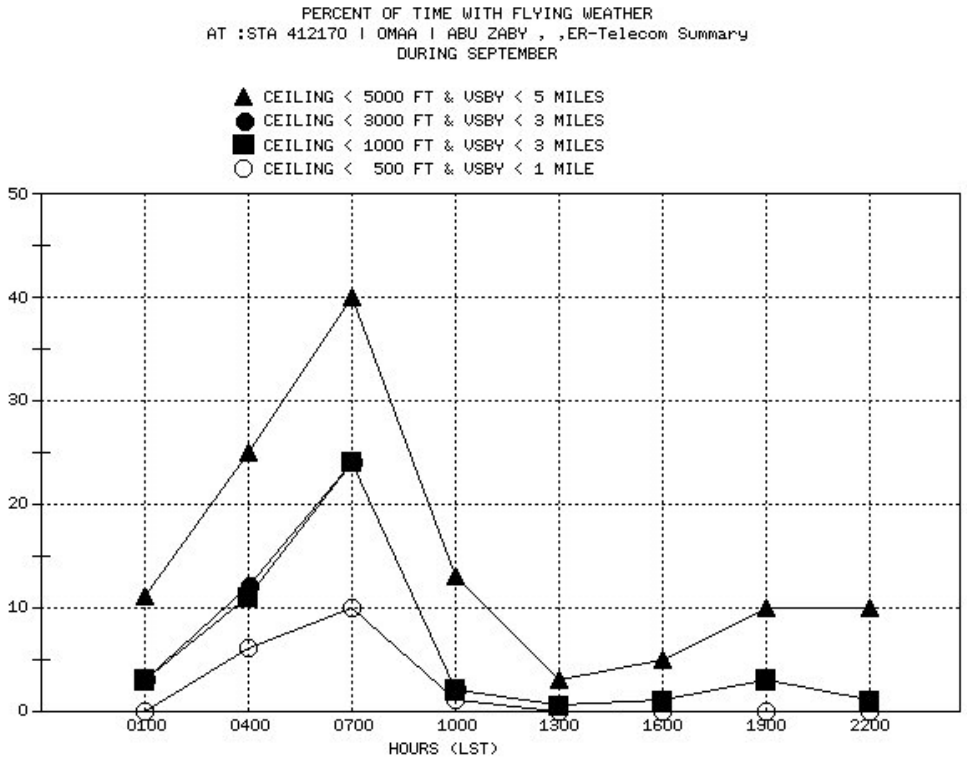


Figure K.2 Diurnal plot of ceiling and visibility probability for Abu Dhabi Airport

## Appendix L. Satellite Overpass Schedules.

### L.1 MISR

| ID# | Site Name | Path | Date | Orbit# | GMT Day (Df) | X-Track(km) | Lat | Lon |
|---|---|---|---|---|---|---|---|---|
| #306t | Ar_Ruways, | Path 162, Block 71 | 31-Jul-04 | 24566 | 2004/213/07:13:00 | 76.0 E | 24.1 | 52.8 |
| #307t | Abu_Dhabi, | Path 160, Block 71 | 2-Aug-04 | 24595 | 2004/215/07:00:00 | 78.0 W | 24.4 | 54.4 |
| #308t | Al_Fujayrah, | Path 160, Block 70 | 2-Aug-04 | 24595 | 2004/215/07:00:00 | 63.0 E | 25.1 | 56 |
| #307t | Abu_Dhabi, | Path 161, Block 71 | 9-Aug-04 | 24697 | 2004/222/07:06:00 | 76.0 E | 24.4 | 54.4 |
| #306t | Ar_Ruways, | Path 161, Block 71 | 9-Aug-04 | 24697 | 2004/222/07:07:00 | 75.0 W | 24.1 | 52.8 |
| #308t | Al_Fujayrah, | Path 159, Block 71 | 11-Aug-04 | 24726 | 2004/224/06:54:00 | 89.0 W | 25.1 | 56 |
| #306t | Ar_Ruways, | Path 162, Block 71 | 16-Aug-04 | 24799 | 2004/229/07:13:00 | 76.0 E | 24.1 | 52.8 |
| #307t | Abu_Dhabi, | Path 160, Block 71 | 18-Aug-04 | 24828 | 2004/231/07:00:00 | 78.0 W | 24.4 | 54.4 |
| #308t | Al_Fujayrah, | Path 160, Block 70 | 18-Aug-04 | 24828 | 2004/231/07:00:00 | 63.0 E | 25.1 | 56 |
| #307t | Abu_Dhabi, | Path 161, Block 71 | 25-Aug-04 | 24930 | 2004/238/07:06:00 | 76.0 E | 24.4 | 54.4 |
| #306t | Ar_Ruways, | Path 161, Block 71 | 25-Aug-04 | 24930 | 2004/238/07:07:00 | 75.0 W | 24.1 | 52.8 |
| #308t | Al_Fujayrah, | Path 159, Block 71 | 27-Aug-04 | 24959 | 2004/240/06:54:00 | 89.0 W | 25.1 | 56 |
| #306t | Ar_Ruways, | Path 162, Block 71 | 1-Sep-04 | 25032 | 2004/245/07:13:00 | 76.0 E | 24.1 | 52.8 |
| #307t | Abu_Dhabi, | Path 160, Block 71 | 3-Sep-04 | 25061 | 2004/247/07:00:00 | 78.0 W | 24.4 | 54.4 |
| #308t | Al_Fujayrah, | Path 160, Block 70 | 3-Sep-04 | 25061 | 2004/247/07:00:00 | 63.0 E | 25.1 | 56 |
| #307t | Abu_Dhabi, | Path 161, Block 71 | 10-Sep-04 | 25163 | 2004/254/07:06:00 | 76.0 E | 24.4 | 54.4 |
| #306t | Ar_Ruways, | Path 161, Block 71 | 10-Sep-04 | 25163 | 2004/254/07:07:00 | 75.0 W | 24.1 | 52.8 |
| #308t | Al_Fujayrah, | Path 159, Block 71 | 12-Sep-04 | 25192 | 2004/256/06:54:00 | 89.0 W | 25.1 | 56 |
| #306t | Ar_Ruways, | Path 162, Block 71 | 17-Sep-04 | 25265 | 2004/261/07:13:00 | 76.0 E | 24.1 | 52.8 |
| #308t | Al_Fujayrah, | Path 160, Block 70 | 19-Sep-04 | 25294 | 2004/263/07:00:00 | 63.0 E | 25.1 | 56 |
| #307t | Abu_Dhabi, | Path 160, Block 71 | 19-Sep-04 | 25294 | 2004/263/07:00:00 | 78.0 W | 24.4 | 54.4 |
| #307t | Abu_Dhabi, | Path 161, Block 71 | 26-Sep-04 | 25396 | 2004/270/07:06:00 | 76.0 E | 24.4 | 54.4 |
| #306t | Ar_Ruways, | Path 161, Block 71 | 26-Sep-04 | 25396 | 2004/270/07:07:00 | 75.0 W | 24.1 | 52.8 |
| #308t | Al_Fujayrah, | Path 159, Block 71 | 28-Sep-04 | 25425 | 2004/272/06:54:00 | 89.0 W | 25.1 | 56 |
| #306t | Ar_Ruways, | Path 162, Block 71 | 3-Oct-04 | 25498 | 2004/277/07:13:00 | 76.0 E | 24.1 | 52.8 |
| #307t | Abu_Dhabi, | Path 160, Block 71 | 5-Oct-04 | 25527 | 2004/279/07:00:00 | 78.0 W | 24.4 | 54.4 |
| #308t | Al_Fujayrah, | Path 160, Block 70 | 5-Oct-04 | 25527 | 2004/279/07:00:00 | 63.0 E | 25.1 | 56 |

## Appendix M. UAE Master Directory

Robert Arnone
Code 7330
Naval Research Laboratory
Stennis Space Center, MS 39529
Phone: 228-688-5268
Fax: 228-688-4149
e-mail: Bob.Arnone@nrlssc.navy.mil

Hamid Ahmed Sulaiman AL Brashdi
Department of Meteorology
Directorate General of Civil Aviation and Meteorology
Seeb International Airport - Muscat
P.O.Box:190 - P.C.:323
Sultanate of Oman
UAE (+971 50 3101412)***Available!!
Oman ( +968 9359977)(cell)
Office: +968 519363
Fax: +968 519364
E-Mail: h.albrashdi@met.gov.omT

Dan Breed
NCAR
3450 Mitchel Ln
Boulder, CO 80301
Phone: 303-497-8933
Fax: 303-497-8401
email: breed@ucar.edu

Roelof T. Bruintjes
NCAR
3450 Mitchel Ln
Boulder, CO 80301
Phone: 303-497-8909
Fax: 303-497-8401
email: roelof@ucar.edu

Anthony Bucholtz
Naval Research Laboratory
7 Grace Hopper St., Stop 2
Monterey, CA 93907
Phone: 831-656-5024
Fax: 831-656-4769
email: bucholtz@nrlmry.navy.mil

Steve Burk
Naval Research Laboratory
7 Grace Hopper St., Stop 2
Monterey, CA 93907
Phone: 831-656-4797
Fax: 831-656-4769
email: burke@nrlmry.navy.mil

Gerrit de Leeuw
TNO-Fysisch en Electronisch Lab
P.O. Box 96864
2509 JG The Hague
The Netherlands
Phone: +31 70 374 0462
Fax: +31 70 374 0654
e-mail: deleeuw@fel.tno.nl

Tom F. Eck
Goddard Space Flight Center/GEST
Code 923
Greenbelt, MD 20771
Phone: 301-614-6625
Fax 301-614-6695
e-mail: teck@ltpmail.gsfc.nasa.gov

Rebecca Eager
NC State University
4219-2 Avent Ferry Rd
Raleigh, NC 27606
e-mail: reeager@ncsu.edu

Maha Al Fahim
Dept. of Water Resources
Office of the President, UAE
e-mail: Amandoos@almiyah.gov.ae

Sufian K. Farrah
Dept. of Water Resource Studies
Office of H.H. The President
PO Box 4815
Abu Dhabi, UAE
Tel.: +971 2 642-7777
Fax: +971 2 642-7711
Mobile: +971 50 416-9823
e-mail1: sfarrah@almiyah.gov.ae
e-mail2: Sufian_farah@hotmail.com

Piotr Flatau
Scripps Institution of Oceanography
Visiting Scientist Naval Research Laboratory
7 Grace Hopper St., Stop 2
Monterey, CA 93907
Phone: 831-656-4759
Fax: 831-656-4769
e-mail: flataup.ucar@nrlmry.navy.mil

Charles Gatebe
Climate and Radiation Branch
Mailstop 913
NASA Goddard Space Flight Center
Greenbelt, MD 20771
Tel.: 301-614-6228
Fax: 301-614-6307/6420
e-mail: gatebe@climate.gsfc.nasa.gov

Ahmed H. Ibrahim
Dept. of Water Resource Studies
Office of H.H. The President
PO Box 4815
Abu Dhabi, UAE
Tel.: +971 2 642-7777
Fax: +971 2 642-7711
Mobile: +971 50 416-9502
e-mail1: AHabib@almiyah.gov.ae
e-mail1: ahabib@hotmail.com

Brent Holben
Goddard Space Flight Center
Code 923
Greenbelt, MD 20771
Phone: 301-614-6658
Fax 301-614-6695
e-mail: brent@ltpmail.gsfc.nasa.gov

Christina Hsu
Goddard Space Flight Center/GEST
Code 916
Greenbelt, MD 20771
Phone: 301-614-5554
Fax 301-614-5903
e-mail: hsu@wrabbit.gsfc.nasa.gov

Sufian K. Farrah
Dept. of Water Resource Studies
Office of H.H. The President
PO Box 4815
Abu Dhabi, UAE
Tel.: +971 2 642-7777
Fax: +971 2 642-7711
Mobile: +971 50 416-9823
e-mail1: sfarrah@almiyah.gov.ae
e-mail2: Sufian_farah@hotmail.com

Tara Jensen
NCAR
3450 Mitchel Ln
Boulder, CO 80301
email: jensen@ucar.edu

Ralph Kahn
MS 169-237
Jet Propulsion Laboratory
4800 Oak Grove Drive
Pasadena, CA 91109 USA
Phone: 818-354-9024
Fax 818-393-4619
e-mail: ralph.kahn@jpl.nasa.gov

Olga Kalashnikova
MS 169-237
Jet Propulsion Laboratory
4800 Oak Grove Drive
Pasadena, CA 91109 USA
Phone: 818-393-4154
Fax 818-393-4619
e-mail: olgak@jord.jpl.nasa.gov

Michael D. King
Goddard Space Flight Center
Code 900
Greenbelt, MD 20771
Phone: 301-614-5636
Fax 301-614-5620
e-mail: michael.d.king@nasa.gov

Jolanta T. Kusmierczyk
TNO Physics and Electronics Laboratory
Oude Waalsdorperweg 63
2509 JG The Hague
The Netherlands
Phone: +31 70 374 07 91
Fax: +31 70 374 06 54
email: michulec@fel.tno.nl

Abdulla Al Mandoos
Dept. of Water Resources
Office of the President
PO Box 4815
Abu Dhabi, UAE
Phone: +971-2-642-7777
Fax:: +971-2-642-7711
e-mail-AMandoos@almiyah.gov.ae

Abdulla Al Mangoosh
Dept. of Water Resources
Office of the President
PO Box 4815
Abu Dhabi, UAE
Phone: +971-2-642-7777
Fax:: +971-2-642-7711
e-mail-AMangoosh@almiyah.gov.ae

Hal B. Maring
Radiation Science Program
Code YS
NASA Headquarters
Washington, DC 20546-0001
Phone: 202-358-1679
Fax: 202-358-2770
email: hal.maring@nasa.gov

Krzysztof Markowicz
Institute of Geophysics
Warsaw University
Pasteura 7
02093 Warsaw, Poland
Phone: (48 22) 55 46 836
e-mail: kmark@uninet.com.pl

John Martonchik
MS 169-237
Jet Propulsion Laboratory
4800 Oak Grove Drive
Pasadena, CA 91109 USA
Phone: 818-354-2207
Fax 818-393-4619
e-mail: jvm@jord.jpl.nasa.gov

Steve Miller
Naval Research Laboratory
7 Grace Hopper St., Stop 2
Monterey, CA 93907
Phone: 831-656-5149
Fax: 831-656-4769
email: miller@nrlmry.navy.mil

Mufeed Oden
Abu Dhabi Dept. of Water and
Electricity Authority
Abu Dhabi, UAE
Phone: +971-2-508-1505
Fax:: +971-2-508-1506
e-mail-AMangoosh@almiyah.gov.ae

Norm O'Niell
CARTEL, Universite de Shebrooke
Sherbrooke, Quebec, Canada
J1K 2R1
on sabbatical 2003/2004 GEST/UMBC;
GSFC/NASA, Code 923,
Greenbelt, MD, 20771
Phone: (301)-614-6638
Fax: (301)-614-6695
e-mail: norm.oneill@USherbrooke.ca

Stuart Piketh
Climatology Research Group
University of the Witwatersrand
Johannesburg, South Africa
Phone: +2711 717 6532
Fax: +2711 717 6535
e-mail: stuart@crg.bpb.wits.ac.za

John Porter
University of Hawaii
Hawaii Institute of Geophysics
2525 Correa Rd.
Honolulu, HI 96822
Phone: 808 956-6483
fax 808 956-3189
e-mail johnport@hawaii.edu

Elizabeth A Reid
Naval Research Laboratory
7 Grace Hopper St., Stop 2
Monterey, CA 93907
Phone: 831-656-4712
Fax: 831-656-4769
email: reidb@nrlmry.navy.mil

Jeffrey S. Reid
Naval Research Laboratory
7 Grace Hopper St., Stop 2
Monterey, CA 93907
Phone: 831-656-4725
Fax: 831-656-4769
email: reidj@nrlmry.navy.mil

Sethu Raman
1005 Capability Dr., Suite 213
Campus Box 7236
North Carolina State University
Raleigh NC 27695-7236
Tel: 919-515-1440
Fax: 919-515 -1441
e-mail: sethu_raman@ncsu.edu

Joanna Remiszewska
Institute of Goephysics
Polish Academy of Sciences
Ksiecia Janusza 64
01-452 Warsaw Poland
Tel: (+48 22) 37 98 20
Fax: (+48 22) 37 05 22
e-mail: jrem@igf.fuw.edu.pl

Kristy Ross
Climatology Research Group
University of the Witwatersrand
Private bag 3
Wits, South Africa
2050
Tel: +27 11 717-6534
Fax: +27 11 717-6535
e-mail:Kristy@crg.bpb.wits.ac.za

Ben Ruston
Naval Research Laboratory
7 Grace Hopper St., Stop 2
Monterey, CA 93907
Phone: 831-656-4725
Fax: 831-656-4769
email: ruston@nrlmry.navy.mil

Adnan Sharaf
Dept. of Water Resource Studies
Office of H.H. The President
PO Box 4815
Abu Dhabi, UAE
Tel.: +971 2 642-7777
Fax: +971 2 642-7711
Mobile: +971 5 451-5593
e-mail: asharaf@almiyah.gov.ae

Robin M. Schoemaker
TNO-Fysisch en Electronisch Lab
Oude Waalsdorperweg 63
2597 AK, The Hague
The Netherlands
phone: +31.70.37.40593
e-mail:schoemaker@fel.tno.nl

Alexander Smirnov
Goddard Space Flight Center/GEST
Code 923
Greenbelt, MD 20771
Phone: 301-614-6626
Fax 301-614-6695
e-mail: asmirnov@aeronet.gsfc.nasa.gov

Si-Chee Tsay
NASA GSFC Code 913
Greenbelt, MD 20771
Phone: 301-614-6188
Fax 301-286-1759
e-mail: tsay@climate.gsfc.nasa.gov

Dominick Vincent
Dept. of Meteorology
Naval Postgraduate School
(Code MR/Qg)
589 Dyer Rd, Rm 254
Monterey, CA 93943
Phone: 831-656-3666
e-mail: davincen@nps.navy.mil

Annette L. Walker
Naval Research Laboratory
7 Grace Hopper St., Stop 2
Monterey, CA 93907
Phone: 831-656-4722
Fax: 831-656-4769
email: walker@nrlmry.navy.mil

Nicola Walton
Climatology Research Group
University of the Witwatersrand
Private bag 3
Wits, South Africa
2050
Tel: +27 11 717-6531
Fax: +27 11 717-6535
e-mail: Nicola@crg.bpb.wits.ac.za

Marcin Witek
Institute of Geophysics
Warsaw University
Pasteura 7
02093 Warsaw, Poland
e-mail: mwit@igf.fuw.edu.pl

Ellseworth Judd Welton
NASA GSFC
Greenbelt, MD 20771
Phone: 301-614-6279
Fax: 301-614-5492
e-mail: Ellsworth.J.Welton@nasa.go

Douglas L. Westphal
Naval Research Laboratory
7 Grace Hopper St., Stop 2
Monterey, CA 93907
Phone: 831-656-4745
Fax: 831-656-4769
email: westphal@nrlmry.navy.mil